Multifunctional Cellulose-Paper for Light Harvesting and Smart Sensing Applications

António T. Vicente, Andreia Araújo, Manuel J. Mendes*, Daniela Nunes, Maria J. Oliveira, Olalla Sanchez-Sobrado, Marta P. Ferreira, Hugo Águas, Elvira Fortunato, Rodrigo Martins*

CENIMAT/I3N, Departamento de Ciência dos Materiais, Faculdade de Ciências e Tecnologia, FCT, Universidade Nova de Lisboa and CEMOP/UNINOVA, 2829-516 Caparica, Portugal

**Corresponding authors: mj.mendes@fct.unl.pt; rm@uninova.pt*

Abstract

A novel generation of flexible opto-electronic smart applications is now emerging, incorporating photovoltaic and sensing devices driven by the desire to extend and integrate such technologies onto a broad range of low cost and disposable consumer products of our everyday life.

Several flexible polymeric materials are now under investigation to be used as mechanical supports for such applications. Among them, cellulose, the most abundant organic polymer on earth used in the form of paper or membrane, has attracted much research interest due to the advantages of being recyclable, flexible, lightweight, biocompatible and extremely low-cost, when compared to other materials. Cellulose substrates can be found in many forms, from the traditional micro-cellulose paper used for writing, printing and food/beverage packaging (e.g. liquid packaging cardboard), to the nano-cellulose paper which has distinct structural, optical, thermal and mechanical properties that can be tailored to its end use.

The present article reviews the state-of-the-art related with the integration and optimization of photonic structures and light harvesting technologies on paper-based platforms, for applications such as Surface Enhanced Raman Scattering (SERS), supporting remarkable 10^7 signal enhancement, and photovoltaic solar cells reaching ~5% efficiency, for power supply in standalone applications. Such paper-supported technologies are now possible due to innovative coatings that functionalize the paper surfaces, together with advanced light management solutions (e.g. wave-optical light trapping structures and NIR-to-Visible up-converters).

These breakthroughs open the way for an innovative class of disposable opto-electronic products that can find wide spread use and bring important added value to existing commercial products. By making these devices ubiquitous, flexible and conformable to any object or surface, will also allow them to become part of the core of the Internet of Things (IoT) revolution, which demands systems' mobility and self-powering functionalities to satisfy the requirements of comfort and healthcare of the users.

Keywords: *Paper-based technology, Photovoltaics, Light Management, Optical Sensing*

Table of Contents

1 Introduction

Cellulose is the most abundant biopolymer on Earth. Besides its traditional uses in books, newspapers, printing paper, packaging, or cleaning, it is nowadays envisaged for several thin film opto-electronic applications given its unique set of properties.[1]Cellulose is biocompatible, biodegradable, 100% recyclable, lightweight, flexible, foldable and low cost (0.3 – 0.6cent/m^2) when compared with the most common flexible substrates (e.g. polyethylene terephthalate - PET, or polyimide- PI) used in electronics which are above one order of magnitude more expensive.[2–4] Nevertheless, the use of cellulose in opto-electronic applications is not free of challenges, namely the lower working temperature range, its surface roughness, porosity, or lower mechanical properties compared to certain polymers, which will require reengineering cellulose to be compatible with the intended application.

It is the high adaptability of thin film technologies that is fueling the growing interest in developing novel flexible platforms for fully autonomous intelligent devices. The demands for efficient regulation, reliable quality control, monitoring, and intelligent systems will require the incorporation of power-demanding flexible opto-electronic devices (e.g. sensors, logic circuits, antenna, lighting elements, and power systems) into clothing,[5]personal objects,[6]packages,[7] diagnostic/monitoring platforms[8] or even electronic-skin.[9]Nevertheless, for thin film technology to be suitable for implementation on flexible substrates, such as paper, plastics, fabrics, and membranes, it must be adapted to allow conformal shaping and bending to some degree without losing function. In this way, besides incredibly broadening the applicability of thin film devices in various consumer electronic products, the technology is also made compatible with roll-to-roll (R2R) manufacture, the preferred industrial process for mass-production.

Solutions to power devices on textiles (*electronic textiles*, or *e-textiles*),[10] polymers,[11] or paper[12] have boomed in recent years, which shows how promising these segments can be for the market of thin film solar cells (TFSC). Plastic substrates, such as PET, PI, and PEN (polyethylene naphthalate), are the traditional options when considering flexible optelectronics.[13–18] However, from an economic and raw material life-cycle perspective, these petroleum-based substrates are expensive and environmentally less attractive than other easily recyclable or biodegradable materials. Substrate materials which could be synthesized at low cost, from renewable feedstock's, or energy-efficient carbon-based green materials (e.g. cellulose, starch, chitosan, collagen, soy protein, and casein), are particularly attractive to achieve sustainable technology.[19]

Among the classes of carbon-based materials, paper, or cellulose-based materials (extracted from cotton, wood, hemp, algae, bacteria, among others[20]), can be one of the best alternatives to ceramics, metal, glass, and polymer substrates given its biodegradability, cost effectiveness and abundance. Paper has been used ubiquitously since ancient times and, in the future, paper-supported photovoltaics could create other attractive new paradigms, including seamless integration into window shades, wall coverings, intelligent packaging and documents. Module installation may be as simple as cutting paper to size with scissors or tearing it by hand and then stapling it or gluing it. Additional cost savings can be anticipated given the low weight of paper and its ability to achieve a compact form factor by rolling or folding for facile transport from the factory to the point of use.[21]

Advantageously, the physical properties of cellulose-based materials can be easily engineered to a high degree, allowing the construction of ideal substrates with flat surface and good mechanical and chemical stability that are compatible with various fabrication processes and enable an inexpensive and scalable production,[22] especially when accompanied by fast direct-write methodologies such as inkjet printing[23]for low cost disposable applications. In addition to the use of paper as a bendable mechanical support, it can also be engineered to exhibit beneficial optical properties for flexible optoelectronic devices, such as high transparency and haze (ratio between diffuse and total light intensity) to improve light transmission and coupling.

In light of the world of possibilities, this review explores recent progress concerning the applications that cellulose-based materials have in the field of opto-electronics, focusing on devices, which exploit light for either energy harvesting or sensing. Section 2 starts by overviewing fabrication methodologies and strategies to address the challenges of paper to obtain devices with comparable properties to those fabricated on conventional substrates. Section 3 evaluates thin film solar cell technology and latest breakthroughs in its adaptation to flexible platforms such as paper, together with promising innovative research pathways to boost the efficiency via light management/trapping solutions. The use of paper for optical bio-sensing applications is reviewed in Section 4, where focus is given to Raman and Photoluminescence based detection. To complete the review, Section 5 comments on another important field outside opto-electronics, related with electronic circuitry, where the physical properties of paper are becoming of emerging interest. Lastly, the main conclusions and future prospects of these promising emergent technologies are presented in Section 6.

2 Paper engineering

The main application of paper in opto-electronics is in the form of a physical substrate to support the different functional materials. Another class of applications is the use of the paper porosity as a scaffold to immobilize photoactive nano-materials, where paper thereby becomes a more active part of the opto-electronic devices. This review covers recent advances in distinct paper-based technologies, focusing mainly in devices for solar energy harvesting and optical sensing. Nevertheless, in all the cases described here, it is crucial to properly modify the physical properties of paper (both bulk and surface) in order to optimize it for the targeted applications.

The most common type of paper engineering techniques consists in covering the natural porosity of paper surfaces with sealing layers, yielding a closed surface which does not allow penetration of the functional materials into the paper.[24]In general, most devices benefit from the surface smoothness of the substrate, as it enables the use of narrower and thinner features without risk of pinholes. In multilayer structures, for example thin film solar cells, excessive surface roughness can lead to non-uniform coverage of the different coatings and even penetration of one cell layer into another, making the devices inoperable due to short-circuiting caused by an excessive number of pinholes that connect the selective contact layers for electrons and holes. Barrier/sealing layers can provide not only a smooth surface but also act as encapsulants preventing oxygen or moisture from destroying the functionality of the patterned devices. A well-known example is the use of high-performance gas/moisture barriers in conventional paper cardboard products used in liquid packaging of beverages, where an alumina-coated aluminium barrier layer is needed conformal deposited onto the porous paper

surface.[25] Besides roughness and encapsulation, the surface chemistry of paper can also play a role in the performance of functional materials in contact with it. While a chemically inert surface can be created through coating, to decouple the paper from the device, some surface chemical groups can potentially improve the performance of a functional material, for example, through doping.

When it comes to material engineering, cellulose-based materials are particularly versatile and highly adaptable via these or other approaches mentioned along the next sections.

2.1 Cellulose and its derivatives

Cellulose, mainly obtained from the skeletal component of plants, is an almost inexhaustible green material with an annual production of about 1.5 trillion tons.[26]The molecular structure of cellulose, $(C_6H_{10}O_5)_n$, is a polysaccharide consisting of a linear chain of glucose units linked together through β 1,4 glycosidic bonds[27]by condensation reaction.[28] The cellulose chains are then organized into elementary fibrils (nanosized fibers), which aggregate into larger microfibrils and microfibrillar bands.[29,30] In microfibrils, the multiple hydroxyl groups on the glucose form hydrogen bonds with each other, holding the chains firmly together and contributing to their high tensile strength.[31,32]The solid-state structure of the microfibril is represented by the areas of both high (crystalline) and low (amorphous) orders range. Variations in crystalline content and crystallite size dictate the differences in morphology, mechanical properties,[33] or thermal stability[34] of the resulting microfibril, which are then reflected in the final cellulosic product.[35]

An in-depth review of cellulose materials, properties and fabrication methods, can be found in the work of Moon *et al*.[35] Here, the main purpose is to provide a brief overview of the available cellulose materials in order to contextualize the topics under discussion.

Cellulose can be chemically modified to yield cellulose derivatives. These are widely used in various industrial sectors (e.g. rayon/viscose as a textile fiber used in the clothing sector, cellulose ethers in pharmaceutical as excipient, or cellulose gum in cosmetics and food)as thickeners, binding agents, adhesives, swelling agents, protective colloids, emulsion and suspension stabilizers, and film-forming agents.[36] Some of the most important cellulose derivatives are methyl cellulose (MC), hydroxypropylmethyl cellulose (HPMC), ethyl cellulose (EC), hydroxypropyl cellulose (HPC), and carboxymethyl cellulose (CMC). The cellulose derivatives get their names from the substituting groups that replace the free hydroxyl groups of cellulose.

Alternatively, cellulose can be purified/extracted from both cellulose I sources (such as wood fibers, cotton, and agricultural crops) and cellulose II sources (such as lyocell fibers)[37] to obtain fibers with characteristic dimensions and unique properties. By mechanical pressure, chemical (e.g. acid hydrolysis), or enzymatic pretreatments followed by high-pressure homogenization, the micrometer-sized cellulose fibers can be disintegrated to obtain microfibrillated cellulose (MFC), cellulose nanofibrillated (CNF), cellulose nanocrystalline (CNC), among other cellulose materials.[38] Another important nanocellulose material, named bacterial cellulose (BC), is synthesized from the fermentation of sugar, mainly by gram-negative bacteria, such as the *Gluconacetobacter xylinus* (reclassified from *Acetobacter xylinum*).[39,40] Comparatively to regular cellulose materials, purified cellulose materials have higher Young's

modulus, dimensional stability, lower coefficient of thermal expansion (CTE), outstanding reinforcing potential, smoother surface, and transparency.[41] Moreover, the reactive surface of –OH side groups facilitates grafting chemical species to achieve surface functionalization.[35]

Amid the variety of envisioned applications it includes, for instance: barrier films, antimicrobial films, flexible displays, reinforcing fillers for polymers, biomedical implants, pharmaceuticals, fibers and textiles, energy storage, and templates for green electronic components.[35]

The cost of nanocellulose, however, can be higher than traditional cellulose materials, due to the additional production steps that add to the energy and materials consumed.[42]Prices based on the raw material cost of CNF range from 0.7 to 7 $\$\cdot g^{-1}$, considering a low weight nanopaper (20 g m^{-2}), but the price is expected to decrease with industrialization.[43]

2.2 Device fabrication on paper-based substrates

Despite all the envisioned applications of paper-based optoelectronics, implementation is not straightforward. For instance, devices like solar cells or OLEDs (organic light-emitting diodes), and printed electronics, require a smooth and non-porous substrate to prevent cracks, breaks and shunts in the films. Some applications and fabrication processes also require the substrate to withstand high temperatures (up to 250 °C) without undergoing degradation (e.g. sintering of Ag nanoparticles commonly used in nanocomposite inks[44]). These and other challenges[45] are intrinsically linked to the properties of paper. Traditional paper, made of cellulose fibers with diameters of ~20 μm, is usually extremely rough, with peak-to-valley roughness values of up to hundreds of micrometers.[38]Furthermore, most commercially available papers also add mineral fillers, seizers, and clays to fill the pores and optimize printability[46] (e.g. capillary action, ink drying and absorption), as well as pigments and fluorescent whitening agents to improve the whiteness of the paper and image quality.[21,46] All these additives can severely limit the quality of the devices fabricated on regular paper, especially if solution processes are involved.[47]

Fortunately, there are several ways to overcome these challenges, such as smoothing the paper surface by cast-coating followed by super calendaring, as exemplified in Figure 1. This process gives a smooth finishing to the paper surface, turning its microscopic porosity into a nanoscopic roughness. It also decreases its wettability, which may be problematic for liquid deposition processes like printing, but can make it suitable for gas-phase coating by physical vapor deposition (PVD) and chemical vapor deposition (CVD) methods that are typically used in thin film Si solar cell fabrication. This innovative approach allowed the realization of flexible a-Si:H solar cells on paper with sunlight-to-electricity conversion efficiencies (3.4%) similar to those (4.1%) attained on rigid (glass) substrates.[48]

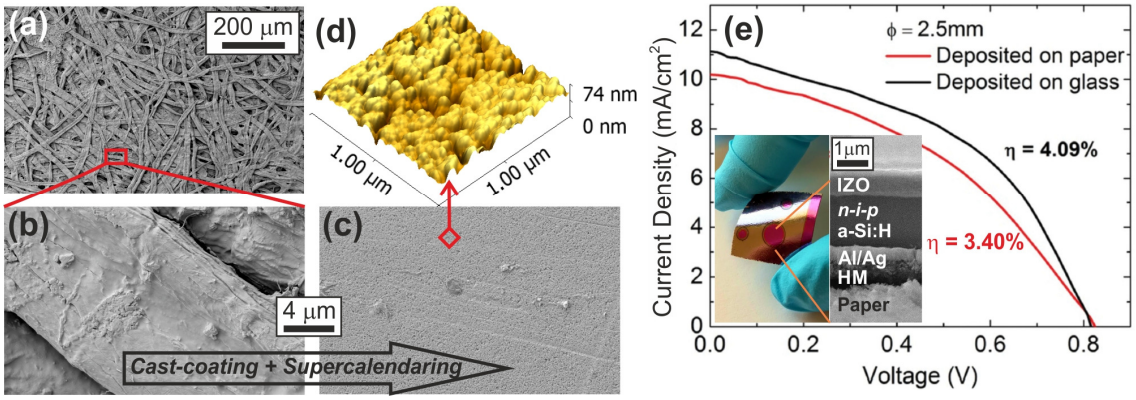

Figure 1 – a,b) SEM images of the fibrous morphology of the untreated paper at low (a) and high(b) magnification. **c,d)** Images of the same paper after the cast-coating plus supercalendaring process, yielding a smooth surface with 9.42 nm RMS roughness as shown in the AFM image (d). **e)** Current density (*J*) vs. voltage (*V*) characteristics of the a-Si:H solar cells deposited either on glass substrate (reference) or on the treated paper. The inset shows a photograph of the solar cells together with a cross-section SEM of the layer structure obtained by a FIB cut.[48] Reprinted with permission of Wiley.

Nonetheless, there is nowadays a broad range of distinct strategies under development to tackle the issue of the high paper roughness and porosity and to allow coating its surface with different types of functional materials, as listed in the following sub-section.

2.3 Coating and printing techniques

A thorough overview of coating and printing techniques for solar cell applications was reported by Frederik Krebs.[49] Here, the goal is to briefly list the available coating and printing techniques compatible with cellulose-based substrates to contextualize the following sections dealing with devices fabricated on the same substrates.

Coatings can be applied on a variety of substrates using non-contact (e.g. inkjet) and contact (e.g. offset, flexographic, screen printing, and doctor blade) techniques (see Figure 2).[50–52] These techniques open numerous possibilities to obtain, not only coated substrates, but also multilayer structures and devices. Multilayer structures, however, constrain the properties of the materials in use to not destroy or dissolve the previously casted layers. A small variation in properties (viscosity, surface tension, solid contents, evaporation rate etc.) of the solution, or of the substrate (surface energy, roughness, and porosity), can greatly change the coating/printing quality.[53] In an ideal process, the fabrication steps should be minimum, the materials environmentally friendly, and the final product recyclable.[54]

The most common coating and printing methods are described below and depicted in Figure 2, with special emphasis on those that are R2R compatible:

- **Casting** - Casting is probably the simplest technique for film forming since it does not require any equipment. This technique simply involves the casting of a solution containing the desired material onto the surface of the substrate followed by the solvent evaporation. However, it has limitations in the area coverage, lacking control over the film thickness and often picture framing effects are observed near the edges of the film or during drying.[49]

- **Dip Coating -** In dip coating, the substrate is dipped into the coating solution and a film is made either by removing the substrate from the solution or by draining the solution.[55] Film thickness can be controlled with several parameters, including the rate at which the substrate is immersed and removed from the liquid, the immersion time, the liquid and substrate intrinsic properties (concentration, viscosity, rate of interaction between the surface and the liquid etc.), and the number of times that the process is repeated.[56] There are advantages for the use of this technique such as good uniformity, very thin layers, large area coverage, and the simplicity of the method.[57–59]However, there is a substantial waste of material and both sides of the substrate become coated. This technology has also been successfully employed in fabrication of solar cells. For example, Hu *et al*.[60] developed organic solar cells with a power conversion efficiency (PCE) of 3.93% and a 63% fill factor using dip coating technology.

- **Spin Coating -** Spin coating is a well-established technology commonly used, for instance, to coat silicon wafers with photoresist, fabrication of sensors, casting protective coatings, optical coatings, and membranes.[61,62]Spin coating involves the application of a small volume of liquid on the surface followed by acceleration of the substrate with a chosen rotation speed producing a centrifugal force.[61] Due to the angular velocity of the substrate the excess liquid flows to the perimeter and is ejected, leaving behind a thin film on the substrate.[49]High reproducibility of Perovskite solar cells was obtained by a complete spin-coating sequential solution deposition (spinning-SSD) process and it is a promising approach to achieve high-performance Perovskite solar cells.[63]

- **Doctor Blade -** Doctor blade is a continuous process that produces thin films on large area surfaces with a well-defined thickness and minimum waste of materials.[59,64]The doctor blade operates at a speed up to several meters per minute and the films' thickness can range from microns to several hundred microns.[59]Uses of this technique in the fabrication of organic solar cells can be found in literature.[64,65]

- **Spray Coating -** In recent years, spray coating has been used as a viable technique for low-cost fabrication in many applications like solar cells.[66–68] In spray coating, the solution is forced through a nozzle by a high pressure, whereby a fine aerosol is formed which is accelerated towards the substrate with an inert carrier gas.[69] The quality of the coating depends on several process parameters such as distance of the spray nozzle to substrate, coating speed, and the number of sprayed layers.[51]

- **Screen-Printing -** Screen-printing is widely used due to its simplicity, speed, and compatibility with various substrates in which the ink is pushed through a fine mesh with a defined pattern producing functional structures with large aspect ratio.[52]This technique requires high-viscosity inks[70] with thixotropic (shear-thinning) behavior, as inks with lower viscosity can simply run through the mesh.[51] The print resolution and print thickness depends on the density of the mesh and ink properties.[54] This technique is also scalable to industrial level and R2R compatible.[71]For instance, screen printing has been used in the fabrication of conductive composites[72] and transistors[73] on paper substrates. In the photovoltaic industry, screen printing accounts for the majority of the metallization processes for silicon wafer solar cells.[74] Nevertheless, organic photovoltaic (OPV) fabrication process often explores screen-printing to deposit active layers.[49,75]

- **Inkjet Printing -** Inkjet printing is a digital noncontact printing technique, capable of reproducing complex patterns, which can also be used to deposit functional materials.[49]It is a low-cost technique, highly adaptable, and has low material consumption.[51,54] These materials, or inks, consist of a solute dissolved or otherwise dispersed in a solvent and can be classified to aqueous, non-aqueous, phase change, or UV-curable inks,[46] that are deposited in form of droplets by a pressure pulse in the nozzle head.[76] Inkjet inks generally have low viscosities and low evaporation rate for a fast droplet generation and prevent clogging. Inkjet printing is being widely used to fabricate RFID antennas[77] and was also successfully implemented in the fabrication of solar cells.[78]

- **Gravure Printing -** Gravure printing is commonly used reproduce catalogs and magazines in high-volumes.[79]This technique employs direct transfer of functional inks through physical contact of predefined engraved structures (metallic or a plastic roll) with the substrate, after which the excess ink is removed by doctor blade.[80,81] The gravure rolls have a long lifetime but are expensive to produce, so this approach is mostly used in industrial mass printing.[52,82] Advantages of the technology include high printing speed (up to 15 m/s) and good printing resolutions due the possibility of engrave different depths into the printer roller.[52]The gravure printing technique can be applied to fabricate devices like organic solar cells,[83] transistors,[84] and OLEDs.[85]

- **Offset Printing-** Offset (lithography) printing, is one of the most common contact techniques. The roll is first chemically patterned and then covered with ink, however the patterning creates surface sections that bind with the ink (by strong adhesive and cohesive forces) and form a thin film, and other sections that repel the ink.[52,82]The ink is then transferred to a substrate by high pressure. However, offset printing for printing electronics is limited by the required high viscosity of the ink, the transferring high pressure, and the typical presence of water.[86,87]

- **Flexographic Printing -** In flexographic printing, the print pattern is present as a protruding relief on a printing roll, made of rubber or a photopolymer.[88]The ink is first transferred from a reservoir onto the printing roll by an anilox cylinder with engraved microcavities embedded into the surface. The anilox cylinder supplies ink by contact with a fountain roller that is partly immersed in an ink bath.[51] The pressures applied must be low to prevent excessive mechanical deformation of the protrusions which decrease the printing quality.[52] A wide variety of inks (solvent-based, water-based, electron-beam curing inks, UV curing inks, etc.) can be printed by flexographic printing, whereas the typical viscosities are rather low, usually less than 500 mPa·s.[51,52]The applicability of flexographic printing on printed electronics devices is reported, for instance, in the fabrication of OTFT (Organic thin-film transistors),[89]logic gates,[90]electroluminescent layers, and OPV.[91] In photovoltaics, flexographic printing is mainly used in front side metallization of silicon solar cells.[92] However, Hübler *et al*.[91] successfully fabricated a solar cell on paper with a PCE of 1.3% (see section 3.2.2), where the transparent PEDOT:PSS [poly(3,4-ethylene-dioxythiophene):poly(styrene-sulfonate)]anode was deposited by flexographic printing on top of the active layer of P3HT:PCBM [poly(3-hexylthiophene-2,5-diyl):[6,6]-phenyl-C_{61} butyric acid methyl ester].

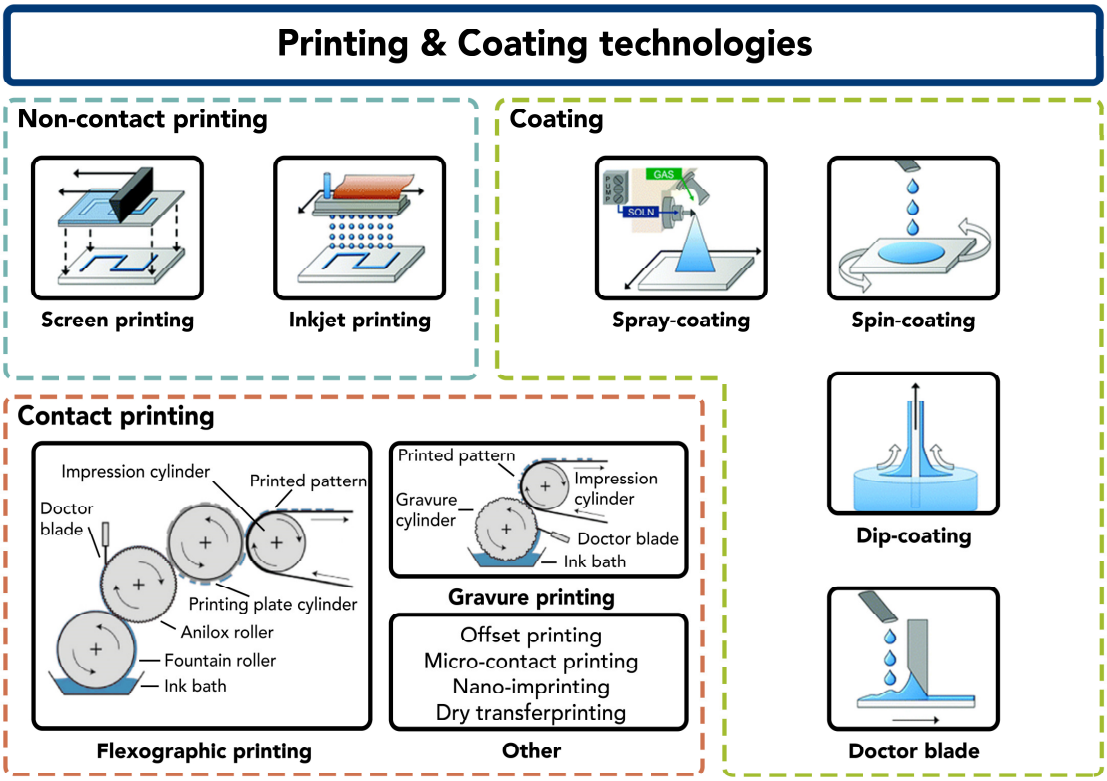

Figure 2 –Sketches of the most common wet-patterning methods employed on paper-based substrates, divided in three types: coating, non-contact and contact printing.[50,51] Reprinted with permission of Royal Society of Chemistry and Wiley, respectively.

Table 1summarizes the main distinctive features and evaluation parameters of the afore mentioned wet-coating techniques.

Table 1 - Comparison of the characteristics of the printing technologies commonly applied to paper coating.[49,82,93]

Coating technique	Pattern	Wet thickness (μm)	Speed	R2R compatible	Ink		
					Viscosity	Preparation	Waste
Dip/Casting	None	1-500	<1 m/min	No	<10 cP	Moderate	Some
Spin	None	0-100	<1 m/min	No	<10 cP	Simple	Very High
Doctor Blade	None	0-100	<10 m/min	Yes	<10 cP	Simple	Some
Spray	None	1-500	$<10^2$ m/min	Yes	10-10^3 cP	Moderate	High
Screen	2D	10-500	$<10^2$ m/min	Yes	10^2-10^5 cP	Demanding	Little
Inkjet	Digital master	1-500	<10 m/min	Yes	<10 cP	Moderate	Little
Gravure	2D	5-80	10-10^3 m/min	Yes	$<10^3$ cP	Difficult	Little
Offset	2D	0.5-10	1-10^2 m/min	Yes	10^3-10^5 cP	Demanding	Little
Flexographic	2D	5-200	10-10^3 m/min	Yes	$<10^3$ cP	Demanding	Little

Coating and printing technologies are assisting and revolutionizing the field of flexible electronics devices by simplifying the process steps, reducing the waste of materials, lowering fabrication and maintenance costs, and speeding up production.[82]

3 Paper-based photovoltaics and light management

Over the last decade, references to the use of photovoltaics (PV) to power printable electronics on paper started to emerge[94] and it is nowadays a hot topic in the development of autonomous high-end applications,[95,96] introducing new directions for intelligent paper electronics. Taking in consideration the current technology stage of paper-based solar cells, where a single cell can generate a current of 5–20 $mA \cdot cm^{-2}$ and voltage of 0.7 – 1.1 V, it is realistically conceivable that a simple integration of 2 – 3 rows of solar cells connected in parallel, and each row with 3 – 5 cells connected in series, can yield a power density output anywhere between 15 $mW \cdot cm^{-2}$ to 150 $mW \cdot cm^{-2}$, which is in line with the power requirements of many paper electronic systems under development. For example, in the work of Barr *et al*., the fabricated paper PV arrays produced > 50 V.[21] Tentzeris and Kawahara have roughly calculated the power specifications of future sensor devices in ICT (information and communications technologies) and μW Computing.[23] Most commonly used wireless sensor nodes (e.g. RFID-enabled sensor nodes) consume dozens of μW in sleep mode and hundreds μW in active mode. Although the above study is directed towards scavenging of potential frequencies, such power requirements can be readily obtained by PV to endow such devices with full autonomy. Moreover, next generations of these nodes consume significantly less power, for instance sensor nodes (sensor + readout circuit) are already able to absorb 1.2 – 1.8 μW in active mode[97] and full wireless nodes (sensor + readout + radio transmitter) are able to absorb 40 μW in active mode.[98]Kim *et al*. later explored such possibility in which is one of the first references to flexible solar powered wireless transmission devices fabricated on paper.[94] Inkjet printing was used to fabricate the conductive circuit traces and the folded slot antenna. Autonomous operation was successfully achieved by powering the 800 MHz antenna-based beacon with an a-Si:H solar cell (drain current 4 mA and supply voltage 1.8 V).[94]

Among the numerous paper-based optoelectronic devices that could exploit PV power sources, OLED devices are one of the most studied.[22,99–102] The power requirements of OLEDs are already in line with those PV can deliver. For instance, one of the most efficient OLED produced (external quantum efficiency of 11.7%) is reported in the work of Jung *et al*.[103] Here, they demonstrate the fabrication of OLEDs by inkjet printing with similar electrical performance to those deposited by vacuum processes. The OLED device with the lowest current density had a driving voltage at 1000 $cd \cdot m^{-2}$ of 6.3 V.

Paper-based batteries[104–106] or supercapacitors[26,107] coupled with PV is another promising strategy to extend autonomy and self-sufficiency of devices, when a light source is unavailable. For instance, Wee *et al*. demonstrated a novel printable module in which organic solar cells were integrated with an all-solid-state flexible supercapacitor.[108]

The present section starts by introducing the current picture of the distinct solar cell technologies (Section 3.1), paying particular attention to thin film photovoltaics. This is the branch where paper can find most application in PV, mainly as flexible platform to

mechanically support the solar cell layers. Therefore, the use of paper for PV substrates is the main focus here, where the chief technological challenges are identified: not only related with the adaptation of the paper materials and devices fabrication conditions to allow stable operation on such substrates (Section 3.2), but also concerned with the improvement of their conversion efficiency via the implementation of advanced light trapping mechanisms (Section 3.3). Besides the use of paper as substrate, there are other classes of applications where cellulose-based materials perform a more active role in the solar cells, as media to incorporate or immobilize nanostructures that assist in the sunlight-to-electricity conversion process (Section 3.4).

3.1 Current picture of solar cell technologies

Climate change poses one of the greatest threats to our life and is rapidly altering the dynamics of the Earth. To prevent irreversible damage to our planet, sustainability concerns must be taken in consideration in all our daily choices. Nowadays there is a great concern with the development of sustainable technologies to curb the negative impacts of humanity to the environment. This search for green technology promotes the manufacture of fully recyclable products, minimizes consumption of natural resources, and exploits renewable energy sources to power devices.

In the particular case of energy consumption, solar energy – the largest global renewable energy source[109] – is one of the most promising options,[110] given its sustainability and high adaptability. Depending on the intended application, solar energy is converted in other energy forms. The most efficient conversion is solar energy to heat, but a wider range of applications can be envisioned when solar energy is converted to electricity. This conversion can be done indirectly by mechanical work (e.g. with steam turbines, or a Sterling engine), or directly, using semiconducting materials that exhibit the photovoltaic effect, called photovoltaics. The direct conversion of solar energy into transportable and storable energy forms, by artificial photosynthesis/photocatalysts (e.g. to reduce CO_2 into renewable hydrocarbon solar fuels), or by photo electrochemical cells (e.g. to produce hydrogen from water splitting),[32] is also possible but still far from reaching industrial viability.

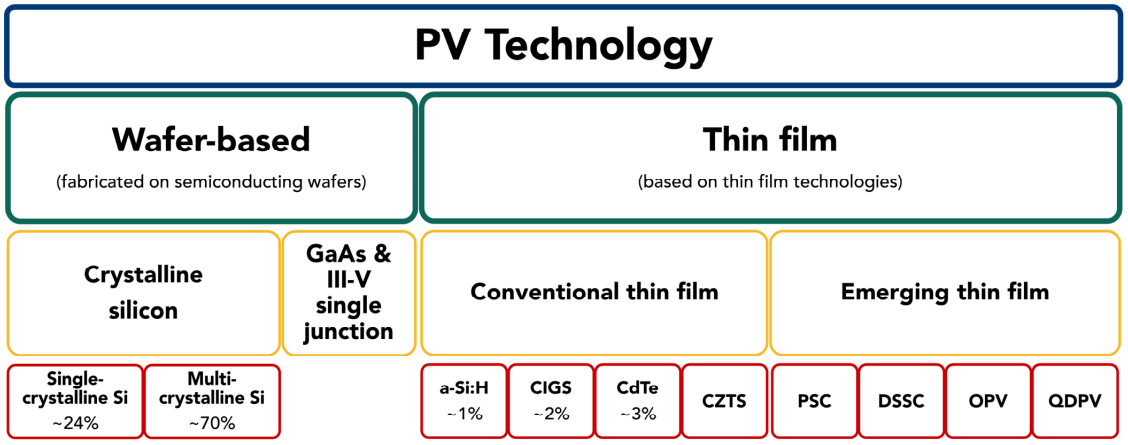

Figure 3 - PV technology classification under two main groups: wafer-based materials (single/multi- crystalline silicon, gallium arsenide (GaAs), and other III-V semiconductors such as InGaAs and AlGaAs), and thin film materials. The group of thin film solar cells (TFSC) can be subdivided in conventional thin film materials

(amorphous silicon, a-Si:H), copper indium gallium selenide (CIGS), cadmium telluride (CdTe), and copper zinc tin sulphide (CZTS)) and emerging thin film materials: dye-sensitized solar cells (DSSC), organic photovoltaics (OPV), quantum dots photovoltaics (QDPV) and perovskite solar cells (PSC). Percentage values refer to global market shares in 2016.[111] Adapted from He *et al*.[112]

The global PV installed capacity in 2015 was of 227 GW,[113] corresponding to a market growth of 25% over 2014; and until 2040 it is expected to grow above 8% yearly.[114] Despite the numerous types of PV technologies (see Figure 3), the market is dominated by first generation wafer-based crystalline silicon (c-Si) cells, which account for 94% of the total production in 2016.[111] Given the reliability, maturity, and continuous cost reduction of c-Si solar cells (in addition to the fact that Si is the second most abundant element in the Earth's crust), it is foreseeable that this standard PV technology will continue to lead the market in the near to mid-term future. The remainder of the PV market is held by second generation thin film solar cells (TFSC), based on cadmium telluride (CdTe), copper indium gallium (di)selenide (CIGS) and silicon (either hydrogenated amorphous silicon, a-Si:H, or microcrystalline silicon, μc-Si:H).[115,116] TFSC technologies were developed to provide other important advantages compared to wafer-based SCs:[117,118]

- High production capacity and shorter energy pay-back time, given the reduced material consumption and energy input in the fabrication process (lower amount of purified semiconductor materials);
- Lower material and energy requirements lead to lower fabrication costs, thus reduced cost per Watt of solar energy conversion, and lower levels of CO_2 equivalent emissions per kWh;
- The decommission and recycling stage is more favorable because the materials used as substrates are mostly composed of glass or plastics.

CdTe SCs takes about ~3% of the total market, while CIGS and silicon account for ~2% and 1%, respectively.[111] The emerging TFSC of third generation PVs, have the potential to overcome the Shockley-Queisser limit for single bandgap and the cell efficiencies are already approaching those of commercialized second generation technologies. Particularly interesting is the case of Perovskite solar cells (PSC), the fastest-advancing solar technology, whose efficiencies soared from 3.8% in 2009[119] to 22.1% in 2016.[120,121] In addition, a mechanically-stacked Perovskite-on-Silicon tandem solar cell has recently reached an efficiency of 26.4%, which rivals the current record efficiency of c-Si wafer-based cells of 26.7%.[122]

Wafer-based SC require thick layers – 100 to 1000 times thicker than thin films – to efficiently absorb sunlight and are extremely fragile, which limits their applicability since they need to be mounted on rigid and heavy structures – features that also raise the balance of system (BOS) costs. Their limited applicability opened a market opportunity for PV solutions that can take advantage of thinner, flexible, and lightweight characteristics like those provided by second and third generations TFSC. Small and flexible modules with power ranging from 3 to 50 W_P are used as portable battery chargers, in a variety of leisure products[123] and can be easily transported and installed in remote areas; there is also a rising interest in providing autonomy and self-sustainability to devices and sensors to achieve concepts such as the Internet of Things (IoT),[124] wearable electronics,[10] and smart environments in general.[125] These electronic

systems will contribute to our future lifestyles at the level of communications, logistics, and healthcare[48] and by being solar powered, the load to the energy grid will not increase.

Paper-based photovoltaics as previously discussed, can be applied as in situ power source for paper electronics. In the fabrication process of solar cell devices, cellulose can have three main purposes: (i) as matrix/binder/dispersion medium for polymer solutions; (ii) as substrate for flexible (and, in times, transparent) SCs; (iii) to enhance surface and optical properties. The different uses of cellulose and solar cells produced are summarized in **Table 2, 3 and 4**,respectively according to those categories. As can be seen, when used in polymer mixtures, most of them rely on ethyl cellulose; whereas as substrate for solar cells, numerous devices are fabricated on nanocellulose composites, as they are porous free, with nanometer scale roughness, and low impregnation volume, comparing to traditional paper. These nanocellulose composites are also the preferable choice to enhance the optical properties of SC, given their high transparency and haze.

3.2 Paper as photovoltaic substrate

The first step in the fabrication of solar cells is to choose the appropriate substrate according to the device requirements. By far, glass, for its rather low cost, transparency, and stability against the conditions of the fabrication process, is the most frequently-used substrate. However, its rigidity, weight, and thickness, does not take fully advantage of thin film solar cells, which are thin and flexible. Flexible glass, in turn, is extremely fragile.

The subject of fabricating solar cells on flexible substrates is not novel. In 1960s the first flexible solar cell arrays were fabricated for space power applications. These cells were made with thin silicon wafers (< 180 μm) assembled on plastic substrates to provide mechanical support. In 1976, Wronski *et al*. successfully fabricated a Pt/a-Si:H Schottky barrier solar cell on stainless steel (SS).[126] At the beginning of the 80s decade, Staebler *et al.* successfully fabricated a single junction *p-i-n* SCs on stainless steel (SS/*p-i-n*/ITO),[127] while Okinawa *et al.* produced SCs on polyimide substrates (PI/SS/*p-i-n*/ITO/Ag).[128] However, during the following decades, this subject was not explored in detail as the competition to maximize efficiency was hot, and new materials and multiple junctions were being developed. With the efficiency of silicon TFSC reaching a bottleneck in the last decade, attentions returned to reducing cost per Watt by using flexible substrates. The price of flexible substrates is generally cheaper than glass coated with TCO and its compatibility with R2R lowers the fabrication costs. The lightness of flexible substrates also leads to lower transportation costs.

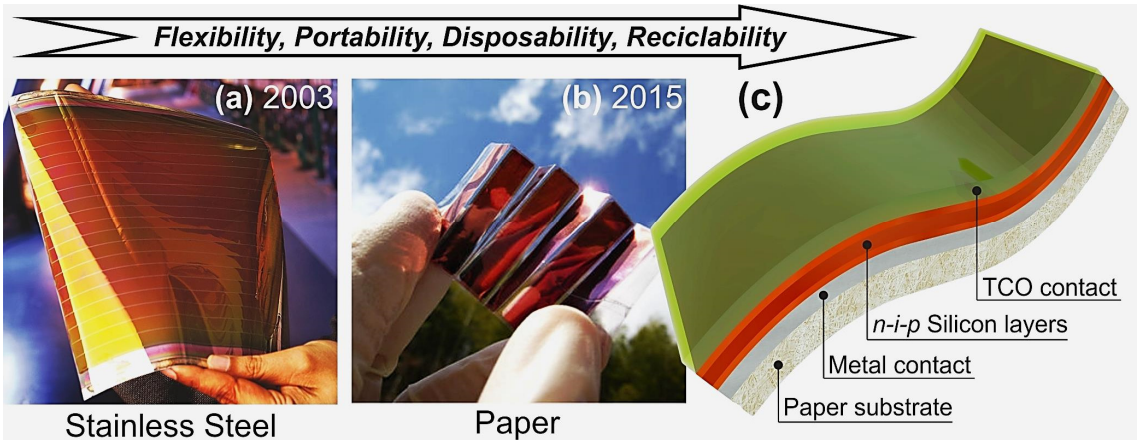

Figure 4–Summarized illustration of advances in TFSC technology implemented of flexible platforms. **(a)** Thin film silicon solar module produced by United Solar Ovonic in 2003, supported on a stainless steel foil, for air-space applications.[129] **(b)** Foldable OPV module fabricated in 2015using a transparent nanofiber paper as substrate, for lightweight portable electronic devices.[130] **(c)** Schematic drawing of the layer structure of a typical single-junction silicon solar cell deposited on paper substrate.[25,48]

For instance, nowadays, a-Si:H single junction TFSC have achieved, routinely, efficiencies above 8% on both stainless steel[131] (~9% for nc-Si:H[132] and up to 16.3% for triple junction – a-Si:H/a-SiGe:H/nc-Si:H,[133] see Figure 4a) and plastic/polymeric substrates.[134–136] Despite the advantages of these flexible substrates, cellulose-base substrates can be much cheaper, sustainable, and easily recyclable (see Figure 4b,c).[137] Furthermore, the mature coating technology of paper substrate can provide an opportunity for low cost R2R mass production.

3.2.1 Technical requirements of paper substrates

Cellulose-based substrates not only require optimized materials at lower substrate temperatures – when silicon thin films are directly deposited on the surface, such as in the case of PECVD fabrication – but also a set of morphologic properties (Table 2) need to be considered to assure performance and reproducibility:

a) ***Thermal stability.*** It is commonly known paper is sensible to temperature, thus the glass transition temperature (T_g) must be compatible with the maximum fabrication process temperature.[138] Another approach to solve the issue of high deposition temperature are the transfer printing methods, which use conventional substrates for fabrication and then transfer the TFSCs onto flexible substrates. The four major transfer printing methods are: transfer by sacrificial layers; transfer by porous Si layer; transfer by controlled crack; and transfer by water-assisted thin film delamination.[139]

b) ***Mechanical stability.*** Thermal mismatch between the substrate and the deposited layers may cause films to break in the event of a thermal cycling associated with fabrication. The coefficient of thermal expansion (CTE) quantifies the fractional increase of length per unit rise in temperature. Ideally, the tolerable mismatch between CTE of different layers, to avoid bending, rolling or film peeling, is $|\Delta CTE \cdot \Delta T| \leq 0.1 - 0.3\%$, where ΔCTE is the difference in coefficients of thermal expansion between substrate and device film, and ΔT is the temperature applied during fabrication.[18]

c) ***Surface smoothness.*** TFSCs are extremely sensitive to surface roughness, given their nanometer-scale thickness. To assure the proper functioning and prevent shunting issues, asperities and roughness over short distance must be avoided, but roughness over long distance is acceptable.

d) ***Optical transmittance.*** In the case of cellulose-based substrates, there should be enough mechanical support and resistance to the device (to prevent over bending). Such substrates are usually thick and opaque; when cellulose is used as coating or a light trapping structure, high transmittance and high haze factor are essential properties to maximize the efficiency of solar cells.

e) ***Chemical and barrier properties.*** To assure proper device function (namely, prevent degradation of active components, oxidation of electrodes, and delamination of layers) and reproducibility, a substrate should not release contaminants and be inert against process chemicals. The barrier property of a film is usually characterized by the steady state rate at which moisture (water vapor transmission rate, WVTR), or oxygen (oxygen transmission rate, OTR) permeates at a specific temperature and relative humidity over a given time period ($g \cdot m^{-2} \cdot day^{-1}$). Knowing that the encapsulant/substrate material for solar cells should have a WVTR below 10^{-4} $g \cdot m^{-2} \cdot day^{-1}$ and OTR < 10^{-3} $cm^3 \cdot m^{-2} \cdot day^{-1}$, one can see from **Table 2** polymers are far from ideal, and cellulose has the highest WVTR, worsened by its high content of water. Thus, to overcome the low barrier properties of these materials, additional barrier layers need to be added to the substrate to prevent the degradation of devices.

Table 2–Set of morphologic properties (glass transition temperature, T_g, coefficient of thermal expansion, CTE, and water vapor transmission rate, WVTR) of different solar cell substrates: aluminium (Al), stainless steel (SS), Corning® glass, polyethylene naphthalate (PEN), polyethylene terephthalate (PET), polyimide (PI), and cellulose.

	Al	**SS**	**Corning® Glass**	**PEN**	**PET**	**PI**	**Cellulose**
T_g (°C)	N/A	N/A	620[140]	120[82]	70[82]	270[82]	~80[138](a)
CTE($ppm \cdot K^{-1}$)	23 – 27[141]	9.3 – 17[142]	3.2 – 3.6[143]	16 – 20[18,144]	33[82]	8 – 20[82]	28 – 40[145]
WVTR ($g \cdot m^{-2} \cdot day^{-1}$) [test conditions](b)	~0.007 [9 µm; 38 °C; 90%][146]	~0	7×10^{-6}-5 $\times 10^{-5}$ [100 µm; 45 - 85°C; 85%][147] (c)	0.23 - 0.65 [200 µm; 70 °C; 25 - 80%][148]	1.1 - 11 [100 µm, 45 - 85°C, 85%][147]	2.4-54 [25 µm, 23°C, 50%][149]	435 - 1209 [120µm, 25°C, 33 - 75%][150] (d)

(a) Estimated value for microcrystalline cellulose powder(~20 µm, $\overline{M}_n \cong 74\,500$; from Sigma-Aldrich), with 70% crystallinity index and 5% water content.
(b) Test conditions [µm; °C; RH%]provide, respectively, the thickness of the material tested, the temperature, and the relative humidity.
(c) Value for the 100 µm thin Corning® Willow® Glass
(d) Value for the bleached Kraft paper (70 $g \cdot m^{-2}$) from the Limerick Pulp and Paper Centre

3.2.2 Thin film solar cells on paper substrates

To our knowledge, the first solar cell fabricated on a paper substrate was in 2005.[151] Lamprecht *et al*. produced an organic solar cell on common newspaper, coated with a Parylene C film (to

act as a chemical and moisture barrier) followed by a film of ORMOCER® to smooth the paper surface. The PCE was < 0.3% (J_{SC} = 0.22 mA·cm^{-2}, V_{OC} = 0.4 V, under 17 mW·cm^{-2} illumination from a halogen lamp). Despite the low efficiency, the interest in the field of solar cells on paper has seen a steady growth, with researchers successfully implementing different SC technologies to paper substrates. Different types of solar cells recently fabricated on distinct paper-based substrates are summarized in

Table **3**.

Like in the inception work of Lamprecht *et al*.,[151] following works on solar cells fabricated on regular paper require a coating layer, prior to the actual device fabrication. The high surface roughness and porosity of regular paper-based substrates affect the PCE, cell integration, and reproducibility, and in the case of solution-based PV, it also hinders the coating process and limits the surface wetting and coverage.[68]Hence the need to coat the paper-surface with an organic or resin paste, to achieve a porous-free and smooth surface.

Conventional methods of cast-coating aqueous dispersions of pigments and binders, and calendering are viable options.[152,153] In this way, planarized paper substrates with good barrier properties can be achieved. Nevertheless, Barr *et al*.[21] were also successful in coating multiple paper substrates (e.g. tracing, copy, and tissue paper) with PEDOT by oxidative chemical vapor deposition (OCVD). In this method, the PEDOT thin film is formed by simultaneously exposing the monomer (EDOT) and oxidant ($FeCl_3$) reactants to vapor-phase at low substrate temperatures (20 °C to 100 °C) and moderate vacuum (~0.1 Torr).[21]

There are few examples of paper coated with recyclable coatings (e.g. starch, latex, mineral pigments) and used as substrate for electronic devices,[154,155] and even less when applied in PV devices.[156] The majority are polymers, like polyethylene (PE),[157] wax/glue (see Figure 5),[91] or metal pastes.[47,158,159] Despite these paper coatings could compromise the low cost and recyclability,[153] they might still be acceptable for relatively high-value electronic applications that require relatively expensive materials, multiple processing steps, and encapsulation.[160] Moreover, the higher quality surfaces they produce yield solar cells with higher efficiencies; while metal paste or PEDOT coatings,[161,162]in addition to the planarization, can function as a thin, flexible and conductive electrode (see Figure 5).[91,161]

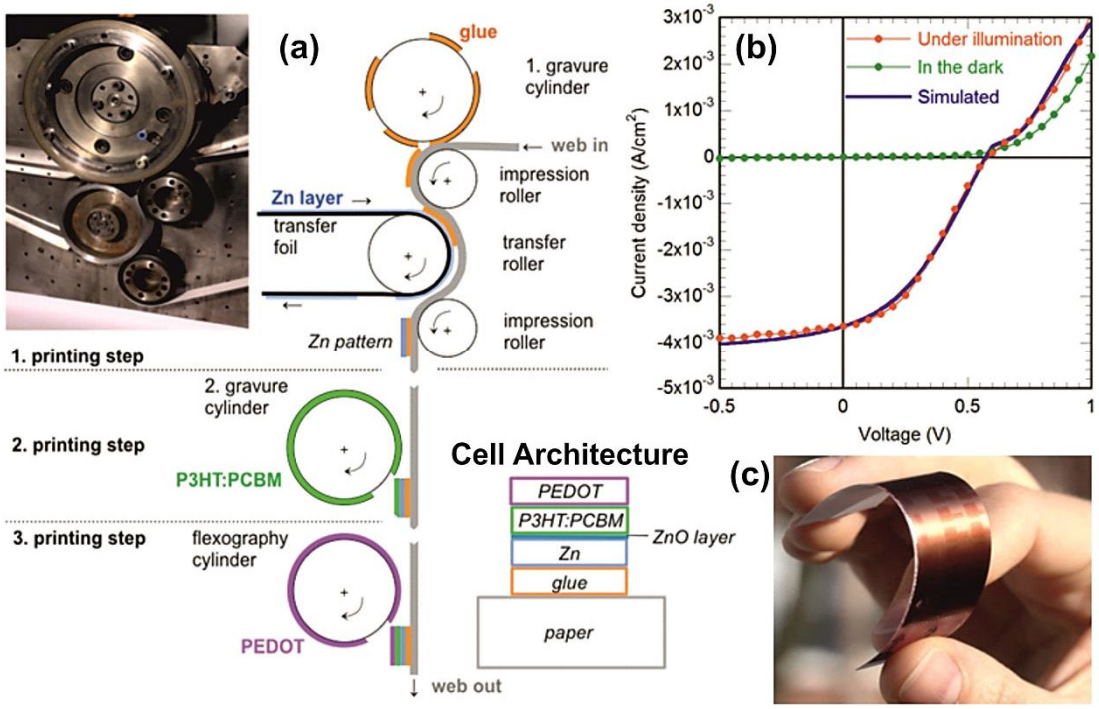

Figure 5 – a) Flexographic printing process and resulting layer architecture of an OPV solar cell. **b)** Current density (J) vs. voltage (V) characteristics of the cell under dark or under a 60 mW·cm^{-2} illumination level fitted with a macroscopic device simulation program. **c)** Photograph of the printed solar cells on paper.[91]Reprinted with permission of Wiley.

An interesting alternative paper conductive coating is reported by Dasari *et al*.[163] They coated a regular paper with graphite obtained by gently rubbing a H2B pencil on the paper and fabricated a QDPV with a PCE of ~1.80% (under 130 mW·cm^{-2} illumination).

In the particular case of amorphous silicon solar cells, given the silicon layer thickness in the order of hundreds of nanometers and the involved deposition techniques, the surface of the substrate must be totally free of defects, hence there are very few reports on the successful fabrication of solar cells on paper. The first published works on a-Si:H solar cells on paper (see Figure 4c), from Vicente *et al*.[25] and Águas *et al*.[48] explore two different coated paper-based substrates. In the work of Vicente *et al*. the selected substrate is the liquid-packaging cardboard (LPC) commonly use in the food and beverage industry (see Figure 6). This packaging cardboard is coated with a low density polyethylene (LDPE) layer and an aluminium (Al) foil, which provides a porous-free surface ideal for solar cell deposition and at the same time functions as back contact.[25] In turn, Águas *et al*. selected a paper substrate coated with a hydrophilic mesoporous layer. Upon heating, the surface slightly modifies, becoming denser, and reducing the density and size of the mesopores, which results in a smoother and compact surface (root mean square (RMS) roughness of 9.42 nm), compatible with silicon thin film deposition.[48] Recently, Smeets*et al*.[164] and van der Werf *et al*.[165] applied an UV curable acrylate lacquer, not only to planarize and cover the porosity of the paper substrate, but also to nanoimprint light trapping structures, by UV nanoimprint lithography. The solar cells obtained by van der Werf *et al*.have the highest reported PCE, reaching 6.70% (J_{SC} = 13.9 mA·cm^{-2}, V_{OC} = 0.90 V, and FF = 53.3% under AM 1.5G illumination).

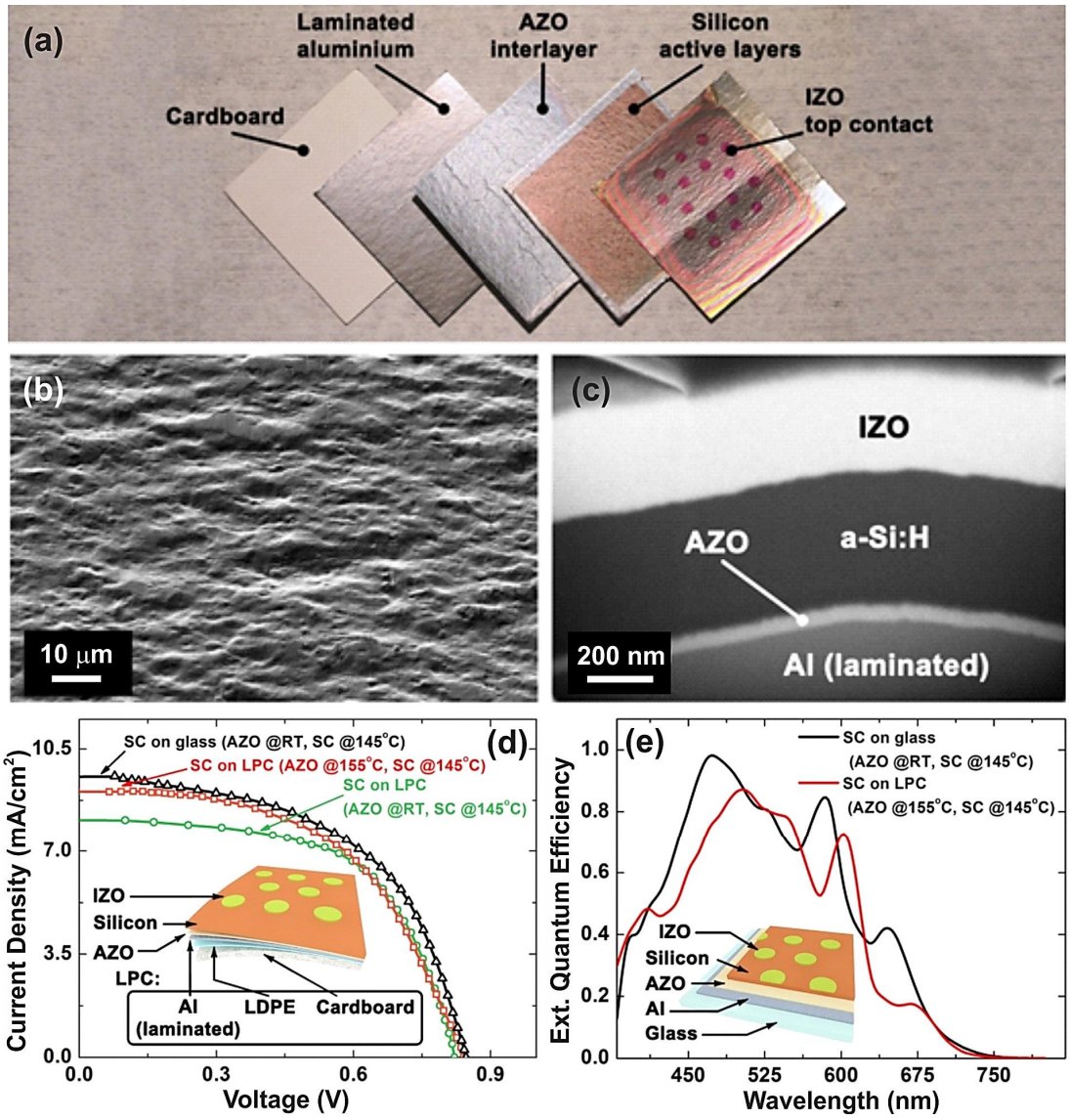

Figure 6 - a) Photograph of the different layers composing the TFSC, starting with the cardboard paper, the Al foil (acting as back contact) laminated with a low-density polyethylene (LDPE) layer, the 60 nm of aluminium zinc oxide (AZO) interlayer (~60 nm), the *n–i–p*a-Si layers (~350 nm) and the indium zinc oxide(IZO)front contact (~300 nm).**b)** SEM of the Al-coated cardboard surface, revealing a highly rough but defect-free surface. **c)** cross-cut SEM-FIB image depicting the solar cell layers. **d, e)**Performance of the a-Si:H solar cells deposited on glass and LPC characterized by the *J(V)* curves (d) and External Quantum Efficiency (EQE) spectra (e). For the LPC substrate, two process temperatures were used for the AZO interlayer (room temperature and 155 ºC), while the Si layers were always deposited at 145 ºC. The inset in (d) shows the device structure used, wherein the LPC comprises the 3 layers: cardboard, LDPE and laminated Al. The inset in (e) shows the layer structure of the glass reference cell.[25]

In order to avoid the need of a pre-coating, to address the challenge of micro-size porosity and surface roughness, and for applications that require very thin/transparent substrates, nanocellulose-based materials can be of high interest. The diameter of some nanocellulose fibers can be as low as 4 nm, which gives paper a high optical transparency and excellent light scattering, or haze. Thus, nanocellulose can be an excellent candidate for production of ultra-thin paper solar cells. Moreover, when using paper as superstrate, when light transverses the

cellulose layer it is scattered, which enhances the optical path and increases the light absorption probability.[38]

The first example of a solar cell deposited on nanocellulose-based substrates is in the work of Hu *et al.*[38] Their work describes the fabrication process of organic solar cells on cellulose nanofibrillated (CNF) with PCE of 0.40%. The substrate was not pre-coated and an ITO electrode was directly deposited, by radio frequency (RF) magnetron sputtering, on CNF, with resistivity of 12 $\Omega \cdot sq^{-1}$, which is comparable with plastic substrates.[38] Subsequent works on nanocellulose-based substrates mainly relate to organic solar cells.[19,41,130,166] Of these, we highlight the work of Zhou *et al.*,[166] which reports the highest PCE for a nanocellulose-based OPV of 4% (J_{SC} = 7.8 mA·cm^{-2}, V_{OC} = 0.81 V, and FF = 64.0% under AM 1.5G illumination).A level of performance identical to that of solar cells fabricated on polyethersulfone (PES) substrates. To achieve this efficiency they used a cellulose nanocrystalline substrate (CNC) and employed a new device structure wherein polyethylenimine-modified Ag is used as the bottom electron-collecting electrode and the high-conductive and transparent PEDOT:PSS is used as the semitransparent top hole-collecting electrode. Another important development is the fact that the PEDOT:PSS electrode was first deposited onto a poly(dimethylsiloxane) (PDMS) stamp and then transferred by lamination onto the photoactive layer (P3HT:indene-C_{60} bisadduct, P3HT:ICBA). This method prevented the damage to the CNC substrate that the aqueous processing of PEDOT:PSS causes.[166]

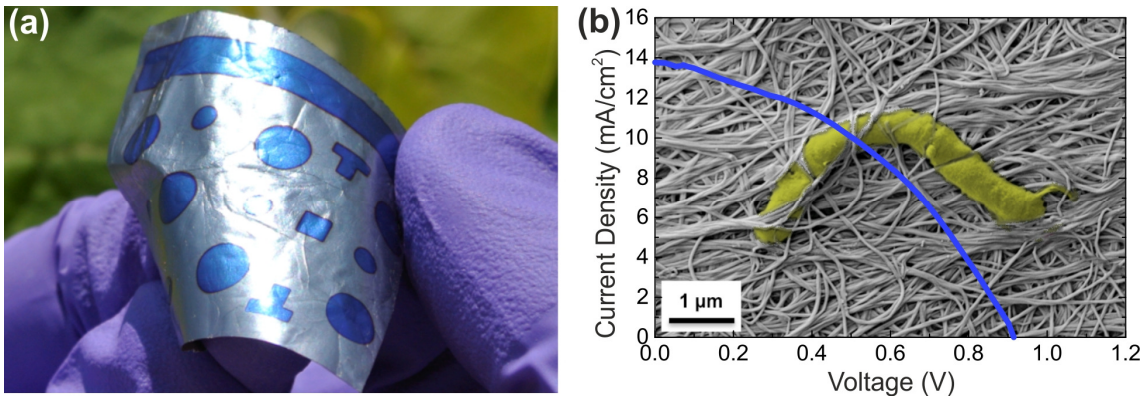

Figure 7 –(a) Photograph of a set of thin film a-Si:H solar cells deposited on a transparent bacterial nanocellullose substrate. **(b)***J(V)* characteristic of a 5.1% efficient solar cell deposited on the substrate. The background SEM image shows a *Gluconacetobacter xylinum*bacteria entangled within the nanocellulose network.[101] Reprinted with permission of Elsevier.

Nanocellulose-based substrates were also successfully used in the fabrication of a-Si:H solar cells[101] and perovskites.[167] In the case of the reported a-Si:H solar cells (PCE = 5.10%, see Figure 7), the substrate selected was the bacterial cellulose, which given its high smooth surface (RMS roughness ~60 nm) it allowed the direct deposition of a porous-free aluminium back contact.[101] Regarding the fabrication of perovskites on cellulose nanofibrillated, Jung *et al.* achieved a PCE of 6.37% (J_{SC} = 15.4 mA·cm^{-2}, V_{OC} = 0.86 V, and FF = 48.2% under AM 1.5G illumination), which is highest PCE achieved for solar cells on nanocellulose-based substrates. Moreover, they showed that by changing the mixture of halide perovskite ($CH_3NH_3Pb(I_{1-x}Br_x)_3$, where x = 0.1 – 0.15) different PV coloration could be obtained (see Figure 8).[167]

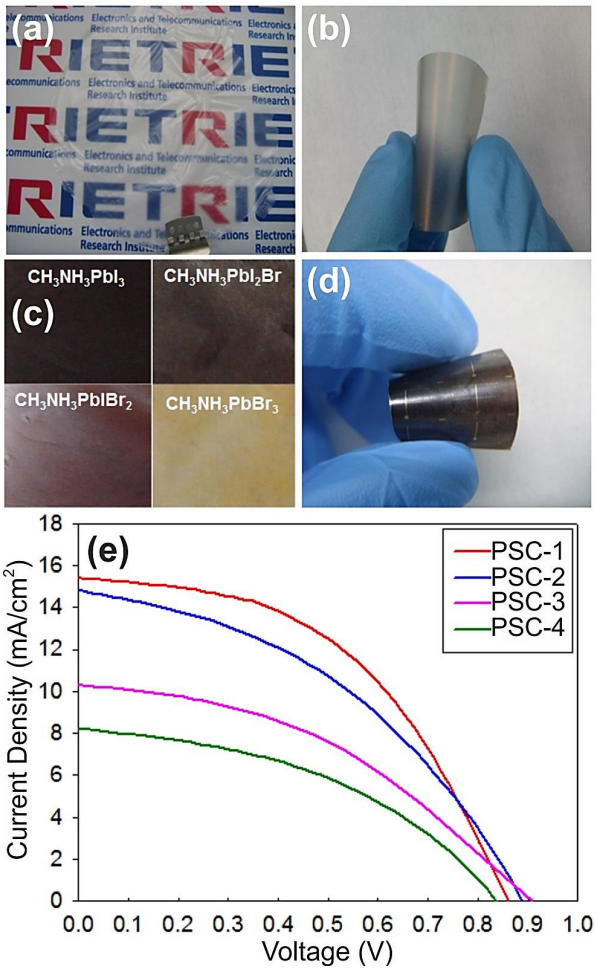

Figure 8 – Perovskite solar cells (PSC) fabricated on transparent nano-fibrillated cellulose substrates (*nanopaper*), with the structure: nanopaper/dielectric-metal-dielectric (DMD) structure/Zinc oxide (ZnO)/$CH_3NH_3PbI_3$/Spiro-OMeTAD/Au.**a)** Photograph of transparent hydrophobic-treated nanopaper and **b)** nanopaper with the conductive electrode (TiO_X/ag/TiO_X, DMD). **c)**The color of the nanopaper changes according to the Perovskite ($CH_3NH_3PbI_{3-x}Br_x$) composition.**d)** Perovskite (with composition $CH_3NH_3PbI_3$) cells supported on the nanopaper substrate. **e)***J(V)* characteristics of the different PSCs on nanopaper, reaching 6.37% efficiency (PSC-1).[167] Reprinted with permission of Elsevier.

Table 3summarizes the different types of solar cells fabricated on diverse cellulose-based substrates, from 2005 to 2017.

Table 3 - Comparison of different cellulose-based materials used as substrates for solar cells.OPV – organic photovoltaic, DSSC – dye-sensitized solar cell, QDPV – quantum dots photovoltaic, a-Si:H – thin film hydrogenated solar cell. COP – common office paper (general term to described common paper with grammage ~80 – 120 $g \cdot m^{-2}$), CNF –cellulose nanofibrillated, CNC – cellulose nanocrystalline, LPC – liquid packaging cardboard (general term to describe paper commonly used in the food and beverage packaging industry), BC – bacterial cellulose. “Cardboard” describes a class of paper made from pressed cellulose fibers with grammage exceeding 200 $g \cdot m^{-2}$ or 300 µm,

whereas "gloss paper" describes a type of common office paper commercially available with a coating layer for high quality printing. SC characteristics refer to 100 mW·cm^{-2}AM1.5G illumination, unless stated otherwise in the efficiency column. N/D stands for "not disclosed", or that data is not explicitly stated.

SC type	Cellulose type	Coating/contact layer	J_{SC} (mA·cm^{-2})	V_{OC} (V)	FF (%)	Efficiency (%)	Year[Ref]
OPV	Newspaper	Parylene + ORMOCER®	0.22	0.40	N/D	< 0.30 (17 mW·cm^{-2})	2005[151]
	COP	Amylum film	0.10	0.39	33	0.13‰	2010[156]
	Trancing (best), COP, tissue	PEDOT	~9	~0.27	N/D	N/D (0.5 W·cm^{-2})	2011[21]
	Gloss paper	Glue+Zn	3.64	0.59	37	1.31	2011[91]
	LPC	Polyethylene+ hcPEDOT:PSS (anode)	2.24	0.42	43	0.40	2011[157]
	CNF	ITO	2.41	0.38	23	≤ 0.40	2013[38]
	CNC	Ag+PEIE	7.50	0.65	54	2.70	2013[19]
	CNC	Ag+PEI	7.80	0.81	64	4.00	2014[166]
	Gloss paper	Glue+polypropylene+Zn	10.60	0.71	55	4.10 (80 mW·cm^{-2})	2014[47]
	CNF	Ag nanowire suspension	9.58	~0.74	N/D	3.20	2015[130]
	CNC	Ag+AZO	3.50	0.90	40	1.40	2016[41]
	CNF	Ag+AZO	2.00	0.70	0.30	0.50	2016[41]
DSSC	Cardboard	Ni	6.70	0.56	33	1.21	2011[158]
	Glass paper (used as substrate and electrolyte medium)	Pt (electrocatalytic); Ru-complex dye-loaded TiO_2 (photoelectrode)	3.90	0.68	76	2.05	2012[168]
	Manila paper	Ni	7.97	0.65	56	2.90	2012[159]
	Carbon fiber composite	PEDOT	13.09	0.72	63	6.13	2016[161]
	COP	Graphene dots+PEDOT:PSS	12.08	0.70	58	4.91	2017[162]
QDPV	COP	Graphite	2.30	0.78	N/D	1.80 (0.13 W·cm^{-2})	2016[163]
Perovskite	CNF (hydrophobic treated)	TiO_2+Ag+TiO_2 (DMD structure)	15.37	0.86	48	6.37	2016[167]
a-Si:H	LPC	Polyethylene+Al	9.05	0.84	53.7	4.08	2015[25]
	Gloss paper	Hydrophilic mesoporous material+Al	10.19	0.82	40.7	3.40	2015[48]
	COP	UV cured acrylate lacquer+Ag	13.90	0.90	53.3	6.70	2015[165]
	BC	Al	~13.80	~0.91	~40.6	5.10	2016[101]
	Gloss paper	Hydrophilic mesoporous material+UV cured photoresist+Ag	13.50	0.86	47.6	5.50	2017[164]

3.3 Improving thin film solar cells with light management

Despite the considerable number of technological efforts described in the previous section to produce high performing TFSCs on flexible paper platforms, the best efficiencies attained so far are, in most cases, still below the record ones achieved on rigid glass substrates. The main reason is the low mechanical robustness of the TFSC structures when mounted on the rough paper surface and upon bending, resulting in film cracking, peeling and general increase of defect density. These aspects can be much improved by further reducing the cells thickness, since:[169,170]

1. The flexural rigidity of a film increases proportionally to the cube of its thickness;
2. The peak strains associated with bending are proportional to the thickness;

3. The ability to heterogeneously integrate PV films on polymeric substrates (e.g. paper,[48] plastics[171]), improves since the energy release rates for interface failure reduce linearly with thickness.

Therefore, highly-bendable TFSC require ultra-thin thicknesses in order to enable their applicability in the flexible substrates of consumer-oriented products (e.g. wearable PV, solar-powered intelligent packaging,[25] portable/disposable electronics, building-integrated PV),[172] with efficiencies and stabilities comparable to state-of-art rigid devices. Besides, lowering the cells' thickness brings additional advantages as lower cost, lighter weight and faster fabrication, which are crucial at industrial level allowing, for instance, large-scale roll-to-roll manufacturing. Moreover, thickness reduction can lead to higher open-circuit voltages (and consequently efficiencies) due to lower bulk recombination.[173,174]

In this context, the development of optical strategies to boost the broadband light absorption in TFSC, while allowing the reduction of their absorber thickness, is becoming of increasing importance.[175] Many ideas and research efforts have been conducted since the turn of the century to develop light-trapping (LT) solutions that allow the engineering of optically-thicker but physically-thinner devices, by amplifying their photocurrent generation and, consequently, efficiency.[174–177] Conventional LT strategies, as those applied in wafer-based devices that rely on textured rear/front surfaces, which provide anti-reflection and scattering,[48,177–179] can be detrimental to thin film PV, since the increased roughness (hence surface area) leads to higher defect density in the PV material, which deteriorate the cells' electrical transport via the increase of charge carrier trapping and recombination. Suitable alternatives for thin film PV are, for instance, plasmonic back reflectors (PBR) or wave-optical dielectric front structures, not only due to their proven effectiveness but mainly because these LT structures are composed of arrays of nano/micro-particles that can be applied in any type of PV device by low-temperature (hence *paper-friendly*) patterning processes.

The plasmonic back-reflector (PBR) structure makes use of the intense light scattered from metal nanoparticles (NPs) sustaining surface plasmons, such as those resulting from monodisperse arrays of silver (Ag) or gold (Au) NPs.[180] The conventional technique employed to fabricate such NP structures is via ultra-thin film annealing, where a metallic precursor layer transforms into a drop-like NP array by a solid-state dewetting mechanism.[181–183] Nevertheless, the high temperatures (400-500ºC) required for the annealing treatment make this technique incompatible with the most common flexible substrates (as paper or PEN/PET) used in thin film PV, as flexible materials can only withstand temperatures up to ~150-200 ºC without degradation. An alternative low-temperature (<120 ºC) approach was demonstrated by Mendes *et al.*[184,185] who developed a wet coating method to precisely pattern arrays of spherical Au NP colloids, with more appropriate dimensions for pronounced far-field scattering, on the rear contact of any solar cell (see Figure 9a-c). Nevertheless, metallic NPs can present significant parasitic absorption in the NIR range,[180] as discussed by Schuster *et al.*[186] In this paper, the authors established a comparison between the LT efficiency in thin film solar cells produced by PBRs and that produced by dielectric diffractive nanostructures placed at the front, in an identical absorber configuration consisting in 240 nm thick amorphous silicon layers. Both LT strategies show pronounced enhancement of the absorption in the red/NIR range, but parasitic absorption increases in the metal nanoparticles for the longer wavelengths, which reduces the overall performance of the plasmonic relative to the dielectric approach. This is clearly seen in the absorption measurements showed in Figure 9d.

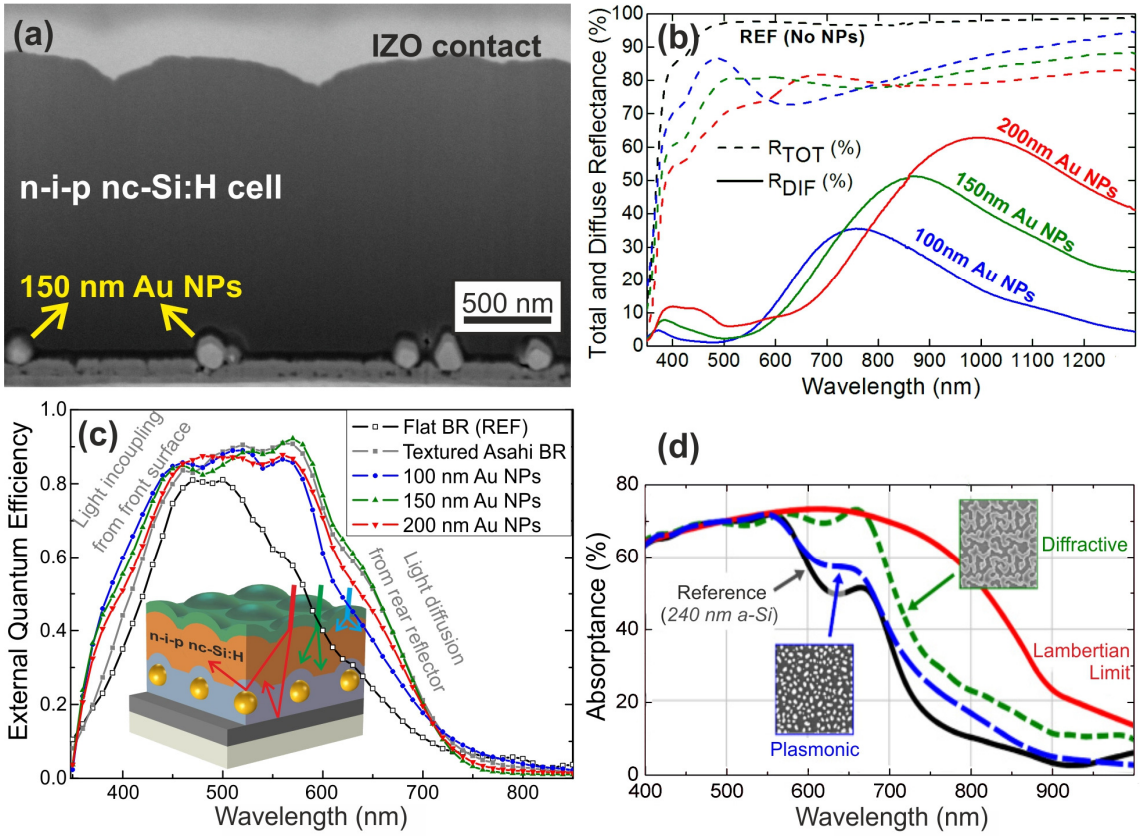

Figure 9- a) SEM picture of a thin film Si solar cell cross-section. The cell is deposited on a colloidal PBR containing 150 nm Au nanoparticles. **b)** Total (*dashed lines*) and diffuse (*solid lines*) reflectance of PBR structures (120 nm Ag/50 nm AZO/Au NPs/40 nm AZO) made with colloidal NPs of different diameters (100, 150 and 200 nm). The total reflectance of a reference BR (*black dashed line*) without NPs is shown for comparison. **c)** EQE curves of the *n-i-p* Si solar cells, like the one in a), fabricated on the three colloidal PBRs, with 100, 150 and 200 nm diameter Au NPs. The EQE curves corresponding to reference cells with a flat (REF, *open symbols*) and an Asahi textured (*black closed symbols*) back reflector are shown for comparison.[185] **d)** Comparison of absorption in a thin film Si layer enhanced by either a PBR or a diffractive quasi-random front structure. The plasmonic structure (*blue dashed line*) can enhance the absorption of an unstructured a-Si slab (*black solid line*) by 7%, while the diffractive structure (*green dashed line*) is able to do so by 25%. The red solid line refers to the theoretical absorption of the Lambertian backscattered light.[186] Reproduced with permission of OSA Publishing.

In view of that, dielectric-based structures applied in the cell's front are nowadays considered preferential LT approaches relative to PBRs.[25,175,187] Dielectric structures provide the highest LT effects in SC when their dimensions are comparable to those of the illuminating wavelengths, thus they operate in the so-called regime of *wave-optics* (sometimes simply called *photonics*).[188,189] An important advantage of dielectric materials, relative to the previous metallic ones, is that they can be lossless (non-absorbing) in most solar spectrum. Therefore, the photonic elements can be incorporated on the top (front surface) of completed cells with flat layers. In this way, the structures do not increase the roughness neither the surface area of the cell layers; and so, do not degrade the cells' electric performance via increase of carrier recombination.

High refractive index media are often preferable for front-located LT structures,[190–192] since they provide the best light in coupling (i.e. minimum reflection) towards the absorber medium when their refractive index is comparable to that of such medium (e.g. Si with n~4).[189]

Regarding the preferential geometry for the LT structures, it strongly depends on the refractive indices of both the photonic and absorbing materials of the cells as reported in the work of Mendes *et al.*[193] (see Figure 10a). The physical mechanisms responsible for such enhancement, i.e. anti-reflection and scattering effects, are schematized in the diagram of Figure 10b, providing a deeper understanding of the advantageous characteristics of the optimized geometries. The authors concluded that optimized structures, composed of TiO_2 half-prolates patterned on the cells' top surface, can yield two times higher photocurrent (up to 32.5 mA/cm^2 in 1.5 μm thick Si layer) than the same flat devices without an anti-reflection coating (ARC) or any LT scheme.

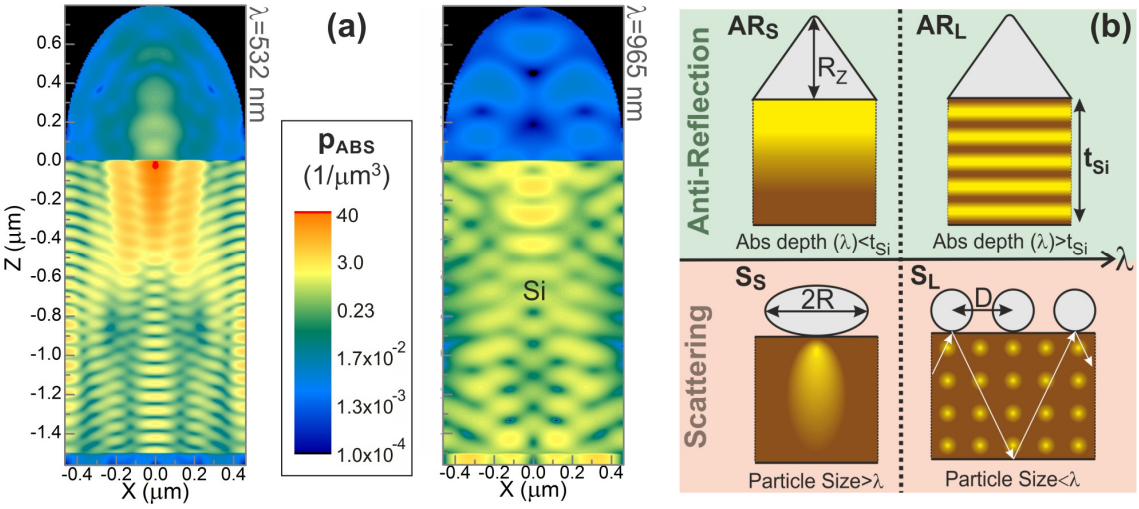

Figure 10 - a) Log scale profiles of the absorption density (p_{ABS}) along a cross section of a thin film Si solar cell patterned with an array of TiO_2 half-prolates on the cell front. The profiles are shown within a unit cell of the array and for two illumination wavelengths (λ) associated with peaks in the absorption spectrum of the structure. **b)** Illustrative diagram of the E-field enhancement profiles resulting from the LT mechanisms generated by dielectric front structures in distinct spectral ranges. The main parameters influencing the absorption enhancement are indicated by the black arrows in each case.[193] Reprinted with permission from Elsevier.

Following this theoretical work, Sanchez-Sobrado *et al.*[192] developed a low-cost soft-lithography method, known as colloidal-lithography (CL), to fabricate the TiO_2-based micro-structures (Figure 11). The method allows forming nano/micron-scale structures with a wide range of materials and is compatible with the PV industry scalability requirements, employing the 4 main steps illustrated in Figure 11a:i) deposition of periodic close-packed arrays of polystyrene colloids which act as the mask, ii) shaping the particles and increasing their spacing via dry etching, iii) infiltration of TiO_2 in the inter-particles spacing and iv) removal of the polystyrene particles to leave only the structured TiO_2 layer. The resultant array of wavelength-sized features acts as a nanostructured high-index anti-reflection coating, which not only suppress the reflected light at short wavelengths but also increases the optical path length of the longer wavelengths, via light scattering, within the absorber. The measured optical absorptance of the a-Si sample with and without the TiO_2 nanostructure (NS) is plotted in Figure 11b and a significant 27.3% enhancement in the cells photocurrent is anticipated with these TiO_2 structures, relative that attained with a conventional indium zinc oxide (IZO) ARC.

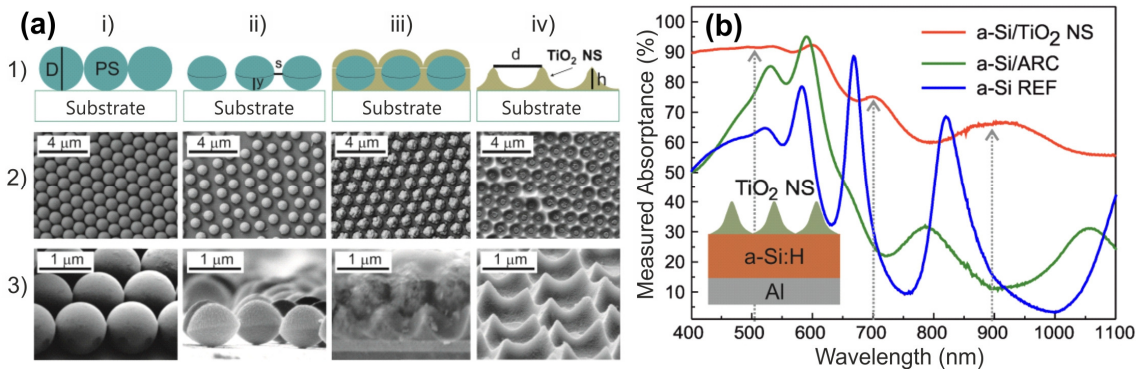

Figure 11- a) Schematic drawings (1) and SEM pictures of the top views (2) and tilted views (3) of the samples obtained after the different steps of the TiO_2 nanostructure (NS) construction *via* colloidal lithography. **b)** Measured absorptance of the samples with a base structure, composed of a rear mirror Al and an a-Si:H absorber, coated with distinct top layers: none (REF), 80 nm IZO (ARC) and the TiO_2 nanostructures (NS) produced by colloidal lithography.[192]

Although the method developed by Sanchez-Sobrado *et al.* was tested with SC structures deposited on glass, it can be straightforwardly applied with paper-based substrates since it involves only low-temperature (<100 ºC) steps and the wet-coating technique used to deposit the colloids can be easily adapted to prevent immersion of the substrate, for instance employing doctor blade surface patterning.

3.3.1 Light trapping with cellulose-based materials

The previous LT schemes based in particle scattering are attractive solutions for the majority of TFSC technologies. However, the non-uniform distribution of particles in the cell, or their aggregation, are practical obstacles that can hinder the overall LT performance of the array.[194]To overcome such challenges, an alternative LT approach can rely in the use of transparent substrates or encapsulates with built-in high transmission and haze, that effectively enable light coupling and show broadband and angle insensitive responses.[22] This is where paper-based materials can have an attractive LT potential, as substrates/encapsulates with a desirable combination of these properties. The enhancement of light scattering is directly linked to the haze property, which is defined as the percentage of light transmitted through a specimen that deviates the incident light beam by a scattering of more than 2.5° angle on average.[195] As previously mentioned, maximizing light scattering into solar cells enhances the absorption by increasing the path length of light in the active layer, resulting in increased photocurrent and thereby efficiency.[194]

Paper scatters light heavily due to its porous structure and the random cellulose matrix. Fine tuning the size and shape of cellulose fibers by chemical and mechanical treatments can result in different optical properties with broad angle absorption and angle scattering; therefore, more light absorbed or emitted.[22] Transparent anisotropic paper can be produced following a "top-down" process straight from delignified natural wood,[196] whereas opaque paper can be directly turned into a transparent substrate via polymer impregnation.[22] Such transparent papers can achieve transmittances up to 90% – 96% and haze factors about 80% – 90%.[30,167,196] The transparent paper (with n~1.5) reduces the index contrast between air and the semiconducting absorber layer, which ultimately increases light absorption within the solar cell.[197]

Furthermore, the surface roughness of the paper leads to angle insensitive behavior over all wavelengths, hence the interest of considering cellulose-based materials as a potential candidate for the next generation anti-reflection coatings (ARC) compatible with green, disposable optoelectronic devices.[197]

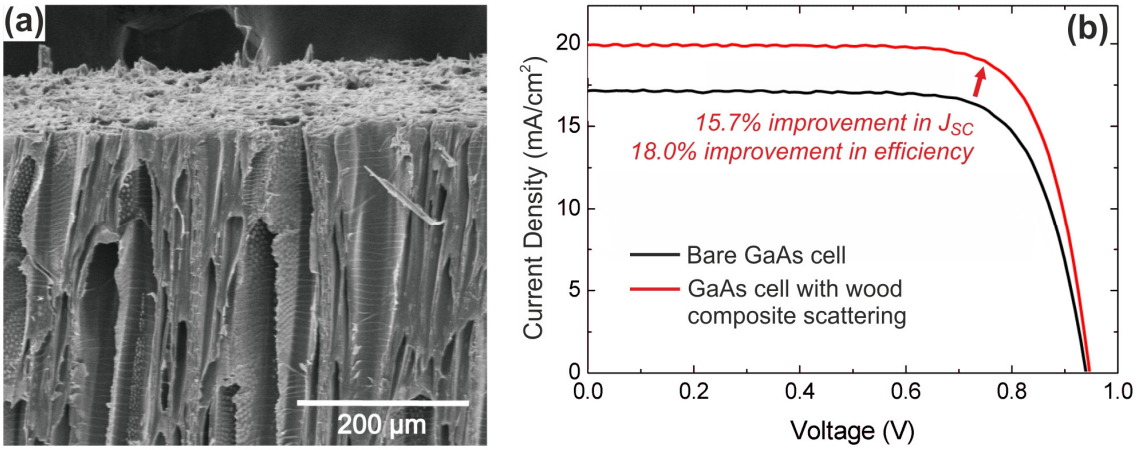

Figure 12 - a) SEM cross section of a wood microstructured ARC. **b)** *J(V)* curves for both bare GaAs cell (*black*) and the GaAs cell with the light trapping wood coating (*red*).[30] Reprinted with permission of Elsevier.

A significant share of publications regarding cellulose-based coatings with LT properties focuses on GaAs solar cells.[22,30,196,197] For instance, the work of Zhu *et al.*[30] developed mesoporous wood-based LT structures (see Figure 12) displaying a high optical transmittance and, at the same time, high haze in a broad wavelength range (400-1100 nm). These transparent wood composites with cellulose nanofibers can substantially improve the overall conversion efficiency by as much as 18% when simply coated over a GaAs thin film solar cell. Gains of ~13% in current density of a thin Si wafer coated with nanofibrillated cellulose have also been reported,[99] as well as improvements for Perovskite solar cells.[198]

Table 4 summarizes the literature on the subject of solar cells coated with cellulose-based materials, either for LT or simply as sealants. As expected, the highest improvement due to the application of the different types of "photonic-paper" is seen in the current density, with gains between 13% to 20%, which leads to efficiency enhancements as high as ~24%.[197]

Table 4 - Comparison of solar cell properties with and without different cellulose-based materials used as anti-reflection coating, light trapping, or encapsulation/sealant. CNF – cellulose nanofibrillated, EC – ethyl cellulose, BC – bacterial cellulose, OSC – organic solar cells, DSSC – dye-sensitized solar cells, GaAs – thin film gallium arsenide, c-Si – crystalline silicon. SC characteristics refer to 100 mW·cm^{-2} AM1.5G illumination, unless stated otherwise in the efficiency column. N/D stands for "not disclosed", or that data is not explicitly stated.

SC type	Cellulose type	Cellulose function	J_{SC} (mA·cm^{-2}) | Δ (%)[a]	V_{OC} (V) | Δ (%)[a]	FF % | Δ (%)[a]	η % | Δ (%)[a]	Year[Ref]
OSC	CNF	Light trapping	1.46 | 7.4	0.89 | 1.1	N/D	5.88 | 10.1 (13 mW·cm^{-2})	2014[199]
	Gloss paper	Back reflector	7.70 | 46.7	0.81 | 5.2	57 | 1.8	3.54 | 55.3	2015[200]
DSSC	EC + glass frit + terpineol	Sealant film	N/D	N/D	N/D	N/D	2012[201]

	(ratio 1:5:4) CNF dispersed in polyester polyurethane	Sealant film	~6.22 | ~1.8	~0.76 | ~2.7	N/D	3.19 | 2.9	2017[202]
	BC dispersed in polyester polyurethane	Sealant film	~6.22 | ~1.8	~0.77 | ~4.1	N/D	3.25 | 4.8	2017[202]
GaAs	CNF	Anti-reflection coating	22.49 | 20.5	1.00 | 0.2	74.4 | 2.6	16.79 | 23.9	2014[197]
	Delignified basswood infiltrated with PVP	Anti-reflection coating + Light trapping	19.78 | 15.7	0.97 | 0.6	76.0 | 1.2	14.41 | 18.0	2016[30]
	COP infiltrated with epoxy resin	Light trapping	14.4 | 13.4	~0.95 | ~0	N/D	N/D | ~15.0	2016[22]
	Anisotropic delignified basswood	Light trapping	20.17 | 18.1	0.91 | 0.3	76.1 | 1.3	13.94 | 14.2	2017[196]
c-Si	CNF	Light trapping	~13% [(b)]	N/D	N/D	N/D	2015[99]

[(a)]The given solar cell parameters correspond to the solar cell with the cellulose layer. Relative change of each solar cell parameter is given by:
$\Delta = \frac{\text{coated-uncoated}}{\text{uncoated}} \times 100(\%)$, where "uncoated" stands for the solar cell parameter without the cellulose layer, and "coated" corresponds to the solar cell parameter with the cellulose layer.

[(b)]Simulated value according to the absorption spectra of 10 μmthick and smooth Si wafer, with and without the CNF coating

Apart from their LT capabilities, cellulose-based materials can also be functionalized to strengthen their thermal, mechanical and barrier properties, in order to improve their role as encapsulates for solar cells. Chen *et al.* reported for the first time, in 2012, the enhancement that a cellulose-based coating can achieve.[201] They prepared a glass frit sealant mixed with terpineol and ethyl cellulose with a 5:4:1 ratio and obtained a uniform sealant film free of porosity and cracks. When used to seal a DSSC it retained 80% of the initial PCE, and the electrolyte leakage rate was 0.12% after 800 hours of tracking test at room temperature.[201] Yuwawech *et al*. demonstrated the enhancement of a DSSC encapsulated with EVA (ethylene vinyl acetate copolymer) reinforced with bacterial cellulose (BC).[37] The introduction of BC enhanced the thermal, mechanical and barrier properties of EVA film, and delayed the degradation of the EVA film, via deacetylation, without compromising the transparency (> 75%) of the EVA film.[37] In another work, Yuwawech *et al.*[37] enhanced the barrier properties of DSSC with polymer composites of polyurethane mixed with esterifies nanocellulose composites (PU:BC, or PU:CNF) as reinforcing agents. By encapsulating the DSSC with the PU:Nanocellulose composites, the lifetime of the devices could be extended by more than 336 hours without PCE loss, whereas the WVTR dropped by 34% – 56%.[37] Besides DSSC, these solutions could also find important application in the emerging field of Perovskites solar cells, as this technology requires highly effective encapsulation to prevent their strong degradation upon exposure to ambient conditions.

3.4 Paper as binder for nanostructures

In addition to the use of paper-based compounds as substrates, encapsulants or light trapping media, another extensively-studied set of PV-related applications of cellulose materials is concerned with their use as scaffolds/binder to incorporate/immobilize different types of photo-

active nanostructures that assist in the sunlight-to-electricity conversion mechanism. This section reviews some of the core advances in this class of applications, which historically were actually the first implementations of cellulose materials in the fields of opto-electronics. With the rise of nanotechnology, the use of paper matrices for incorporation and/or immobilization of nanostructures has been progressing at a rapid pace.[49] Among the numerous benefits of paper matrices are the important advantages of reducing the dependency on petrochemical-based polymers, its biodegradability, cost effectiveness, and abundance.[45,203,204] The work of Matsubara *et al*. in 1995 marks the emergence of the research area of incorporation of nanostructures in paper matrices by a standard hand sheet making method.[205] In this work, TiO_2-containing paper sheets were prepared by dispersing TiO_2 powder in paper pulp, which led to a highly efficient photocatalyst.

In the third generation thin film PV field, metal oxide nanostructures (e.g. TiO_2, ZnO, Fe_2O_3/Fe_3O_4, CuO, ITO, SiO_2, MoO_2, and WO_3) can play a central role as photoactive elements. Nonetheless, these nanostructures have also shown great potential also in other fields like piezoelectric, magnetic, gas sensors, and bio-devices due to their unique optical, electronic, conductivity, catalytic and antimicrobial properties.[45]To properly disperse metal oxide nanostructures, or fabricate mesoporous films with intended properties and tailored to the chosen coating/printing method, the addition of a suitable surfactant or binder to the precursor paste, such as cellulose, can be crucial. Independently of the role played by the nanostructures, it is well known that the morphology, film thickness, porosity, and surface features (homogeneity, presence of cracks or aggregates, etc.) will significantly affect the performance, hence the fabrication method developed is essential to achieve solar cells with high efficiency.[206]

TiO_2 is by far the most studied metal oxide. Since Fujishima and Honda discovered in 1972 that TiO_2 can be used for water photolysis under UV light irradiation,[207,208] it has received great attention.[32] The significant share of initial investigations focused on TiO_2 nanoparticles and they showed excellent performances in photocatalysis,[209] hydrogen production, solar cells, adsorbents, and sensors due to their large surface, broadened band gap, and electron transport properties.[210] TiO_2 plays three main roles in photovoltaic devices: (i) as antireflection coating or a scattering layer,[211] (ii) the interlayer in organic photovoltaics (OPV),[212] (iii) as selective contact layer of the device (mesoporous film) responsible for electron transport in dye sensitized solar cells (DSSC), quantum dot solar cells (QDSC), and perovskite solar cells.[213]

When using paper as a matrix for the incorporation of metal oxide nanostructures, adhesion occurs by weak interactions such as hydrogen bonding, and van der Waals forces, which poses retention problems. One way to solve this issue is through the use of suitable linkers, binders or retention aids for the incorporation/immobilization of the nanostructures in the paper matrices (see Figure 13).[43,214] Alternatively, novel methodologies that avoid the use of binders, linkers or retention aids are being developed. For instance, the hydrothermal treatment (at 150 °C for 20 h) allows one to immobilize metal oxide nanostructures on the cellulose fibers of paper as reported by Chauhan *et al*.[215] A non-hydrothermal and mass-producible synthesis of mesoporous TiO_2 spheres is also reported by Lee *et al*. where the concentration of ethyl cellulose controls the bulk calcination.[216] Cellulose fibers have also been used as a template to prepare nanostructured TiO_2 hollow fibers to be applied in photocatalytic and dye-sensitized solar cells. These porous cellulose-template TiO_2 nanostructures, exhibit a significantly enlarged surface area and improved electron transport properties, whereas the PCE of the fabricated DSSC reached 7.2%.[217]

Typical mesoporous semiconductor films comprise three main components, the metal oxide nanoparticles, a solvent and the surfactant (binder). The surfactant plays an important role in controlling the porosity, viscosity, rheology, and overall morphology properties of the pastes used mainly in OPV and DSSC,[43] which deeply influence the charge transport properties in the nanostructure matrix under illumination.[206] Cellulose is commonly used as a surfactant that enhances the interconnection of the nanoparticles, and does not leave undesired residues when the pastes undergo thermal processes.[218] Applications of these pastes range from electrodes to electrolytes. Ethyl cellulose (EC) is the binder usually chosen,[219–222] however, there are numerous studies on other cellulose materials applied to solar cell fabrication, such as: hydroxyethyl cellulose (HEC),[223] hydroxypropyl cellulose (HPC),[224–226] cyanoethylated cellulose (CN-HPC),[227] cellulose acetate (CA),[228,229] cellulose acetate butyrate (CAB),[230] carboxymethyl cellulose (CMC),[231–234] trimethylsilyl-cellulose (TMSC),[204] cellulose nanocrystalline (CNC),[235] microfibrillated cellulose (MFC),[232] and bacterial cellulose.[144]

The importance of the properties of metal oxide pastes is reported in the work of Jiang *et al*, for instance.[236] They studied the influence of pore size, pore distribution and porosity of TiO_2 films prepared by changing the cellulosic thickener concentration in the pastes. The best results were achieved for a paste containing 15 wt % cellulosic thickener (60MP-50), which lead to a DSSC with a PCE of 6.4%. The short-circuit photocurrent density (J_{SC}) was 13.0 $mA \cdot cm^{-2}$, the open-circuit photovoltage (V_{OC}) 0.72 V, and the fill factor (FF) 68.0%.

Likewise, Dhungel *et al*.[237] obtained the best TiO_2 pastes when adding a cellulosic binder (ethyl cellulose, EC) along with the solvent, α-terpineol. The best DSSC had a PCE of 7.3%. Mori *et al*.[238] also confirmed the importance cellulose has as a critical binder for TiO_2. Their TiO_2 dispersions, for DSSC electrodes, exhibit the best conversion efficiency when prepared using EC and α-terpineol (PCE = 5.07%, J_{SC} = 10.9 $mA \cdot cm^{-2}$, V_{OC} = 0.83 V, and FF = 56.0%). Recently, Maldonado-Valdivia *et al*.[206] also studied the importance EC has in the performance of TiO_2 photoelectrodes for DSSC. The DSSCs with the highest PCE were systematically obtained with EC as surfactant, instead of polyethylene glycol (PEG).[237]

Despite the general interest that TiO_2 mesoporous films have received, cellulose polymers are also considered a reliable thickener/binder for alternative mesoporous metal oxides.[239] For example, alternatives such as Nb_2O_5,[226] and ZnO,[239–241] or mixed systems of mesoporous metal oxides like ZnO/SnO_2,[242] have been explored over the last decade. The main reason behind the development of reliable substitutes to TiO_2 is the fact that TiO_2 has a high photocatalytic activity. Under UV light in natural sunlight, it decomposes organic materials in DSSCs during outdoor use and causes long-term reliability problems for the conversion efficiency.[243] Zinc oxide, in particular, is a high candidate for photoanodic material in QDPV and DSSC given its advantageous intrinsic characteristics, such as a stable wurtzite crystal structure with a wide band gap (~3.37 eV), high carrier mobility (~115 – 155 $cm^2 \cdot V^{-1}s^{-1}$), and large exciton binding energy (~60 meV).[244]

Most of the studies published refer to a sole single cell component bearing a cellulose polymer, however, earlier this year, Bella *et al*.[245] have moved from this usual approach, to interfacing different paper-based components within the same device (the photoanode and the electrolyte). Such process gave rise to a DSSC with 3.55% efficiency and retained 96% of the efficiency value after 1000 h of accelerated aging test. Moreover, it is a step towards truly sustainable energy conversion devices.

Further applications of cellulose as a binder can be found for other types of solar cells, such as c-Si (mainly used in the preparation of high quality screen-printed metal paste electrodes),[246–249] CIGS/CIS,[250,251] CZTS/CZTSSe,[252] or perovskites.[253] It is interesting to note that one of the earliest references to the use of ethyl cellulose is in the work of Szlufcik *et al.*,[246] from 1988, where they employed it as a binder for screen-printed TiO_2 anti-reflection coating for c-Si solar cells (the improvement in J_{SC} and efficiency was more than 30%). Clemminck *et al.* also used ethyl cellulose to replace the commonly used binder at that time, the propanediol, to obtain high quality screen printing CdS pastes for CdS-based solar cells.[254]

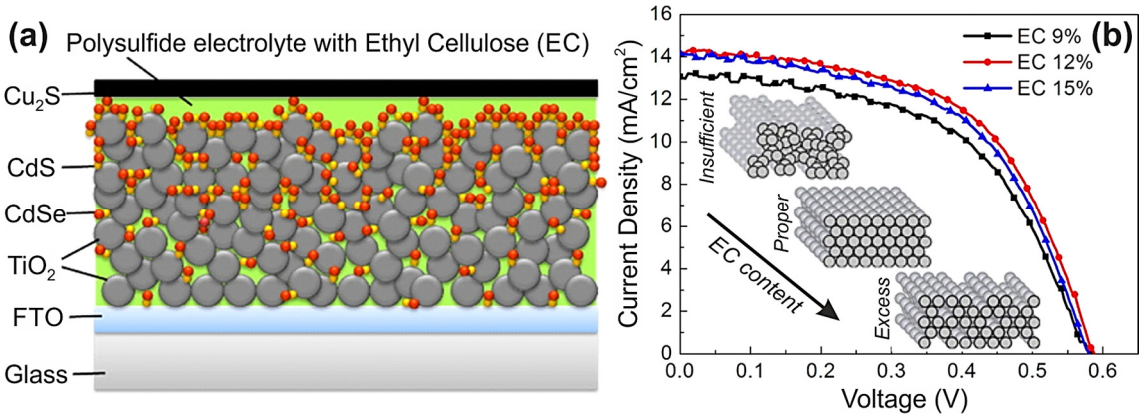

Figure 13 - (a) Quantum-dot (QD) solar cell structure, depicting the distribution of CdS/CdSe QDs in a mesoporous film composed of TiO_2 nanoparticles. **(b)** *J(V)* curves of the cells with different ethyl cellulose (EC) content mixed in the polysulfide electrolyte.[255] The inset sketches illustrate a structural model describing the arrangement of TiO_2 nanoparticles in the printed films fabricated with insufficient, proper, and excess EC content.[214] Reprinted with permission of Springer.

In the field of perovskite solar cells, Liu *et al.*[253] fabricated a mesoporous TiO_2 film by annealing a mixture of EC:P25 TiO_2:α-terpineol and saw a 20% improvement in efficiency comparatively to the commonly used titanium isopropoxide. For QDPV, Tian *et al.*[255] reported on homogeneously distributed CdS/CdSe quantum dots in a TiO_2 mesoporous film (see Figure 13). The thickness and porosity of the film was optimized by adding 12 wt% EC and the PCE of the QDPV reached 4.62%. The major concern regarding perovskite solar cells is the stability of the organic-inorganic perovskite, since it is highly sensitive to moisture and light.[256] He *et al.* observed that the incorporation of EC into the perovskite film can significantly improve photostability and moisture stability.[198] The stability gain they found arises from the hydrogen bonds between the EC mesostructure and the crystal structure of the $CH_3NH_3PbI_3$. The perovskite solar cell with EC incorporated does not show degradation over 5 days under ambient indoor light and 60% RH.[198]

Other mixtures where cellulose solutions have been used with PV applications are for instance in the preparation of polymer electrolyte membranes,[257] nanocellulose aerogel membranes,[258] hydrocalcites,[259] electrospun nanofibers,[228] and carbon counter electrodes.[260]

It is important to highlight the significant interest the employment of cellulose as binder for carbon nanostructures has gained over the last years. The work of Cruz *et al.*[261] focuses on the use of single-wall carbon nanohorns (SWNH) as counter electrodes of DSSC (decorated with

and without Pt nanoparticles). The counter electrode assembled with SWNH and 10 wt.% of hydroxyethyl cellulose (HEC) had the highest electrocatalytic activity (the charge-transfer resistance, R_{ct}, reached 141 $\Omega \cdot cm^2$). Applications for OPV can also be found. For example, Valentini *et al*.[262] developed transparent and conductive CNC/graphene nanoplatelets(GNPs) layers and Hu *et al.*[102] reported on the roll-to-roll production of PEDOT:PSS:graphene:ethyl cellulose (PEDOT:PSS:G:EC) electrodes (13 $\Omega \cdot sq^{-1}$ and 78% optical transmittance) for flexible transparent electrodes.

Other developments over the last decade explored the fabrication of conductive papers and the functionalization of cellulose fibers also with photovoltaic applications. Surface functionalization allows the tailoring of particle surface chemistry to facilitate self-assembly, controlled dispersion within a wide range of matrix polymers, and control of both the particle–particle and particle-matrix bond strength.[35]For example, Small and Johnston developed photoluminescent cellulose fibers by adding ZnS crystals doped with Mn^{2+} and Cu^{2+} Ions (emission at ~600 nm and ~530 nm, respectively).[31] Sakakibara and Nakatsubo functionalized cellulose films with porphyrin for photocurrent generation, although the absorption band was very narrow (from 400 nm to 420 nm).[263] Later on, the same research group addressed the limitation of the narrow absorption band by adding polypyridyl ruthenium (II) complexes (photocurrent generation range from 400 nm to 600 nm)[264] as a new complementary material for porphyrin-bound, or phthalocyanine-bound (photocurrent generation range from 600 nm to 700 nm)[265] cellulose derivatives. Shi *et al*. reported the assembly of bacterial cellulose and polyaniline (PAni) to obtain electro conductive composite hydrogels (10^{-2} $S \cdot cm^{-1}$),[266] which could be applied as flexible electrodes for solar cells. Transparent and conductive papers by embedding silver nanowires (AgNWs) is another promising method to develop flexible transparent electrodes for solar cells, as the work of Song *et al*. [267] shows. They successfully fabricated a paper using bamboo/hemp CNF and AgNWs cross-linked by hydroxypropylmethyl cellulose (HPMC) with a sheet resistance of 1.90 $\Omega \cdot sq^{-1}$ and transmittance above 80%, in the wavelength range from 500 nm to 800 nm.

Table 5presents a selection of research works recently published regarding the use of cellulose in the production of pastes with PV application.

Table 5 – Solar cells using cellulose in their formulations and corresponding performances. The different cellulose derivatives are indicated in bold: CNC – cellulose nanocrystalline, EC – ethyl cellulose, TMSC – trimethylsilyl-cellulose, HEC – hydroxyethyl cellulose, HPC – hydroxypropyl cellulose, CMC – carboxymethyl cellulose, CA – cellulose acetate, MFC – microfibrillated cellulose. SC characteristics refer to 100 $mW \cdot cm^{-2}$ AM1.5G illumination, unless stated otherwise in the efficiency column. N/D stands for "not disclosed", or that data is not explicitly stated.

SC type	Cellulose compound/mixture	Layer function	J_{SC} ($mA \cdot cm^{-2}$)	V_{OC} (V)	FF (%)	Efficiency (%)	Year[Ref]
OPV	**CNC**:Graphene NPs	Anode	1.9	0.3	30	0.2 (*)	2013[262]
	PEDOT:PSS:G:**EC**	Cathode	16.52	0.79	72	9.4	2015[102]
	ZnO:Graphene:**EC**	Electron transporter	15.88	0.74	69.0	8.1	2015[241]
	TMSC:CuXa:InXa: $CuInS_2$	Absorber	5.48	0.48	37.7	0.99	2017[204]
DSSC	**EC**:Ag-doped TiO_2:terpineol	Photoanode	10.9	0.83	56	5.07	2011[238]
	TiO_2:Carbon powder:terpineol: **EC**	Counter electrode	14.2	0.79	63	7.11	2011[260]
	NaI:I_2:MPII:TBP: CH_3CN:PEO:**CMC**	Electrolyte	10.3	0.75	69.0	5.18	2013[231]
	Pt:SWNH:**HEC**	Counter electrode	6.85	0.71	64	3.08	2013[261]

	Graphene:terpineol:ZrO_2:**EC** (GC-CE)	Counter electrode	13.8	0.64	71	6.27	2013[268]
	TiO_2:Pluronic F127:**EC**	Photoanode	15.3	0.83	60.7	7.70	2014[269]
	HPC:Ethylene carbonate:PC: NaI:MPII	Electrolyte	13.73	0.61	69.1	5.79	2015[224]
	CNC:PEO:NaI:I_2:TBP	Electrolyte	2.8	0.58	66.0	1.09	2016[235]
	CMC:KI:I_2	Electrolyte	~2.6	~0.45	~61	0.72	2017[233]
	CA:NH4I:Ethylene carbonate: ZnS/CuInS	Electrolyte	11.11	1.11	65.0	8.02	2017[229]
	TiO_2:**MFC**:**CMC** **MFC**:PEGDA:PEGMA	Photoanode Electrolyte	8.36	0.66	64.0	3.55	2017[245]
QDPV	**EC:**P25 TiO_2/CdS/CdSe: terpineol	Photoanode	14.23	0.59	55	4.62	2012[255]
	EC:P25 TiO_2/CdSe: terpineol	Photoanode	15.54	0.56	61.0	5.53	2014[270]
	EC:CTAB:ZnO NDs/CdS/CdSe	Photoanode	16.0	0.62	49.0	4.86	2015[271]
	CMC: polysulfide electrolyte	Electrolyte	21.89	0.67	63.1	9.21	2016[234]
PSC	**EC**:TiO_2:terpineol	Electron transporter	20.43	0.89	67	12.48	2016[246]
	EC:$CH_3NH_3PbI_3$	Photoactive layer	21.18	0.99	67.2	14.08	2016[198]
c-Si	Ag:**EC**:DMO:Rosin ester:organic solvents	Back contact	~35.6	0.64	79.2	18.06	2016[248]

(*) Measured with a simulated illumination of 90 $mW \cdot cm^{-2}$

4 Paper substrates for optical sensing

The area of sensors ascribes a high importance to paper substrates. From the healthcare perspective, point-of-care (PoC) tests, which are performed at or near the site of clinical care, provide unique opportunities to speed diagnosis and cost reduction in developing countries. The strengths of paper-based microfluidics and sensors are their low-cost, disposability and minimal external equipment requirements.[272] In the packaging area, the food and beverage industry are aligning their strategy with the consumers' demands of more natural products with less additives, higher regulation, and quality control, to assure food safety. Intelligent sensors can impart packages with the capability to acquire, store and transfer data, communicate and carry out logic functions. Thereby contributing to increase consumer confidence in the products they eat and drink.[7]

The incorporation of electronics and microfluidics has the potential to generate new functions and devices in the field of lab-on-chip.[4,273] Nowadays, most of the devices are constructed by stacking electronic and microfluidic structures, which require multiple fabrication, assembly, mounting, and connection steps. Combining electronics and microfluidics on paper, the so-called lab-on-paper devices, has the advantage of exploring low-cost and scalable printing fabrication techniques with a substrate that is highly compliant (possibility to functionalize cellulose, create hydrophobic barriers or regions to contain biomolecules/reagents, etc.) and has intrinsic microfluidic transport mechanisms.[274,275] The fabrication of lab-on-paper devices explores various patterning techniques (e.g. photolithography,[276] laser treatment,[277] inkjet printing,[278] wax printing,[279][280] plasma treatment,[281] and silanization[282]) to define channels and reaction zones onto paper. In the future, these devices are expected to perform more complex and a wider range of analysis, which could take advantage of PV to power, for instance, a color sensor and display coupled to the lab-on-paper, to increase detection limits and display information/data analysis regarding the tests performed in the device. Hamedi *et al*. are

already exploring co-fabrication processes to simultaneously engineer the electrical and fluidic components.[273] In this work, they demonstrate a printed circuit board on paper, an electroanalytical device (coulometric measurement for ferrocyanide, and a glucose assay) and a paper battery. Regarding the power consumption of these devices, the electrochemical devices require a potential of 0.6V; the electronic paper circuit (microcontroller based heater) requires a 5V power source; whereas the paper battery has an energy output of 6 μWh.[273] Further work on strategies to integrate PV in these devices is feasible, given the power consumptions involved, in order to extend their self-sufficiency. Very recently, Pavinatto *et al*.[283] have reported a printed and flexible impedance based biosensor for antioxidant detection, whereas the biological recognition layer (Tyrosinase-containing ink, where CMC was selected as viscosity enhancer) was deposited by large-area rotogravure. The finished biosensor was then encapsulated with a cellulose acetate dip-coating film to avoid dissolution.

The field of opto-fluidics can also take advantage of PV coupling. There is a growing focus on biological and chemical sensing, and significant research involving the implementation of opto-fluidic concepts using bulk optics and microchannels, that could see more complex design principles by exploiting power sources. Although this is an area that is yet to receive proper attention, there are exciting opportunities to combine opto-fluidic functionality with additional electrical, mechanical and magnetic elements.[284] Erickson *et al*.[285] in their review discuss opportunities for opto-fluidics in the fields of photo-bioreactors and photo-catalytic reactors (for solar-energy-based fuel production), and liquid-based systems (for the collection and control of solar radiation); these are fields where PV can add value[286] by increasing energy/heat production rates, thus higher power densities and yield/revenues. For instance, Zimmerman *et al*. developed a concept for using a solar-collecting adsorbing substrate to provide the heat for a microfluidic-chip-based methanol reformation reaction to improve the efficiency of current micro-reactors.[287]

In view of the aforementioned exciting applications of paper materials for bio-detection, this section reviews two of the most researched technologies that allow such detection, using light-induced optical signals emitted by the analytes (probe molecules), based in either Surface Enhanced Raman Spectroscopy (SERS, Section 4.1) and Photoluminescence (Section 4.2) sensing. In the latter case, luminescent up-converting materials can also find application in the enhancement of solar cells' efficiency, as they can provide improved spectral matching between the illuminating sunlight and the solar cells' photocurrent generation.

4.1 Plasmonic Raman sensing

4.1.1 Basic principles of SERS detection

Raman scattering[3] is based on the inelastic scattering of a photon from a molecule which is excited to higher vibrational or rotational energy levels (see Figure 14a), resulting in a spectrum that reflects the energy differences between the incident and inelastically-scattered photons, allowing the unique identification of one or multiple "fingerprints" from molecular bonds.[14–16] One of the difficulties associated with Raman spectroscopy is the small scattering cross section of many materials and, consequently, Raman signals can be inherently weak (one scattered photon per million incident).[290] Surface-enhanced Raman spectroscopy (SERS) is a surface-sensitive technique that enhances the Raman signal by molecules adsorbed on metal

nanostructured substrates.[291] This technique has attracted intense interest since 1977 because it could produce 3to14 orders of magnitude enhancement in Raman signals.[292,293]The exact mechanism of the enhancement effect of SERS is still a matter of debate in the literature, however two mechanisms have been theoretically accepted to explain this effect: the electromagnetic (EM)[294] enhancement associated to localized surface plasmon resonances (LSPR) and the so-called chemical enhancement (CE)[295] due to charge transfer mechanisms. The former arises from the interaction between an exciting light and metal nanostructures, leading to enhance local EM fields due to the resonant excitation of surface plasmon oscillations in the nanostructures. The resulting localized electric-field enhancement can lead to highly amplified Raman scattering signals at the surface of the nanostructures, resulting in an increase of the signals from molecules that have been adsorbed onto or are in the vicinity of the nanometer-sized metallic particles.[296] The local field enhancement is higher at the overlap of the near-field regions between adjacent nanoparticles, creating the so-called '*hot-spots*',[297] where usually the ideal spacing is in the range of 1–10 nm (see Figure 14b).[298,299]The latter mechanism can be attributed to charge transfer induced by the molecule-metal interaction.[300,301] Generally, its contribution to the enhancement factor (EF) is of the order of one to three orders of magnitude,[302] and significantly smaller than the EM contribution, being the electromagnetic enhancement the common dominant mechanism for SERS. An in-depth review of the SERS mechanisms is beyond the scope of this overview and can be found elsewhere.[295,300–302]

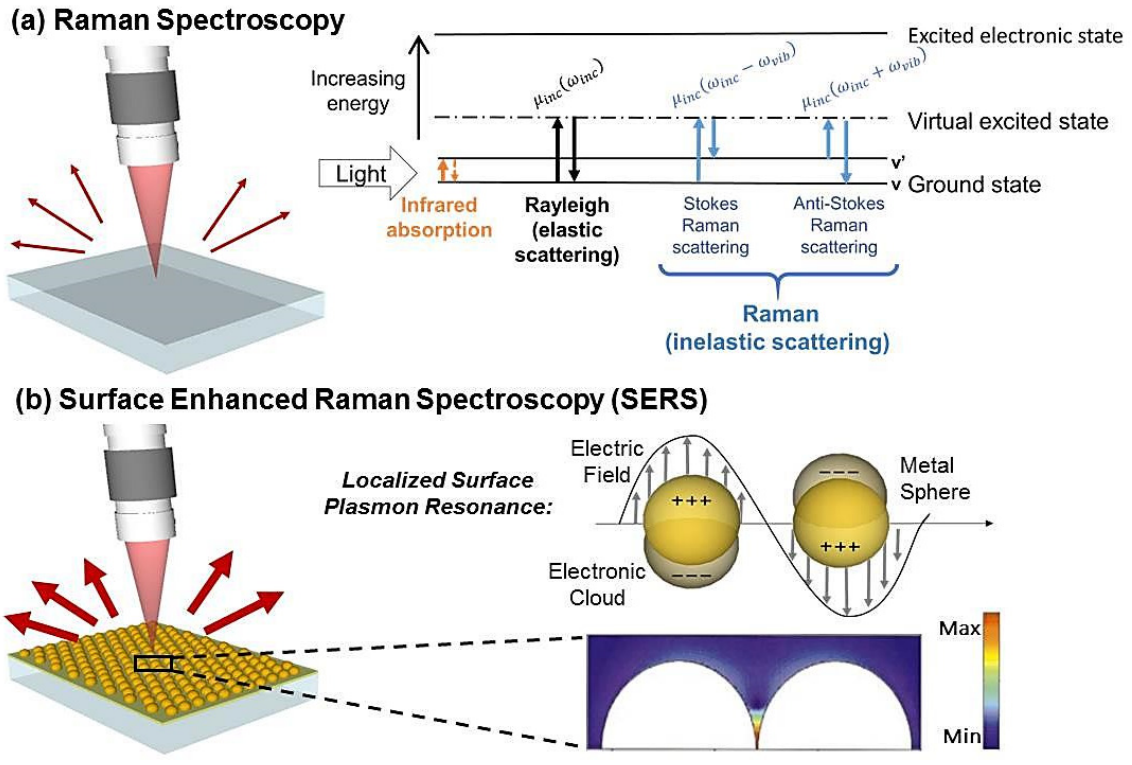

Figure 14–(a) Schematic of Raman Spectroscopy and energy diagram representing (*from left to right*) the infrared absorption, elastic Rayleigh scattering and the inelastic anti-Stokes (*left*) and Stokes (*right*) Raman scattering with ω_{inc}, $\omega_{inc}\pm\omega_{vib}$ and ω_{vib} referring to the frequencies of the incident light, the Raman scattered light, and the molecular vibration, respectively. **(b)** Illustration of Surface Enhanced Raman Spectroscopy and of the LSPR effect. This consists in the collective oscillation of the conduction electrons in a metal nanoparticle (NP) in resonance with the frequency of incident light. The colour plot at the bottom corresponds to the electric field intensity profile in the

inter-space of a dimer with two Au nanospheres having a separation of 1 nm. The colour scale is logarithmic.[303] Reproduced with permission of APS Physics.

4.1.2 Cellulose-based SERS substrates

The performance of the Surface Enhanced Raman Spectroscopy (SERS) technique mainly depends on the choice of the materials and structure of the SERS-active substrate. Ideal SERS platforms should not only exhibit strong signal enhancement with multiple electric-field *hot spots*, but should also present a uniformly distributed signal along the surface. With the advances of nanotechnology in the last decades, there are applications of SERS branched to new fields from environmental to medical care, art, clothing, security, among others.[304–306]The design of effective SERS substrates needs to cover many aspects besides having high SERS enhancement, that are intrinsically related to all sensor requirements for point-of-care (PoC) applications such as: uniformity, reproducibility, shelf life, scalability and cost. SERS studies have largely benefited from the recent advances in the understanding of plasmonic concepts.[307,308] Nanoparticles (NPs) made of noble metals, such as silver (Ag) or gold (Au), became the most studied materials for SERS because of their stronger localized surface plasmon resonance (LSPR)relative to other metals.[296,309–311]The research on nanostructures for SERS is mainly focused in improving the correlation between the NPs' properties and the resulting SERS signal intensities, since both the frequency and magnitude of the maximum field enhancement are strongly dependent on the shape, size and structure of the metallic material.[182,296,312,313] Generally, two typical routes have been pursued to improve SERS platforms, targeting single molecule detection: The most common approach is the optimization of the morphological properties(mainly particle size, shape and surface coverage), of the self-assembled metallic NPs structures.[4,296,314,315] The other one is the development of their supporting material (i.e. the substrate).

The surface onto which the nanomaterials are placed can vary from rigid [e.g. glass, silicon wafers (~200 μm thick) and porous alumina][316–320] to flexible substrates (e.g. paper, cardboard substrate, cotton, plastic, silica sheets and tape)[296,306,321,322]. The traditional rigid substrates have several drawbacks as practical SERS substrates, since the collection efficiency and manipulation of solid samples is difficult. Flexible substrates for SERS can present several advantages over conventional rigid substrates, in terms of cost and processability, achieving Raman signal enhancements ($EF \approx 10^5$-10^7) comparable with the conventional rigid planar supports.[296,306,320,322–332]Such substrates have the advantage of being able to collect analytes by soaking, which allow them to be used for example in contact with the human body and food in packaging, as they can be wrapped around curved surfaces,[333,334]opening doors for the next generation of bio-medical optical sensing. **Table** 6 presents a summary of the principal features of the main SERS platforms.

Table 6 -Advantages and disadvantages of main SERS substrates.[275,305,335–338]

Surfaces	Advantages	Disadvantages
Silicon wafer	• Low background within the Raman fingerprint region (only the characteristic peaks associated with the Si crystal vibrations appear).	• Expensive; • Fragile (need to be handled with care); • Rigid (thickness ~200 μm).

Glass	• Very low SERS background; • Readily integrated into other analytical systems; • Less expensive than Si substrates.	• Fragile; • Rigid.
Paper based	• Available; • Inexpensive; • Made of renewable resources; • Thinness, lightweight; • Biodegradability; • Abundant storage capability; • Flexible (wipe over a surface to collect the analyte); • Cellulose fibres are compatible with biomolecules (important for biosensing).	• Analyte solution spreads out over a large area due the wicking ability of cellulose, so the paper needs to be modified to have varied degrees of hydrophobicity; • Dispersion of the NPs presents difficulties for controlled array formation; • Fragile.

Among all the flexible substrates, there is a currently growing interest towards paper-based SERS substrates, mainly due to the paper composition and cost, which provides flexibility, portability and biodegradability. In fact, paper has already been widely used as a low-cost platform for bio-analytical devices such as colorimetric, biochemical fluorescence electrochemical sensors, among others.[54,279,316,324,326,327,339–344]

4.1.2.1 Solution-processed SERS substrates

The fabrication methods of paper-based SERS substrates can be divided in two classes: chemical methods via patterning from a colloidal solution of metal NPs (e.g. inkjet and screen printing,[316,324,339,341,345–347] deposition by drop-casting,[348,349] filtration,[350]in-situ growth[351–354]) or physical methods via material deposition under vacuum (e.g. vapor deposition of ultra-thin metallic layers,[310] laser induced annealing method[355]). We start here by overviewing the first class of solution-based processes.

Inkjet and screen printing technologies are probably two of the most popular methods to fabricate plasmonic devices on paper, just by direct printing nanoparticle colloidal solutions on paper.[316,324,339,341,345–347]Their major advantage is the ability for printing arrays of SERS-active regions of any shape, which makes these techniques simple and affordable.[305] White's group reported the preparation of SERS-active substrates[324,346,347,350] on chromatography paper prepared by inkjet printing using a low-cost commercial piezo-based inkjet printer. By printing silver nanoparticles (Ag NPs) onto one end of the paper, the remaining part of the paper was used as a swab to collect the analyte's molecules directly from a large-area surface, enabled by the flexible nature of the paper-based SERS device (Figure **15**.1).Using these novel lateral-flow paper SERS devices, they achieved detection limits as low as 95 fentograms of rhodamine 6G (R6G).[347] More recently, Zhigao Dai *et al*.[328] presented a study using an inkjet printing technique to fabricate a SERS substrate based on Au nanorod (NR) inks on printed paper. The neighbouring nanoclusters of Au NRs, aligned side-to-side,were formed on office paper with favourable SERS properties.[328]Even though not yet applied on paper substrates, other methodologies such as direct printing of Ag nanostructures on porous Silicon (p-Si)[356,357]might be a suitable solution for flexible SERS platforms, since the p-Si layers can be easily detached from the Si wafer and subsequently attached to any material such as paper.

Screen printing is another printing technique that has been used to fabricate SERS substrates by printing SERS active nanoparticles arrays on filter paper using concentrated nanoparticles solutions.[316] However, the SERS signal of 5 µL R6G (1×10^{-9} M) recorded on paper was weaker than those from the glass and glass fibre plate (EF = 4.4×10^{6}). Sample delivery was not well

controlled on filter paper, thus diluting the sample and resulting in weak SERS enhancements. Although the printing method offers interesting features for the fabrication of flexible plasmonic devices, it requires agents for the viscosity control of the nanoparticles' ink.[316] Hence, printing can promote aggregation and background signals reducing the capability of detecting the analyte. Moreover, it is generally changeling to achieve simultaneously a good uniformity and high concentration of NPs deposited on paper when they come from solution phase.

An innovative method reported by Polavarapu *et al.*[325]was the development a "*pen on paper*" approach to produce efficient and reproducible SERS substrates in a highly versatile way. With this method, a fountain pen filled with metal NPs ink was used to directly write plasmonic SERS areas on paper, made of gold or silver nanospheres and gold nanorods, without the need of any special training or equipment (Figure **15**.2). The average enhancement factor (EF) of the Ag NPs substrates was calculated using 10 µL droplet of malachite green (MG) as Raman active probe (1×10^{-6} M) and the obtained values were 2×10^{5} and 1.5×10^{5} at 532 nm and 785 nm, respectively.

Possibly an even simpler approach is the drop-casting method. This type of process generally requires lower energy consumption and amount of material. When drop-casting the NPs, the wicking ability of cellulose causes the liquid to spread over a large area, which reduces the SERS signal and reproducibility. Limiting the hydrophilicity of the paper to a defined area, making it possible to concentrate the NPs over a pre-patterned area and consequently obtain high SERS enhancements, surpasses this drawback. Oliveira *et al.*[349] reported the fabrication of office paper SERS substrates using silver nanostars (Ag NSs) drop-casted in wells patterned in the paper using printed wax. These substrates exhibited a high reproducibility with good uniformity and high SERS enhancement (EF~10^{7}). Furthermore, contrary to other methods that require a high concentration of nanoparticles to achieve a high density of near-field *hot spots*, the tip-shaped anisotropic morphology of Ag NSs avoids the need of high NP's concentration (Figure **15**.3).

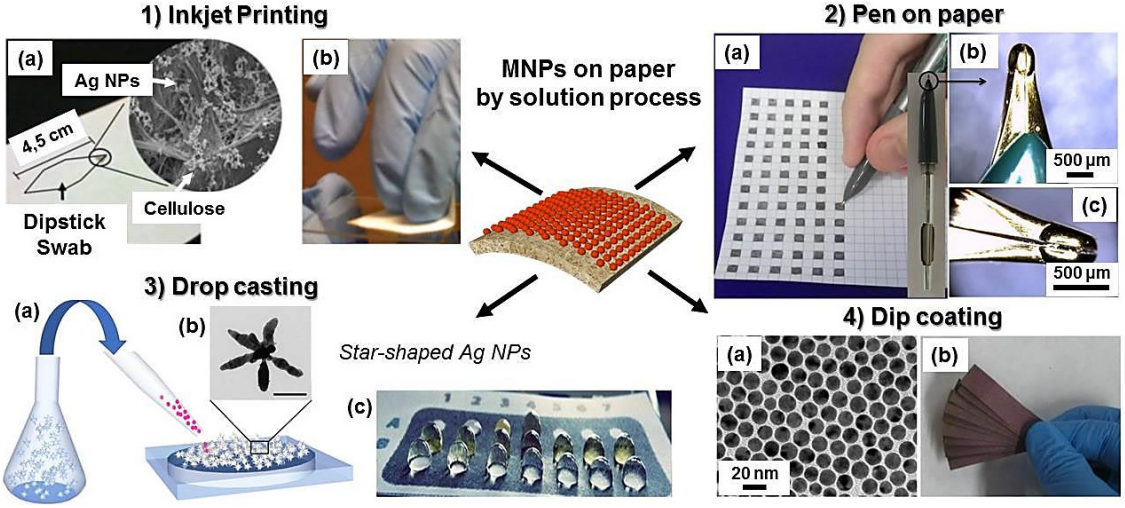

Figure 15- Methods for decoration of paper substrates with plasmonic nanoparticles by solution processes. **1)**Ag NPs printed onto paper by inject printing technology.[347]**2)** Impregnation of Au nanospheres, Ag nanospheres and Au nanorods,using a pen filled with a colloidal solution to directly write SERS arrays on paper substrates.[325]**3)** Schematic representation of the fabrication process of the plasmonic SERS paper substrates by drop-casting colloidal solutions of Ag nanostars (inset shows the TEM of a single nanostar).[349]**4)** (a)TEM image of oleylamine-capped Au

NPs, (b) Photograph of Au NP-doped filter papers by the dip coating method.[332] Panels 1 and 4, 2, and 3 reproduced with permission from Royal Society of Chemistry, Wiley and Nature, respectively.

Another simple process that has been applied to fabricate paper coated with metal NPs is by *dip-coating* (i.e. "soaking") paper substrates into solutions having colloidal metal nanostructures with different morphologies (e.g. nanoparticles, nanorods, bipyramids).[306,338,339,353] Using this method, nanoparticles are uniformly deposited onto the paper by simply dipping the substrate into the nanoparticle's solution of interest, followed by drying. This process provides high sample collection efficiency, does not require complex fabrication methodologies and allows the tunability of the NPs morphology that are deposited on the substrate. However, most of these approaches involve the attachment of NPs from aqueous dispersions, which requires either nanoparticle's solutions in a rather high concentration, like for the printing method, or long dipping times (typically 24–48 hours) to obtain a sufficiently high loading.[323,326] Zheng *et al.*[332] developed a fast fabrication based on a robust and recyclable dip-catalyst. The Au NPs were impregnated into a filter paper by simply dipping the paper into a concentrated NP colloidal dispersion in toluene, followed by drying using a hair-dryer (see Figure **15**.4). This process was repeated five times in order to achieve a close packed Au NP assembly.[332]

Other methods explore the modification of cellulose with different functional groups.[358] For example, the aldehyde groups can be used to help the synthesis of metallic silver. These types of paper-based substrates are included in the category of *in-situ* growth.[351,353,354,359,360] Other examples use reductive agents such as glucose to perform silver mirror reactions to produced 3D SERS paper strips containing Ag NPs. Although an adequate concentration of NPs for SERS signals can be obtained, the background signal of residues from the reagents used for the *in-situ* growth of Ag NPs, and the fast NP's oxidation rate, have quenched the interest for these types of methods.

4.1.2.2 Physically-processed SERS substrates

The physical methods typically employed for the patterning of metal NP arrays on paper are sputtering, pulsed laser (PLD) and e-beam deposition.[296,327] However, there are still few contributions investigating deposition by PLD and laser induced annealing, because generally they require high power lasers,[355] elevated temperatures for fine control of the shape and organization of the nanoparticles, which are incompatible with paper-based substrates. Although lithographic methods also can be used to precisely define the morphologies and sizes of NPs, this approach has major drawbacks, such as a high patterning time and elevated costs, which limit its extensive use in macroscopic scale systems.[361,362]

CENIMAT/i3N group has pioneered a simple, uniform, reproducible and large scale one-step method to deposit metal NPs on cellulose-based substrates.[4,296,363] The methodology employed consists in the thermal evaporation of thin metal films assisted by electron beam, resulting in the direct arrangement of individual nanoparticles' arrays with good control of their size and shape, without post-deposition thermal procedures.[296] Metal NPs are formed in situ during the thermal evaporation of ultra-thin (few nm) metal films (e.g. Ag, Au) onto heated (150 °C) paper substrates, with up to 20 × 20 cm^2 area. Despite the inherent roughness of the paper substrates, highly dense and uniform distributions of individual Ag NPs can be formed, without large-scaled agglomerates, throughout the entire paper area. The uniformity of the nanostructures on paper substrates produced by thermal evaporation greatly contributes to the high reproducibility

of SERS, as the Raman laser spot covers a range of tens of microns that contains several thousands of particles. Thus, a large ensemble of NPs affects the resulting signal. One important concern when paper SERS substrates are used, is the paper-derived fluorescence. The inherent background fluorescence can be prevented through time resolved Raman spectroscopy,[364] shifted excitation Raman difference spectroscopy (SERDS),[365] wavelength modulated Raman spectroscopy,[366] or even by depositing metal nanoparticles that can quench or shield the fluorescence emission signal.[349]

Based on this methodology, Araújo *et al.*[296] reported a flexible SERS substrate, using as support a liquidpackaging cardboard (LPC, see Figure 16). Besides being cost-efficient and amiable to several different environments, like common paper, this LPC substrate has an aluminium layer, which makes it more robust and contributes to amplify and red-shift the LSPR for wavelengths that are not usual for small NPs,[182,313] assisting in the spectral matching of the plasmonic resonance for maximum Raman enhancement (EF ~10^6).

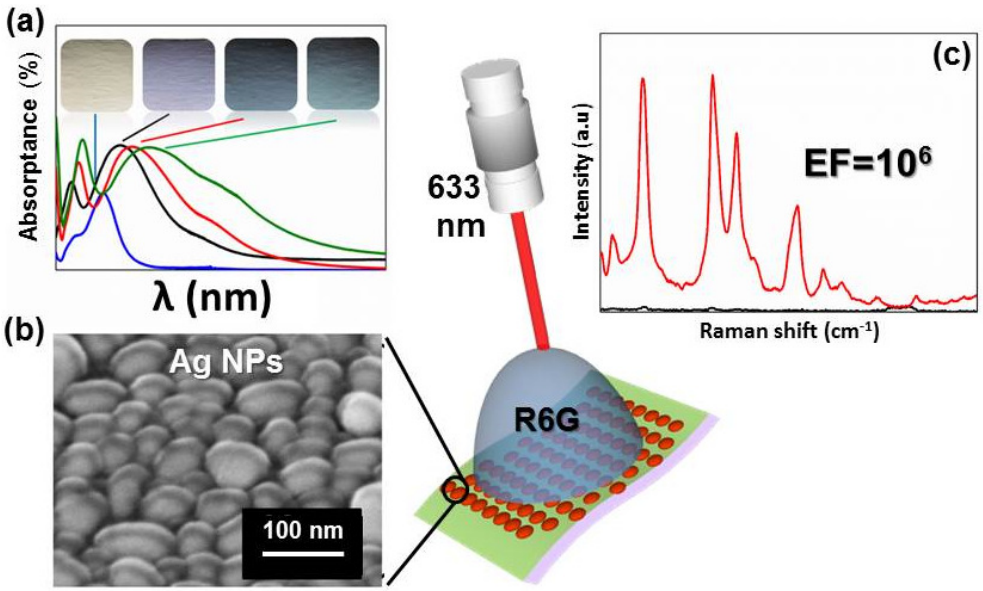

Figure 16 -Nanoplasmonic cardboard SERS substrate for the ultra-sensitive detection of R6G. **a)** UV-Vis-NIR adsorption spectra of laminated cardboard substrates with increases of NPs sizes, together with photographs of the substrates. **b)** SEM image showing the uniformly dense surface of the cardboard substrate with Ag NPs, fabricated from the 6 nm Ag precursor film structure, in which the majority of the nanoparticles have in-plane sizes around 60 nm. **c)** SERS spectra of the cardboard substrates with (*red line*) and without (*black line*) being decorated with the Ag NPs array.[296]

Recently, three-dimensional (3D) hybrid SERS substrates have been demonstrated, improving the performance relative to planar SERS substrates. NPs made of noble metals, such as Ag or Au, were deposited on dielectric nanostructures (Ag@ZnO,[367–369] Ag@SiO_2,[318] Ag@TiO_2[370] Au@ZnO[371] and Au@Si[372]) with different morphologies, such as nanorods (NRs), nanotubes and nanowires, have been proposed as promising SERS substrates due to the larger surface area allowed by the 3D nanostructured supports. Among these, ZnO nanostructures have been considered the most advantageous candidates for fabrication of such SERS substrates, since they allow the fabrication of many different 3D morphologies, employing a variety of

inexpensive and fast growth methods.[367–369]Concerning the various morphologies, ZnO NRs are particularly interesting mainly due to their high surface-to-volume ratio, making them a quite favorable nanostructured support for the development of SERS substrates (see Figure **17**).[320]

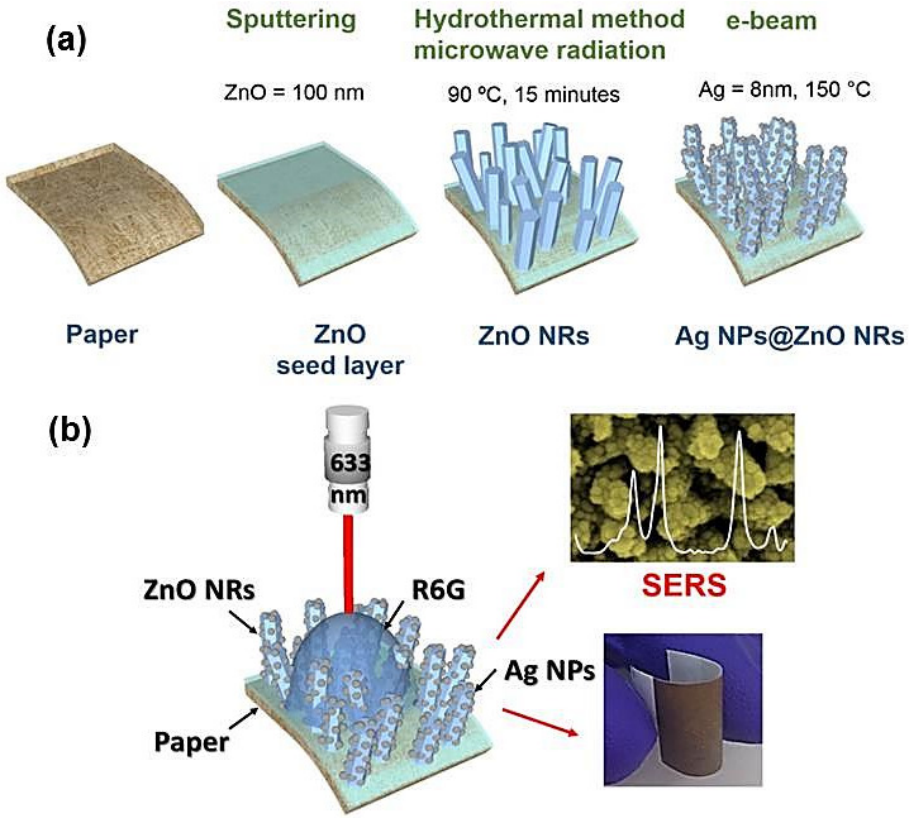

Figure 17- a) Illustration of the fabrication of SERS platforms on paper, composed of ZnO NRs covered with Ag NPs. **b)** Schematic drawing of the Raman measurement of Ag NPs@ZnO NRs on paper substrates in the presence of R6G.[310] Reprinted with permission from IOP Publishing.

Although different materials and morphologies of 3D structures have been employed on different rigid substrates (e.g. c-Si, glass, fused silica, sapphire), there are few reports on the direct growth of 3D nanostructures on flexible paper substrates for SERS. To the best of our knowledge, Araújo *et al.*[310]reported the first direct growth of Ag NPs@ZnO NRs on paper substrates for low-cost and flexible SERS devices. Here, a simple and scalable two-step method is presented (see Figure **17**a). ZnO NRs were grown on paper substrates using a low temperature (90 °C) and relatively fast (15 min) hydrothermal method assisted by microwave radiation. The rods were then decorated with Ag NPs by a single-step thermal evaporation process, assisted by electron beam, which resulted in the direct arrangement of a dense array of individual Ag nanoparticles with good control of their size and shape. Using rhodamine 6G (R6G) as a probe molecule, with an amount down to 10^{-9} M, the SERS substrates allowed a Raman signal enhancement of 10^7 (see Figure **17**b). The contribution of the inter-Ag-NPs gaps for the near-field enhancement, the ZnO NRs orientation and the large sensing area provided by the NR scaffolds, were determinant factors for the significant Raman enhancement observed.[310]

4.2 Photoluminescent sensing

Photoluminescent sensing has emerged as an important and growing research field especially when it comes to biological and environmental areas. Moreover, photoluminescence techniques are very versatile and can be introduced to several analytes due to their high sensitivity and selectivity, as well as high spatial resolution.[373] In this sense, semiconductors, with emphasis on semiconductor nanocrystals, play an expressive role, and their optical properties have been studied extensively over the years.[374–376] The optical and electronic properties of these small sized particles present quantum confinement effects, which is their major characteristic.[376]This particularity leads to spatial enclosure of the electronic charge carriers within the nanocrystal,[376] thus these materials exhibit unusually different behaviors compared to their bulk counterparts. Moreover, these materials allow tuning the light emission from ultraviolet to mid-infrared spectral ranges.[376] Semiconductor nanocrystals are already commercially sold nowadays, for example in luminescent labels,[377] electroluminescent devices,[378] among others.

Doped semiconductor nanocrystals have also been largely investigated,[379,380] in which one of the most interesting doping categories in semiconductors are the magnetic ions, followed by luminescent activators. These latter ones have attracted the scientific community interest, mainly due to their ability to increase quantum luminescence efficiency of the semiconductor nanocrystals. Mn^{2+} or Eu^{2+} are examples of doping elements.[381,382] Moreover, Cu, Sn and In doping have also been reported.[383,384]

The semiconductor nanocrystals have been added to different materials or substrates,[385,386]including paper. For instance, Small *et al.*[31]reported the production of photoluminescent cellulose fibers having ZnS nanocrystals doped with Mn^{2+} and Cu^{2+} ions. This process did not influence the inherent properties of the fibers, however it rendered photoluminescent properties to the coating. Moreover, photoluminescence up-conversion emission of ZnS:Mn^{2+} bulk and nanoparticles has been described by Chen *et al.*[387]Another approach using fluorescently labeled cellulose nanocrystals for bioimaging has been reported by Dong *et al*.[388]

Despite these semiconductor nanocrystals, several other materials can be employed for photoluminescent sensing, which includes lanthanide-doped up-conversion materials. These materials are extremely interesting concerning reliability and stability, besides they can be obtained at the nanometer scale, and have their up-conversion emission precisely controlled, in terms of emission color, lifetime and intensity, which are the basic prerequisites for practical applications.[389]

4.2.1 Principles of luminescent up-conversion

Photoluminescence (PL) involves absorption of energy and subsequent emission of light. The phenomena normally obey Stokes' law of luminescence, which states that the wavelength of the emitted light is generally longer than its exciting counterpart.[390] Up-conversion (UC),first suggested as a theoretical possibility by Bloembergen,[391] also referred as Anti-Stokes photoluminescence, violates the Stokes' law. Since the material emits light at shorter wavelengths than its excitation; i.e. the emitted photons have higher energy than the absorbed photons (see Figure 18**Erro! A origem da referência não foi encontrada.**).[392] This occurs due to the additional energy gain induced by multiple photon or thermal (phonon) energy absorption.[392–394] The PL emission of lanthanide-doped materials is based on well-shielded

4felectrons, where the filled shells of the larger 5s and 5p orbitals shield the 4f orbitals from external interactions, which can quench excited states.[395,396] Lanthanide ions have long-lived excited states (10 μs–10 ms).[396] These excited states relax slowly due to $4f^N \rightarrow 4f^N$ electric dipole transitions that are parity forbidden by quantum mechanical selection rules.[395–397]

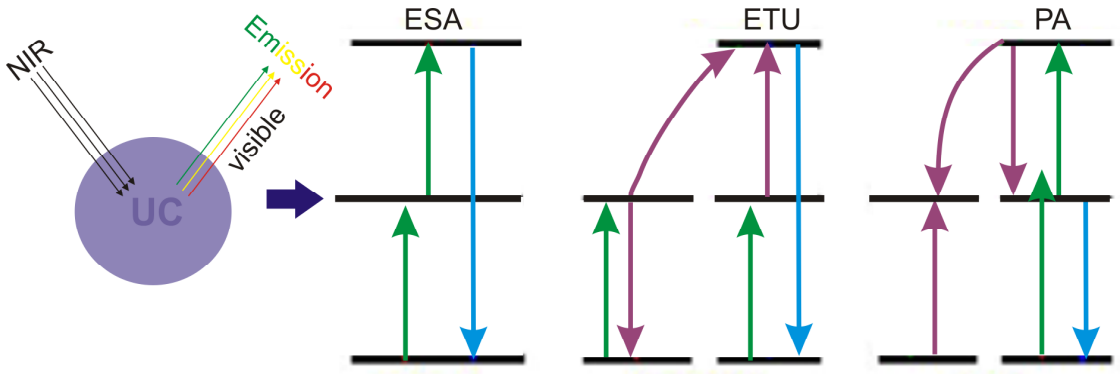

Figure 18 - Scheme of an up-conversion material exposed to a NIR excitation (980 nm) with emission of visible light together with the principal up-conversion mechanisms for lanthanides:[398] excited state absorption (ESA), energy transfer up-conversion (ETU) and photon avalanche (PA).[399] Reprint with permission of ???

Commonly, an emissive up-conversion material consists of an inert host matrix and an activator, however to enhance the up-conversion efficiency, a sensitizer can be employed.[396] The host must have good chemical and thermal stability, low toxicity, high corrosion resistance, and low phonon energy since up-conversion efficiency is determined by the radiative relaxation and the lifetime of the intermediate states involved.[396] The most commonly used host lattices are halides and oxides.[400] Halides hosts (e.g. $NaYF_4$, YF_3, LaF_3) have low phonon vibration energy (< 400 cm^{-1}), however their toxicity and air-sensitivity are drawbacks to their utilization.[396,401] Oxide-based host matrices (e.g. Y_2O_3, ZrO_2) have enhanced chemical stability, in addition to being environmental friendly, however they suffer from relatively high phonon energy (> 500 cm^{-1}).[396,402] Oxysulfides (e.g. Y_2O_2S, La_2O_2S) and oxyfluorides (e.g. ScOF, LaF_3) are also known for their potential applications as luminescent host materials[98] with phonon energies ranging from 350 to 500 cm^{-1}.[401,403,404]

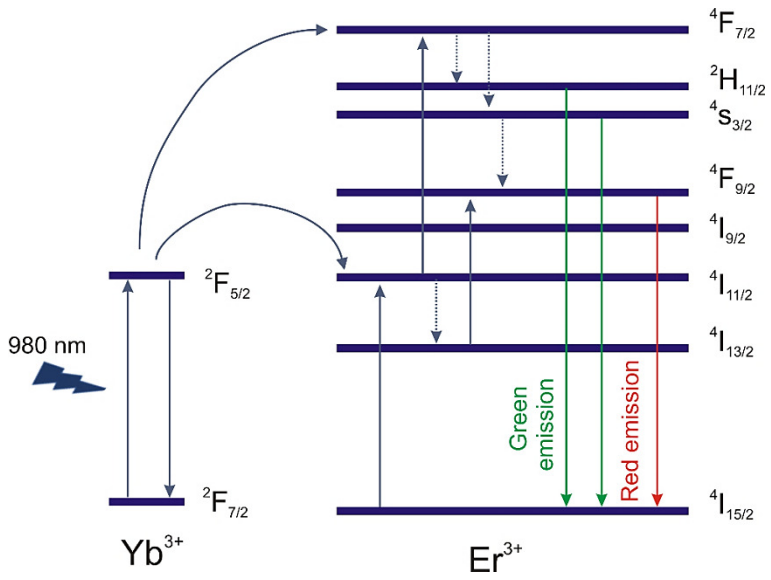

Figure 19 - Scheme of the Yb^{3+} and Er^{3+} up-conversion process (980 nm excitation).[400,405] Reprint with permission of ?

As an example, the up-conversion process observed between Yb^{3+} to Er^{3+} is depicted in Figure 19**Erro! A origem da referência não foi encontrada.**. This process occurs when Yb^{3+} absorbs radiation with wavelength of 980 nm and transfers the energy from the $^2F_{5/2}$ level to the $^4I_{11/2}$ level of Er^{3+}. Afterwards, energy transfer from a second excited Yb^{3+} ion is transferred to Er^{3+} ($^4I_{11/2}$) exciting the Er^{3+} ion to the $^4F_{7/2}$ excited state. After multi-phonon relaxation to the lower lying $^4S_{3/2}$ and $^4F_{9/2}$ states, green and red emissions are obtained.[400,405] The concentration of Yb^{3+} Er^{3+} is a central aspect in luminescence efficiency since high concentrations can cause PL quenching,[402]and energy migration.[406] Moreover, the luminescence efficiency can be further influenced by the distribution of the luminescent centres in the host matrix, organic ligands, size-dependent effects and overall particle structure and morphology.[395,407]

4.2.2 Up-conversion applications

Up-conversion materials have been extensively studied over the years for applications in optical devices ranging from solid-state lasers[408,409] to waveguide amplifiers[399,410] and light harvesting in solar cells.[411–413] Lately, these materials have also been considered as inks for security[389] and biological applications.[389,414–416]

In photovoltaic devices, materials composing the solar cells absorb photons with energy equal or greater than their bandgap. For instance with crystalline silicon, the most common material used in commercial solar cells, this corresponds to energies $E>E_g = 1.09$ eV.[417] Such material is therefore unable to absorb lower energy photons in the NIR region, which constitutes ~50% of the energy of the entire solar spectrum, resulting in a severe energy loss.[418] One possibility to overcome this restriction is to incorporate lanthanide-doped up-converting materials in solar cells, mainly due to their ability to convert low-energy NIR photons to higher energy photons (ultraviolet or visible); thus increasing the device photocurrent and thereby PCE.[419] Up-converting materials have been used in several photovoltaic devices, including crystalline or amorphous Si devices, and organic or dye-sensitized solar cells (DSSCs).[411,419,420] The up-

conversion materials are normally included as an ex-situ planar layer on top of the solar cell rear metallic contact (acting as back reflector), as shown in **Erro! A origem da referência não foi encontrada.**a. This layer can absorb the NIR portion of the solar spectrum transmitted through the cell active layer and then emit visible photons, which are directed back to the cell assisted by the rear reflector.[421]

Regarding the UC materials used in the biological field, they have been reported to serve as an excellent alternative for traditional fluorescent labels.[416] Moreover, their applications in biodetection, medical therapy or multiplexed analysis (**Erro! A origem da referência não foi encontrada.**b), and as reporters for DNA microarrays have been extensively studied.[399,419,422]Innovative approaches and technologies are under investigation to conjugate their favourable luminescent properties, such as multicolour emission capability under single-wavelength excitation, high signal-to-noise ratio and high chemical and photo-stabilities,[389]with long exposure effects.

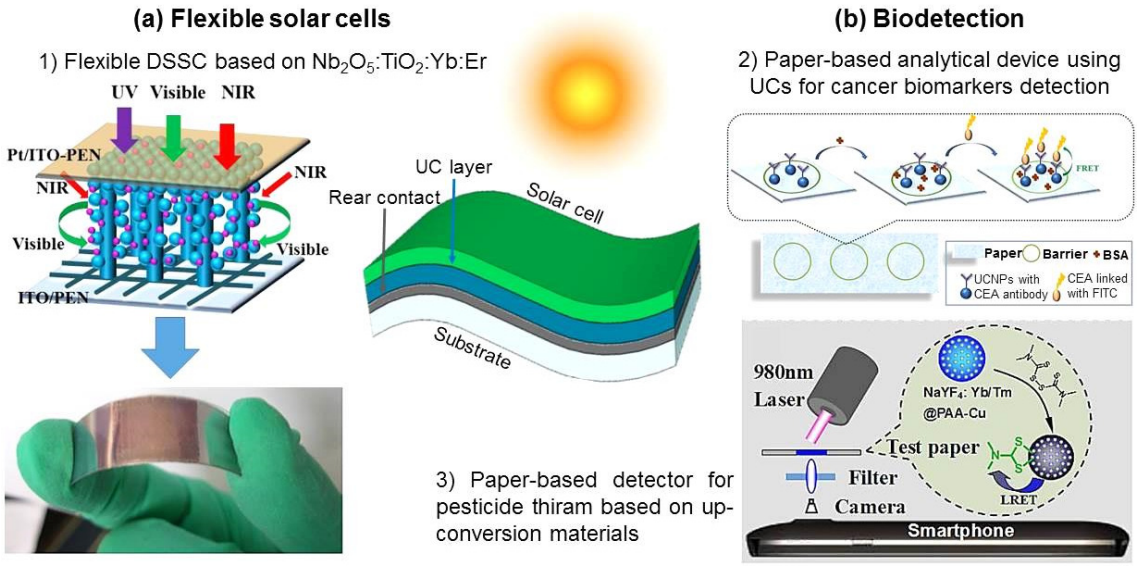

Figure 20– Applications of up-conversion materials in **a)** flexible solar cells and **b)** biodetection. 1) Scheme and photo of a fully flexible thin film dye-sensitized solar cell (DSSC) containing a rear-located up-conversion (UC) layer based on Nb_2O_5-coated TiO_2 nanowire arrays/nanoparticles co-doped with Er-Yb micro-nano structures.[423]2) Scheme of a paper-based analytical device using$NaYF_4$:Yb/Tmup-conversion materials as donors.[424] 3) Schematic of an up-conversion test paper to detect pesticide thiram using $NaYF_4$:Yb/Tm-Cu nanoprobes.[425] Reprinted with permission of Elsevier.

4.2.3 Up-conversion on flexible and paper-supported devices

Most of the studies involving up-converting compounds use materials in the form of powders or nanocrystals, however it has also been reported the production of UC films.[426–428] The introduction of up-conversion materials on flexible optoelectronic devices is recent and under intense investigation. Li *et al.*[409] reported the production of flexible amorphous silicon solar cells on steel foil substrates with up-conversion nanomaterials based on $NaYF_4$:Yb^{3+}/Er^{3+}/Gd^{+3} nanorods with Au nanoparticles. Liu *et al.*[423] demonstrated the improvement of light capturing and conversion efficiency of flexible dye-sensitized solar cells (polyethylene naphthalate as

substrate) using a composite of TiO_2 doped with Er^{3+} and Yb^{3+}, attaining a PCE of 8.10% as compared to 4.82% for the undoped DSSCs.

A flexible and superhydrophobic up-conversion-luminescence fibrous membrane, made ofaLn^{3+}-doped (Yb^{3+}, Tm^{3+} or Yb^{3+}, Er^{3+} co-doped) $NaYF_4$ nanoparticle/polystyrene hybrid material, was used as an ultrasensitive fluorescence sensor for single droplet detection.[429] Organic, transparent, and flexible colour displays based on UC materials have also been reported.[430] Moreover, Park *et al.*[431] reported the production of thin and bright flexible transparent displays using a core/shell structured up-conversion nanophosphor that was incorporated into a polymer waveguide. Regarding the security applications, Blumenthal *et al.* reported the direct-write of a polymer impregnated with luminescent up-conversion phosphors for security application,[431]producing continuous and uniform films on Kapton substrates.

Regarding the application of UC in paper-based devices, an important asset of cellulose-based substrates is the fluid transport via capillary action, in addition to the advantages described in section 1.[432] Paper has a three-dimensional fibrous structure, which provides large surface area, moreover it can be easily chemically modified,[433] and when associated to low-cost printing techniques (see section 2.3), this substrate can be an appealing option for low priced and disposable biological tests. For these sorts of tests, the paper porosity can also serve as a filtering medium to separate particles and aggregated materials from a reaction zone.[434]

An up-conversion fluorescence resonance energy transfer assay device has been developed for the sensitive detection of carcino-embryonic antigen (cancer biomarker), having normal filter paper as substrate and depositing the up-conversion material by nano-imprinting technology (**Erro! A origem da referência não foi encontrada.**.2).[424]Zhou *et al.*[433] reported a paper-based nucleic acid hybridization assay using immobilized up-conversion nanoparticles as donors in luminescence resonance energy transfer (LRET). A paper-based DNA hybridization assay with high sensitivity and fast response has also been demonstrated.[434] In this report, LRET associated with up-converting phosphors (donors) were used to develop a paper-based DNA hybridization assay. Up-conversion nanoparticles were deposited on filter paper to act as paper sensors for the quantitative analysis of pesticide thiram (**Erro! A origem da referência não foi encontrada.**.3).[425] Doughan *et al.*[432]showed the use of covalently immobilized up-conversion nanoparticles on paper as LRET donors for the optical detection of unlabelled nucleic acid targets.

Solar cells fabricated on paper have already been reported as described in section 3.2. With the incorporation of up-conversion particles on paper-based substrates, flexible PV devices could be thought, having the advantage of higher device efficiency due to the decrease of the sub-bandgap sunlight energy loss, via the up-conversion of NIR-to-visible photons. Other opto-electronic devices, such as temperature sensors[435,436]can also benefit from combining cellulose-based substrates with up-converting materials that have unique characteristics, thus improving their overall performance.

Besides the advances regarding SERS and UC based optical sensing covered in this section, other interesting techniques have also shown to be promising for chemical/biochemical analysis, with high sensitivity, specificity, miniaturization potential, and minimal hardware requirements (i.e. electrodes, voltage/current source, and light sensor). For instance, electrochemical devices based on electrolytic gas generation reactions,[437] which can be powered by DC current directly supplied PV to control the reaction velocity. On the other hand, impedance biosensors involve

the application of a small amplitude AC voltage. These sensors are fabricated by immobilizing a bio-recognition molecule (e.g. receptor proteins, single-stranded DNA, aptamer, or peptides) onto a conductive and biocompatible electrode and then detecting the change in the interfacial impedance at the sensor electrode, upon analyte binding, by measuring the in/out-of-phase current response as a function of frequency.[438]

5 Other paper applications in electronic circuitry

Together with the development of opto-electronic devices for photovoltaics and sensing, there is another class of related applications for electronic circuitry where paper is also emerging as a highly attractive material. Even though electronics is not a core subject in this article, it is nonetheless important to briefly comment the latest advances in this field concerning the use of paper-supported or paper-based materials, for completeness of the review.

To develop paper-based logic elements, significant research has been conducted towards the development of thin film transistors (TFT, both organic and inorganic) that are efficient, reliable, and with low operation voltage requirements.[2,439] For instance, the development of low operation voltage (< 3V) organic field effect transistors (OFET), based on naturally occurring materials (including cellulose), and fully compatible with printing fabrication methods are already a reality[440] and can be realistically coupled with paper based solar cells. High-performance nonvolatile memory devices, with reliable data storage, low-power consumption, and low-manufacturing cost are also of key importance to realize intelligent optoelectronic devices.[441,442] In the field of security devices, Liao and co-workers developed, for the first time, a nonvolatile memory with simple metal–insulator–metal device structure on paper using an all printing approach (the writing bias is +6 V and 100 μs width pulse, the erasing bias is a -3 V and 200 μs negative width pulse, and the reading voltage is 0.5 V).[443] In another recent work, Nagashima *et al*.[444] demonstrated a Ag-decorated CNF substrate as an ultra-flexible (350 μm bent radius) nonvolatile resistive memory that can be electrically switched with 6 orders of ON/OFF resistance ratio. The readout voltages were 0.01 V for retention and 0.1 V for endurance, respectively.[444]

Functionalization of cellulose also opens the door to realize devices build exclusively on cellulose multilayers/composite. By stacking different functionalized cellulose composite monolayers with tailored active functions (electro conductive, semiconductor, insulator), one can truly fabricate paper optoelectronic devices. One promising development in this subject is the work of Zang *et al*. where they report a paper-based ionic diode made of two oppositely charged MFC sublayers, and successfully rectified electric current.[445] Kawahara *et al*. reported low voltage operated electrochemical devices produced from electrically conducting polymers and polyelectrolytes cast together with CNF. The mechanical and self-adhesive properties of the films enable simple and flexible electronic systems by assembling the films into various kinds of components using a “cut and stick” method. This concept was demonstrated by detaching and reconfiguring one or several subcomponents by a “peel and stick” method to create yet another device configuration.[446]A similar concept was also shown for *iontronics*, using innovative cellulose-based ion gel electrolytes (see Figure **21**), which is expected to impact several market sectors from health, packaging and printing to the battery industry.[447] As reported by Cunha *et al.*, this approach consists in implementing the electrolyte directly on flexible transistors on paper, in the form of a sticker, employing four steps: cut, transfer, stick and reuse.[447]

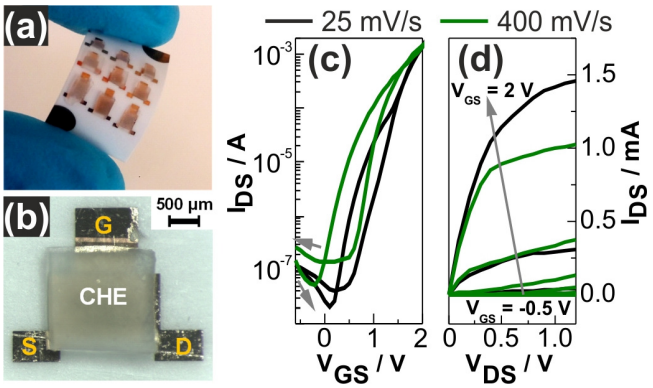

Figure 21–(a) Photo of flexible indium gallium zinc oxide (IGZO) electrolyte-gated transistors (EGTs) on multi-layer coated paper laminated with cellulose-based hydrogel electrolytes **(**CHEs). **(b)** Optical microscope image of the flexible EGTs with indication of the contacts (Gate, Source and Drain). **(c)**Cyclic transfer characteristic curves of an EGT at different V_{GS} scan rates for the saturation regime (V_{DS} = 1.2 V) and **(d)** respective output curves. The arrows represent the sweep direction.[447] Reprinted with permission of Wiley.

Furthermore, as paper-based electronics are easily recyclable, they do not have the disadvantages of producing electronic waste at the product´s end-of-life stage, contrary to common electronic products. The recycling of cellulose-based materials is a mature process, and the recovered cellulose can reenter the device fabrication stage to minimize (ideally replace) the need for raw cellulose pulp. Alternatively, incineration can produce energy; and from char, metals can be recovered and reused. In 2013, Zhou *et al*. demonstrated that polymer solar cells fabricated on CNC can be recycled into individual components using low-energy process at room temperature.[38] Recently, Jung *et al*.[448] demonstrated an alternative method to break down nanocellulose substrates by fungal biodegradation (*Postia placenta* and *Phanerochaete chrysosporium* fungi). Fungus degradation was evaluated for pure CNF films and epoxy-coated CNF films and was found to be efficient for both films. The encapsulated electronic component could be recovered after a biodegradation period of 84 days.[448] In a similar work, Seo *et al*. studied the fungal degradation (*Postia placenta*) of a TFT transistor fabricated on CNF.[449]

A broad range of near-future advances are currently anticipated in this booming field of paper electronics, such as improvement of devices performance, bendability and reliability/stability; as well as the development of clever means to add recycling steps, instead of directly disposing the devices, to reduce material waste. These advances bring new exciting functionalities and added value to cellulose, while providing more sustainable and user-friendly technologies.

6 Conclusions

The advances reviewed here have shown that cellulose can be an appealing option for the next generation of optoelectronic and medical devices. This material can be multi-functional, contributing to the improvement of the performance and applicability of light harvesting technologies, as those aimed at power conversion and bio-detection.Such technologies can find widespread applicability in the market of consumer electronics. Besides wearable/portable electronics, the packaging and healthcare segments are two other main possibilities to integrate

thin film devices. Here, paper-based materials have attracted a growing interest as platforms for solar-powered point-of-care tests and consumer diagnostics.

The combination of cellulose and solar cells is a hot topic nowadays that leaves ample room for photovoltaic innovation. Some of the biggest challenges to the widespread use of PV solar power in consumer electrical products are higher efficiencies, reproducibility, longer stability/lifetime and flexural capabilities for higher integration versatility. Thin film ssolar cells produced on flexible substrates, such as cellulose based materials, can open the possibility of achieving autonomous energy packaging systems.[25] Thus, having the paper advantages, which include bendability, lightweight, recyclability, disposability, low price, among others; thereby making paper one of the most attractive options to be integrated as platform for PV devices.

Although the power conversion efficiency is still low compared to traditional TFSCs supported on glass, the performance of SCs on paper still has potential to be much improved and more easily implemented in large-scale production. For that, two main R&D pathways are being pursued. One addresses the challenge of finding the optimum low-cost and scalable method for SC fabrication on the insulating, porous, and delicate nature of the fibrous paper material. The other concerns the application of light management structures, both for light trapping (via anti-reflection and scattering) and spectral matching (e.g. up-convertion), compatible with the cell architecture and promoting further enhancement of the generated photocurrent. Here, different optical approaches have been investigated to improve the light absorption capability of TFSCs, allowing the reduction of the thickness of the active layers without any detriment of the efficiency. This reduction of the commonly used thickness is important to achieve better structural quality, while reducing the manufacturing costs and enhancing the flexural properties of the devices. Moreover, light trapping structures can also be constructed in paper-based materials, allowing paper to serve not only as mechanical support for the solar cells but also as an active optical medium.

Concerning optical sensing, the combination of paper substrates with the plasmonic properties of Au and Ag nanoparticles has been gaining a substantial interest for applications in Surface Enhanced Raman Spectroscopy (SERS). The low cost of paper allied with its fibrous morphology gives SERS paper substrates soaking capabilities that are not possible to be attained by rigid SERS substrates, giving them a unique capability for many bio-applications. Paper substrates can also integrate microfluidics with SERS detection zones, making them a powerful tool for biosensor diagnostics that can be used in point of care tests. Besides, the SERS fabrication techniques on paper are allowing these types of substrates to attain remarkably high enhancements that are already close to those that can be achieved with rigid substrates.

Another research line that was highlighted concerns the implementation of up-conversion materials in paper-based devices, which turns to be highly appealing in terms of producing low cost and disposable products. Recently, UC materials have been used as fluorescent labels for molecular detection, medical analysis or even therapy. The flexibility and adaptability of these materials in terms of applications, together with their unique physical characteristics, makes them prone to be integrated in many types of flexible functional devices. Another promising example is the incorporation of UC materials in thin film solar cells, which has demonstrated the possibility of overcoming one of their main optical drawbacks, i.e. the limitation of PV semiconductors to absorb photons with energy below their bandgap, by converting lower-energy photons (e.g. in the NIR range) to higher-energy photons (e.g. in the Visible)that can generate a higher amount of photocurrent in the cells.

The complementary advances in the multi-disciplinary research topics reviewed here are likely to open a new era of environmentally-friendly, disposable and recyclable smart products, such as intelligent electronic labels for food-control and medical diagnostic electronics (e.g. point-of-care tests), which have low energy consumption and can therefore operate autonomously powered by PV electricity. Such technological innovations, i.e. making paper intelligent and self-powered, shall open the way for the establishment of paper-based materials as key players in the present IoT revolution.

Acknowledgements

This work was supported by FEDER funds, through the COMPETE 2020 Program, and national funds, through the *Fundação para Ciência e Tecnologia* (FCT), under the projects POCI-01-0145-FEDER-007688 (Reference UID/CTM/50025), ALTALUZ (Reference PTDC/CTM-ENE/5125/2014) and DISERTOX (Reference PTDC/CTM-NAN/2912/2014). The authors also acknowledge funding from the European Commission through the projects 1D-NEON (H2020-NMP-2015, grant 685758-21D) and BET-EU (H2020-TWINN-2015, grant 692373). The work was also partially funded by the Nanomark collaborative project between INCM (Imprensa Nacional-Casa da Moeda) and CENIMAT/i3N.

A. T. Vicente acknowledges the support from FCT and MIT-Portugal through the scholarship SFRH/ BD/33978/2009. A. Araújo, M. J. Mendes, D. Nunes and O. Sanchez-Sobradoalso acknowledge funding from FCT through the grants SFRH/BD/85587/2012,SFRH/BPD/115566/2016, SFRH/BPD/84215/2012 and SFRH/BPD/114833/2016, respectively. The authors would also like to acknowledge Inês Cunha for assistance in the subject of electronic circuitry on paper.

References

[1] S. Ummartyotin, M. Sain, *Cellulose Composites for Electronic Devices*, Nova Science Publishers, New York, **2016**.

[2] R. Martins, I. Ferreira, E. Fortunato, *Phys. status solidi - Rapid Res. Lett.***2011**, *5*, 332.

[3] R. S. Krishnan, R. K. Shankar, *J. Raman Spectrosc.***1981**, *10*, 1.

[4] A. T. Vicente, A. Araújo, D. Gaspar, L. Santos, A. C. Marques, M. J. Mendes, L. Pereira, E. Fortunato, R. Martins, in *Nanostructured Sol. Cells*, InTech, **2017**.

[5] M. Stoppa, A. Chiolerio, *Sensors***2014**, *14*, 11957.

[6] H. Jayakumar, K. Lee, W. S. Lee, A. Raha, Y. Kim, V. Raghunathan, in *Proc. 2014 Int. Symp. Low Power Electron. Des. - ISLPED '14*, ACM Press, New York, New York, USA, **2014**, pp. 375–380.

[7] K. L. Yam, P. T. Takhistov, J. Miltz, *J. Food Sci.***2005**, *70*, R1.

[8] J.-F. Christmann, E. Beigne, C. Condemine, P. Vivet, J. Willemin, N. Leblond, C. Piguet, *IEEE Des. Test Comput.***2011**, *28*, 84.

[9] C. G. Núñez, W. T. Navaraj, E. O. Polat, R. Dahiya, *Adv. Funct. Mater.***2017**, *27*, 1606287.

[10] M. Peng, D. Zou, *J. Mater. Chem. A***2015**, *3*, 20435.

[11] M. Kaltenbrunner, M. S. White, E. D. Głowacki, T. Sekitani, T. Someya, N. S. Sariciftci, S. Bauer, *Nat. Commun.***2012**, *3*, 770.

[12] K. Sakakibara, T. Rosenau, *Holzforschung***2012**, *66*, 9.

[13] P. Barquinha, S. Pereira, L. Pereira, P. Wojcik, P. Grey, R. Martins, E. Fortunato, *Adv. Electron. Mater.***2015**, *1*, 1.

[14] A. Correia, J. Goes, P. Barquinha, in *7th Dr. Conf. Comput. Electr. Ind. Syst.*, **2016**, pp. 533–541.

[15] P. Barquinha, R. Martins, L. Pereira, E. Fortunato, *Transparent Oxide Electronics: From Materials to Devices*, Wiley, **2012**.

[16] F. Villani, P. Vacca, G. Nenna, O. Valentino, G. Burrasca, T. Fasolino, C. Minarini, D. della Sala, *J. Phys. Chem. C***2009**, *113*, 13398.

[17] L. Santos, J. P. Neto, A. Crespo, D. Nunes, N. Costa, I. M. Fonseca, P. Barquinha, L. Pereira, J. Silva, R. Martins, E. Fortunato, *ACS Appl. Mater. Interfaces***2014**, *6*, 12226.

[18] W. S. Wong, A. Salleo, *Flexible Electronics: Materials and Applications*, Springer US, **2009**.

[19] Y. Zhou, C. Fuentes-Hernandez, T. M. Khan, J.-C. Liu, J. Hsu, J. W. Shim, A. Dindar, J. P. Youngblood, R. J. Moon, B. Kippelen, *Sci. Rep.***2013**, *3*, 1536.

[20] S. Kalia, B. S. Kaith, Inderjeet Kaur., *Cellulose Fibers : Bio- and Nano-Polymer Composites*, Springer, Berlin, **2011**.

[21] M. C. Barr, J. A. Rowehl, R. R. Lunt, J. Xu, A. Wang, C. M. Boyce, S. G. Im, V. Bulovic, K. K. Gleason, *Adv. Mater.***2011**, *23*, 3500.

[22] Y. Yao, J. Tao, J. Zou, B. Zhang, T. Li, J. Dai, M. Zhu, S. Wang, K. K. Fu, D. Henderson, E. Hitz, J. Peng, L. Hu, *Energy Environ. Sci.***2016**, *9*, 2278.

[23] M. M. Tentzeris, Y. Kawahara, in *2008 Int. Symp. Appl. Internet*, IEEE, **2008**, pp. 373–376.

[24] M. Toivakka, J. Peltonen, R. Osterbacka, M. (Mihai) Irimia-Vladu, E. D. Glowacki, N. S. Sariciftci, S. Bauer, in *Green Mater. Electron.*, Wiley-VCH Verlag GmbH & Co. KGaA, **2017**, pp. 163–189.

[25] A. Vicente, H. Aguas, T. Mateus, A. Araujo, A. Lyubchyk, S. Siitonen, E. Fortunato, R. Martins, *J. Mater. Chem. A***2015**, *3*, 13226.

[26] X. Du, Z. Zhang, W. Liu, Y. Deng, *Nano Energy***2017**, *35*, 299.

[27] B. L. Browning, *The Chemistry of Wood*, Interscience Publishers, New York, **1963**.

[28] A. Bledzki, *Prog. Polym. Sci.***1999**, *24*, 221.

[29] D. Klemm, B. Heublein, H.-P. Fink, A. Bohn, *Angew. Chemie Int. Ed.***2005**, *44*, 3358.

[30] M. Zhu, T. Li, C. S. Davis, Y. Yao, J. Dai, Y. Wang, F. AlQatari, J. W. Gilman, L. Hu,

*Nano Energy***2016**, *26*, 332.

[31] A. C. Small, J. H. Johnston, *Curr. Appl. Phys.***2008**, *8*, 512.

[32] C. Li, F. Wang, J. C. Yu, *Energy Environ. Sci.***2011**, *4*, 100.

[33] A. Ishikawa, T. Okano, J. Sugiyama, *Polymer (Guildf).***1997**, *38*, 463.

[34] M. Poletto, H. Ornaghi, A. Zattera, *Materials (Basel).***2014**, *7*, 6105.

[35] R. J. Moon, A. Martini, J. Nairn, J. Simonsen, J. Youngblood, *Chem. Soc. Rev.***2011**, *40*, 3941.

[36] J. Bousquières, C. Michon, C. Bonazzi, *Food Hydrocoll.***2017**, *70*, 304.

[37] K. Yuwawech, J. Wootthikanokkhan, S. Tanpichai, *Polym. Test.***2015**, *48*, 12.

[38] L. Hu, G. Zheng, J. Yao, N. Liu, B. Weil, M. Eskilsson, E. Karabulut, Z. Ruan, S. Fan, J. T. Bloking, M. D. McGehee, L. Wågberg, Y. Cui, *Energy Environ. Sci.***2013**, *6*, 513.

[39] R. E. Cannon, S. M. Anderson, *Crit. Rev. Microbiol.***1991**, *17*, 435.

[40] K.-Y. Lee, G. Buldum, A. Mantalaris, A. Bismarck, *Macromol. Biosci.***2014**, *14*, 10.

[41] S. V. Costa, P. Pingel, S. Janietz, A. F. Nogueira, *J. Appl. Polym. Sci.***2016**, *133*, 6.

[42] Z. Fang, H. Zhu, C. Preston, L. Hu, *Transl. Mater. Res.***2014**, *1*, 15004.

[43] F. Hoeng, A. Denneulin, J. Bras, *Nanoscale***2016**, *8*, 13131.

[44] K. Rajan, I. Roppolo, A. Chiappone, S. Bocchini, D. Perrone, A. Chiolerio, *Nanotechnol. Sci. Appl.***2016**, *9*, 1.

[45] I. Chauhan, S. Aggrawal, C. Chandravati, P. Mohanty, *RSC Adv.***2015**, *5*, 83036.

[46] J. Kettle, T. Lamminmäki, P. Gane, *Surf. Coatings Technol.***2010**, *204*, 2103.

[47] L. Leonat, M. S. White, E. D. Głowacki, M. C. Scharber, T. Zillger, J. Rühling, A. Hübler, N. S. Sariciftci, *J. Phys. Chem. C***2014**, *118*, 16813.

[48] H. Águas, T. Mateus, A. Vicente, D. Gaspar, M. J. Mendes, W. A. Schmidt, L. Pereira, E. Fortunato, R. Martins, *Adv. Funct. Mater.***2015**, *25*, 3592.

[49] F. C. Krebs, *Sol. Energy Mater. Sol. Cells***2009**, *93*, 394.

[50] R. M. Pasquarelli, D. S. Ginley, R. O 'hayre, *Chem. Soc. Rev. Chem. Soc. Rev***2011**, *40*, 5406.

[51] R. R. Søndergaard, M. Hösel, F. C. Krebs, *J. Polym. Sci. Part B Polym. Phys.***2013**, *51*, 16.

[52] R. Abbel, E. R. Meinders, in *Nanomater. 2D 3D Print.* (Eds.: S. Magdassi, A. Kamyshny), Wiley-VCH Verlag GmbH & Co. KGaA, Weinheim, Germany, **2017**, pp. 1–26.

[53] F. Shepherd, *Modern Coating Technology Systems*, Emap Maclaren, **1995**.

[54] D. Tobjork, R. Osterbacka, *Adv. Mater.***2011**, *23*, 1935.

[55] J. B. Wachtman, R. A. Haber, *Ceramic Films and Coatings*, Noyes Publications, **1993**.

[56] K. Kalantar-zadeh, B. Fry, *Nanotechnology-Enabled Sensors*, Springer US, Boston, MA, **2008**.

[57] Z. Hu, J. Zhang, S. Xiong, Y. Zhao, *Sol. Energy Mater. Sol. Cells***2012**, *99*, 221.

[58] S. Zhang, *Nanostructured Thin Films and Coatings : Functional Properties*, CRC Press, **2010**.

[59] M. A. Aegerter, M. Mennig, Eds. , *Sol-Gel Technologies for Glass Producers and Users*, Springer US, Boston, MA, **2004**.

[60] Z. Hu, J. Zhang, S. Xiong, Y. Zhao, *Sol. Energy Mater. Sol. Cells***2012**, *99*, 221.

[61] K. Norrman, A. Ghanbari-Siahkali, N. B. Larsen, *Annu. Reports Sect. "C" (Physical Chem.***2005**, *101*, 174.

[62] K. Rajan, S. Bocchini, A. Chiappone, I. Roppolo, D. Perrone, K. Bejtka, C. Ricciardi, C. F. Pirri, A. Chiolerio, *Microelectron. Eng.***2017**, *168*, 27.

[63] Z. Zhang, D. Wei, B. Xie, X. Yue, M. Li, D. Song, Y. Li, *Sol. Energy***2015**, *122*, 97.

[64] R. Mens, P. Adriaensens, L. Lutsen, A. Swinnen, S. Bertho, B. Ruttens, J. D'Haen, J. Manca, T. Cleij, D. Vanderzande, J. Gelan, *J. Polym. Sci. Part A Polym. Chem.***2008**, *46*, 138.

[65] C. H. M. van der Werf, T. Budel, M. S. Dorenkamper, D. Zhang, W. Soppe, H. de Neve, R. E. I. Schropp, *Phys. status solidi - Rapid Res. Lett.***2015**, *9*, 622.

[66] S. Marouf, A. Beniaiche, K. Kardarian, M. J. Mendes, O. Sanchez-Sobrado, H. Águas, E. Fortunato, R. Martins, *J. Anal. Appl. Pyrolysis***2017**, *127*, 299.

[67] K. X. Steirer, M. O. Reese, B. L. Rupert, N. Kopidakis, D. C. Olson, R. T. Collins, D. S. Ginley, *Sol. Energy Mater. Sol. Cells***2009**, *93*, 447.

[68] F. Zabihi, M. Eslamian, *J. Coatings Technol. Res.***2015**, *12*, 489.

[69] C. Girotto, D. Moia, B. P. Rand, P. Heremans, *Adv. Funct. Mater.***2011**, *21*, 64.

[70] K. Suganuma, *Introduction to Printed Electronics*, Springer New York, New York, NY, **2014**.

[71] H. J. van de Wiel, Y. Galagan, T. J. van Lammeren, J. F. J. de Riet, J. Gilot, M. G. M. Nagelkerke, R. H. C. a T. Lelieveld, S. Shanmugam, A. Pagudala, D. Hui, W. a Groen, *Nanotechnology***2013**, *24*, 484014.

[72] R. Barras, I. Cunha, D. Gaspar, E. Fortunato, R. Martins, L. Pereira, *Flex. Print. Electron.***2017**, *2*, 14006.

[73] M. Härting, J. Zhang, D. R. Gamota, D. T. Britton, *Appl. Phys. Lett.***2009**, *94*, 193509.

[74] V. Shanmugam, J. Cunnusamy, A. Khanna, M. B. Boreland, T. Mueller, *Energy Procedia***2013**, *33*, 64.

[75] J. Sakai, E. Fujinaka, T. Nishimori, N. Lto, J. Adachi, S. Nagano, K. Murakami, in *Conf. Rec. Thirty-First IEEE Photovolt. Spec. Conf. 2005.*, IEEE, **2005**, pp. 125–128.

[76] M. Singh, H. M. Haverinen, P. Dhagat, G. E. Jabbour, *Adv. Mater.***2010**, *22*, 673.

[77] L. Yang, A. Rida, R. Vyas, M. M. Tentzeris, *IEEE Trans. Microw. Theory Tech.***2007**,

55, 2894.

[78] A. Lange, M. Wegener, B. Fischer, S. Janietz, A. Wedel, *Energy Procedia***2012**, *31*, 150.

[79] R. R. Søndergaard, M. Hösel, F. C. Krebs, *J. Polym. Sci. Part B Polym. Phys.***2013**, *51*, 16.

[80] N. Kapur, *Chem. Eng. Sci.***2003**, *58*, 2875.

[81] G. Grau, J. Cen, H. Kang, R. Kitsomboonloha, W. J. Scheideler, V. Subramanian, *Flex. Print. Electron.***2016**, *1*, 23002.

[82] S. Khan, L. Lorenzelli, R. S. Dahiya, *IEEE Sens. J.***2015**, *15*, 3164.

[83] M. M. Voigt, R. C. I. MacKenzie, S. P. King, C. P. Yau, P. Atienzar, J. Dane, P. E. Keivanidis, I. Zadrazil, D. D. C. Bradley, J. Nelson, *Sol. Energy Mater. Sol. Cells***2012**, *105*, 77.

[84] J. Kim, T. Hassinen, W. H. Lee, S. Ko, *Org. Electron.***2017**, *42*, 361.

[85] S. Tekoglu, G. Hernandez-Sosa, E. Kluge, U. Lemmer, N. Mechau, *Org. Electron.***2013**, *14*, 3493.

[86] D. Gaspar, E. Polikarpov, Eds. , *OLED Fundamentals*, CRC Press, Boca Raton, FL, **2015**.

[87] D. Tobjörk, R. Österbacka, *Adv. Mater.***2011**, *23*, 1935.

[88] R. Søndergaard, M. Hösel, D. Angmo, T. T. Larsen-Olsen, F. C. Krebs, *Mater. Today***2012**, *15*, 36.

[89] H. Yan, Z. Chen, Y. Zheng, C. Newman, J. R. Quinn, F. Dötz, M. Kastler, A. Facchetti, *Nature***2009**, *457*, 679.

[90] M. Hambsch, K. Reuter, H. Kempa, A. C. Hübler, *Org. Electron.***2012**, *13*, 1989.

[91] A. Hübler, B. Trnovec, T. Zillger, M. Ali, N. Wetzold, M. Mingebach, A. Wagenpfahl, C. Deibel, V. Dyakonov, *Adv. Energy Mater.***2011**, *1*, 1018.

[92] A. Lorenz, A. Senne, J. Rohde, S. Kroh, M. Wittenberg, K. Krüger, F. Clement, D. Biro, *Energy Procedia***2015**, *67*, 126.

[93] S. Mandal, Y.-Y. Noh, *Semicond. Sci. Technol.***2015**, *30*, 64003.

[94] S. Kim, A. Georgiadis, A. Collado, M. M. Tentzeris, *IEEE Trans. Microw. Theory Tech.***2012**, *60*, 4178.

[95] L. Wu, Z. Dong, F. Li, H. Zhou, Y. Song, *Adv. Opt. Mater.***2016**, *4*, 1915.

[96] L. Csóka, D. Dudić, I. Petronijević, C. Rozsa, K. Halasz, V. Djoković, *Cellulose***2015**, *22*, 779.

[97] A. Damilano, P. Motto Ros, A. Sanginario, A. Chiolerio, S. Bocchini, I. Roppolo, C. F. Pirri, S. Carrara, D. Demarchi, M. Crepaldi, *IEEE Sens. J.***2017**, *17*, 2682.

[98] T. Tommasi, A. Chiolerio, M. Crepaldi, D. Demarchi, *Microsyst. Technol.***2014**, *20*, 1023.

[99] W. Wu, N. G. Tassi, H. Zhu, Z. Fang, L. Hu, *ACS Appl. Mater. Interfaces***2015**, *7*,

26860.

[100] H. Zhu, Z. Fang, Z. Wang, J. Dai, Y. Yao, F. Shen, C. Preston, W. Wu, P. Peng, N. Jang, Q. Yu, Z. Yu, L. Hu, *ACS Nano***2016**, *10*, 1369.

[101] E. Fortunato, D. Gaspar, P. Duarte, L. Pereira, H. Águas, A. Vicente, F. Dourado, M. Gama, R. Martins, in *Bact. Nanocellulose*, Elsevier, **2016**, pp. 179–197.

[102] X. Hu, L. Chen, T. Ji, Y. Zhang, A. Hu, F. Wu, G. Li, Y. Chen, *Adv. Mater. Interfaces***2015**, *2*, 1500445.

[103] S.-H. Jung, J.-J. Kim, H.-J. Kim, *Thin Solid Films***2012**, *520*, 6954.

[104] M. Hilder, B. Winther-Jensen, N. B. Clark, *J. Power Sources***2009**, *194*, 1135.

[105] K. B. Lee, *J. Micromechanics Microengineering***2006**, *16*, 2312.

[106] G. Nyström, A. Razaq, M. Strømme, L. Nyholm, A. Mihranyan, *Nano Lett.***2009**, *9*, 3635.

[107] V. L. Pushparaj, M. M. Shaijumon, A. Kumar, S. Murugesan, L. Ci, R. Vajtai, R. J. Linhardt, O. Nalamasu, P. M. Ajayan, *Proc. Natl. Acad. Sci.***2007**, *104*, 13574.

[108] G. Wee, T. Salim, Y. M. Lam, S. G. Mhaisalkar, M. Srinivasan, *Energy Environ. Sci.***2011**, *4*, 413.

[109] P. Moriarty, D. Honnery, *Renew. Sustain. Energy Rev.***2012**, *16*, 244.

[110] P. M. Voroshilov, C. R. Simovski, P. A. Belov, A. S. Shalin, *J. Appl. Phys.***2015**, *117*, 203101.

[111] B. Burger, K. Kiefer, C. Kost, S. Nold, R. Preu, S. Philipps, J. Rentsch, T. Schlegl, G. Stryi-Hipp, G. Willeke, H. Wirth, I. Brucker, A. Häberle, W. Warmuth, *Photovoltaics Report*, Freiburg, **2017**.

[112] X. He, H. Zervos, *Perovskite Photovoltaics 2016-2026: Technologies, Markets, Players*, Cambridge, UK, **2016**.

[113] J. L. Sawin, *Renewables 2016 Global Status Report*, Paris, **2016**.

[114] U.S. Energy Information Administration, *International Energy Outlook 2016*, Washington, **2016**.

[115] A. T. Vicente, P. J. Wojcik, M. J. Mendes, H. Águas, E. Fortunato, R. Martins, *Sol. Energy***2017**, *144*, 232.

[116] A. Lyubchyk, S. A. Filonovich, T. Mateus, M. J. Mendes, A. Vicente, J. P. Leitão, B. P. Falcão, E. Fortunato, H. Águas, R. Martins, *Thin Solid Films***2015**, *591*, 25.

[117] T. M. Razykov, C. S. Ferekides, D. Morel, E. Stefanakos, H. S. Ullal, H. M. Upadhyaya, *Sol. Energy***2011**, *85*, 1580.

[118] M. Bravi, M. L. Parisi, E. Tiezzi, R. Basosi, *Energy***2011**, *36*, 4297.

[119] A. Kojima, K. Teshima, Y. Shirai, T. Miyasaka, *J. Am. Chem. Soc.***2009**, *131*, 6050.

[120] "NREL Efficiency chart.," can be found under www.nrel.gov/ncpv/images/efficiency_chart.jpg, **n.d.**

[121] M. A. Green, K. Emery, Y. Hishikawa, W. Warta, E. D. Dunlop, D. H. Levi, A. W. Y. Ho-Baillie, *Prog. Photovoltaics Res. Appl.***2017**, *25*, 3.

[122] T. Duong, Y. Wu, H. Shen, J. Peng, X. Fu, D. Jacobs, E.-C. Wang, T. C. Kho, K. C. Fong, M. Stocks, E. Franklin, A. Blakers, N. Zin, K. McIntosh, W. Li, Y.-B. Cheng, T. P. White, K. Weber, K. Catchpole, *Adv. Energy Mater.***2017**, 1700228.

[123] M. Zeman, *J. Electr. Eng.***2010**, *61*, 271.

[124] A. Collado, A. Georgiadis, *IEEE Trans. Circuits Syst. I Regul. Pap.***2013**, *60*, 2225.

[125] K. Niotaki, A. Collado, A. Georgiadis, S. Kim, M. M. Tentzeris, *Proc. IEEE***2014**, *102*, 1712.

[126] C. R. Wronski, D. E. Carlson, R. E. Daniel, *Appl. Phys. Lett.***1976**, *29*, 602.

[127] D. L. Staebler, R. S. Crandall, R. Williams, *Appl. Phys. Lett.***1981**, *39*, 733.

[128] H. Okaniwa, K. Nakatani, M. Yano, M. Asano, K. Suzuki, *Jpn. J. Appl. Phys.***1982**, *21*, 239.

[129] "AFRL Program to Enable Solar Cells - Wright-Patterson Air Force Base," can be found under http://www.wpafb.af.mil/News/Article-Display/Article/399668/afrl-program-to-enable-solar-cells/, **n.d.**

[130] M. Nogi, M. Karakawa, N. Komoda, H. Yagyu, T. T. Nge, *Sci. Rep.***2015**, *5*, 17254.

[131] K. H. Jung, S. J. Yun, S. H. Lee, Y. J. Lee, K.-S. Lee, J. W. Lim, K.-B. Kim, M. Kim, R. E. I. Schropp, *Sol. Energy Mater. Sol. Cells***2016**, *145*, 368.

[132] B. Yan, G. Yue, X. Xu, J. Yang, S. Guha, *Phys. status solidi***2010**, *207*, 671.

[133] S. Morawiec, M. J. Mendes, S. A. Filonovich, T. Mateus, S. Mirabella, H. Águas, I. Ferreira, F. Simone, E. Fortunato, R. Martins, F. Priolo, I. Crupi, *Opt. Express***2014**, *22*, A1059.

[134] K. Wilken, V. Smirnov, O. Astakhov, F. Finger, in *2014 IEEE 40th Photovolt. Spec. Conf.*, IEEE, **2014**, pp. 3051–3054.

[135] C. Zhang, Y. Song, M. Wang, M. Yin, X. Zhu, L. Tian, H. Wang, X. Chen, Z. Fan, L. Lu, D. Li, *Adv. Funct. Mater.***2017**, *27*, 1604720.

[136] T. Söderström, F.-J. Haug, V. Terrazzoni-Daudrix, C. Ballif, *J. Appl. Phys.***2008**, *103*, 114509.

[137] Q. Wang, Y. Xie, F. Soltani-Kordshuli, M. Eslamian, *Renew. Sustain. Energy Rev.***2016**, *56*, 347.

[138] L. Szcześniak, A. Rachocki, J. Tritt-Goc, *Cellulose***2008**, *15*, 445.

[139] C. H. Lee, D. R. Kim, X. Zheng, *ACS Nano***2014**, *8*, 8746.

[140] R. C. Welch, J. R. Smith, M. Potuzak, X. Guo, B. F. Bowden, T. J. Kiczenski, D. C. Allan, E. A. King, A. J. Ellison, J. C. Mauro, *Phys. Rev. Lett.***2013**, *110*, 265901.

[141] P. Hidnert, H. S. Krider, *J. Res. Natl. Bur. Stand. (1934).***1952**, *48*, 209.

[142] ASM International. Materials Properties Database Committee, in *ASM Ready Ref. Therm. Prop. Met.* (Ed.: F. Cverna), ASM International, **2002**, pp. 9–16.

[143] "Corning Boro-Aluminosilicate Glass Products," can be found under http://www.delta-technologies.com/products.asp?C=1, **n.d.**

[144] S. Khan, M. Ul-Islam, W. A. Khattak, M. W. Ullah, J. K. Park, *Carbohydr. Polym.***2015**, *127*, 86.

[145] H. Zhu, Z. Fang, C. Preston, Y. Li, L. Hu, *Energy Environ. Sci.***2014**, *7*, 269.

[146] A. Dutta, G. Dutta, *J. Appl. Packag. Res.***2016**, *8*, 52.

[147] J. M. Burst, W. L. Rance, D. M. Meysing, C. A. Wolden, W. K. Metzger, S. M. Garner, P. Cimo, T. M. Barnes, T. A. Gessert, M. O. Reese, *2014 IEEE 40th Photovolt. Spec. Conf. PVSC 2014***2014**, 1589.

[148] J. A. Bertrand, D. J. Higgs, M. J. Young, S. M. George, *J. Phys. Chem. A***2013**, *117*, 12026.

[149] L. K. Massey, in *Permeability Prop. Plast. Elastomers* (Ed.: Plastics Design Library), Elsevier, **2003**, pp. 205–207.

[150] A. H. Bedane, M. Ei??, M. Farmahini-Farahani, H. Xiao, *Cellulose***2016**, *23*, 1537.

[151] B. Lamprecht, R. Thünauer, M. Ostermann, G. Jakopic, G. Leising, *Phys. status solidi***2005**, *202*, R50.

[152] D.-H. Kim, Y.-S. Kim, J. Wu, Z. Liu, J. Song, H.-S. Kim, Y. Y. Huang, K.-C. Hwang, J. A. Rogers, *Adv. Mater.***2009**, *21*, 3703.

[153] P. Ihalainen, A. Määttänen, J. Järnström, D. Tobjörk, R. Österbacka, J. Peltonen, *Ind. Eng. Chem. Res.***2012**, *51*, 6025.

[154] R. Bollström, A. Määttänen, D. Tobjörk, P. Ihalainen, N. Kaihovirta, R. Österbacka, J. Peltonen, M. Toivakka, *Org. Electron.***2009**, *10*, 1020.

[155] B. Trnovec, M. Stanel, U. Hahn, A. C. Hubler, H. Kempa, R. Sangl, M. Forster, *Prof. Papermak.***2009**, *6*, 48.

[156] F. Wang, Z. Chen, L. Xiao, B. Qu, Q. Gong, *Sol. Energy Mater. Sol. Cells***2010**, *94*, 1270.

[157] T. S. Kim, S. I. Na, S. S. Kim, B. K. Yu, J. S. Yeo, D. Y. Kim, *Phys. Status Solidi - Rapid Res. Lett.***2012**, *6*, 13.

[158] B. Wang, L. L. Kerr, *Sol. Energy Mater. Sol. Cells***2011**, *95*, 2531.

[159] K. Fan, T. Peng, J. Chen, X. Zhang, R. Li, *J. Mater. Chem.***2012**, *22*, 16121.

[160] J. R. Sheats, D. Biesty, J. Noel, G. N. Taylor, *Circuit World***2010**, *36*, 40.

[161] B. Anothumakkool, I. Agrawal, S. N. Bhange, R. Soni, O. Game, S. B. Ogale, S. Kurungot, *ACS Appl. Mater. Interfaces***2016**, *8*, 553.

[162] C.-P. Lee, K.-Y. Lai, C.-A. Lin, C.-T. Li, K.-C. Ho, C.-I. Wu, S.-P. Lau, J.-H. He, *Nano Energy***2017**, *36*, 260.

[163] M. Dasari, P. R. Rajasekaran, R. Iyer, P. Kohli, *J. Mater. Res.***2016**, *31*, 2578.

[164] M. Smeets, K. Wilken, K. Bittkau, H. Aguas, L. Pereira, E. Fortunato, R. Martins, V. Smirnov, *Phys. Status Solidi Appl. Mater. Sci.***2017**, *214*, 1700070.

[165] C. H. M. van der Werf, T. Budel, M. S. Dorenkamper, D. Zhang, W. Soppe, H. de Neve, R. E. I. Schropp, *Phys. status solidi - Rapid Res. Lett.***2015**, *9*, 622.

[166] Y. Zhou, T. M. Khan, J.-C. Liu, C. Fuentes-Hernandez, J. W. Shim, E. Najafabadi, J. P. Youngblood, R. J. Moon, B. Kippelen, *Org. Electron.***2014**, *15*, 661.

[167] M.-H. Jung, N.-M. Park, S.-Y. Lee, *Sol. Energy***2016**, *139*, 458.

[168] S. I. Cha, Y. Kim, K. H. Hwang, Y.-J. Shin, S. H. Seo, D. Y. Lee, *Energy Environ. Sci.***2012**, *5*, 6071.

[169] K. J. Yu, L. Gao, J. S. Park, Y. R. Lee, C. J. Corcoran, R. G. Nuzzo, D. Chanda, J. A. Rogers, *Adv. Energy Mater.***2013**, *3*, 1401.

[170] Y. Wang, Z. Li, J. Xiao, *J. Electron. Packag.***2016**, *138*, 20801.

[171] E. Marins, M. Warzecha, S. Michard, J. Hotovy, W. Böttler, P. Alpuim, F. Finger, *Thin Solid Films***2014**, *571*, *Part*, 9.

[172] H. Aguas, S. K. Ram, A. Araujo, D. Gaspar, A. Vicente, S. A. Filonovich, E. Fortunato, R. Martins, I. Ferreira, *Energy Environ. Sci.***2011**, *4*, 4620.

[173] V. E. Ferry, M. A. Verschuuren, M. C. van Lare, R. E. I. Schropp, H. A. Atwater, A. Polman, *Nano Lett.***2011**, *11*, 4239.

[174] A. Polman, H. A. Atwater, *Nat Mater***2012**, *11*, 174.

[175] A. Polman, M. Knight, E. C. Garnett, B. Ehrler, W. C. Sinke, *Science (80-.).***2016**, *352*, 307.

[176] Q. Lin, H. Huang, Y. Jing, H. Fu, P. Chang, D. Li, Y. Yao, Z. Fan, *J. Mater. Chem. C***2014**, *2*, 1233.

[177] D. M. Callahan, J. N. Munday, H. A. Atwater, *Nano Lett.***2011**, *12*, 214.

[178] F. Priolo, T. Gregorkiewicz, M. Galli, T. F. Krauss, *Nat. Nanotechnol.***2014**, *9*, 19.

[179] L. C. Andreani, A. Bozzola, P. Kowalczewski, M. Liscidini, *Sol. Energy Mater. Sol. Cells***2015**, *135*, 78.

[180] S. Morawiec, J. Holovský, M. J. Mendes, M. Müller, K. Ganzerová, A. Vetushka, M. Ledinský, F. Priolo, A. Fejfar, I. Crupi, *Sci. Rep.***2016**, *6*, 22481.

[181] A. Araújo, M. J. Mendes, T. Mateus, A. Vicente, D. Nunes, T. Calmeiro, E. Fortunato, H. Águas, R. Martins, *J. Phys. Chem. C***2016**, *120*, 18235.

[182] S. Morawiec, M. J. Mendes, S. Mirabella, F. Simone, F. Priolo, I. Crupi, *Nanotechnology***2013**, *24*, 265601.

[183] P. Tiberto, S. Gupta, S. Bianco, F. Celegato, P. Martino, A. Chiolerio, A. Tagliaferro, P. Allia, *J. Nanoparticle Res.***2011**, *13*, 245.

[184] M. J. Mendes, S. Morawiec, F. Simone, F. Priolo, I. Crupi, *Nanoscale***2014**, *6*, 4796.

[185] M. J. Mendes, S. Morawiec, T. Mateus, A. Lyubchyk, H. Águas, I. Ferreira, E. Fortunato, R. Martins, F. Priolo, I. Crupi, *Nanotechnology***2015**, *26*, 135202.

[186] C. S. Schuster, S. Morawiec, M. J. Mendes, M. Patrini, E. R. Martins, L. Lewis, I. Crupi, T. F. Krauss, *Optica***2015**, *2*, 194.

[187] J. Grandidier, R. A. Weitekamp, M. G. Deceglie, D. M. Callahan, C. Battaglia, C. R. Bukowsky, C. Ballif, R. H. Grubbs, H. A. Atwater, *Phys. status solidi***2013**, *210*, 255.

[188] M. J. Mendes, I. Tobías, A. Martí, A. Luque, *J. Opt. Soc. Am. B***2010**, *27*, 1221.

[189] M. J. Mendes, I. Tobías, A. Martí, A. Luque, *Opt. Express***2011**, *19*, 16207.

[190] M. L. Brongersma, Y. Cui, S. Fan, *Nat. Mater.***2014**, *13*, 451.

[191] X. H. Li, P. C. Li, D. Z. Hu, D. M. Schaadt, E. T. Yu, *J. Appl. Phys.***2013**, *114*, DOI 10.1063/1.4816782.

[192] O. Sanchez-Sobrado, M. J. Mendes, S. Haque, T. Mateus, A. Araujo, H. Aguas, E. Fortunato, R. Martins, *J. Mater. Chem. C***2017**, *5*, 6852.

[193] M. J. Mendes, A. Araújo, A. Vicente, H. Águas, I. Ferreira, E. Fortunato, R. Martins, *Nano Energy***2016**, *26*, 286.

[194] Z.-Q. Fang, H.-L. Zhu, Y.-Y. Li, Z. Liu, J.-Q. Dai, C. Preston, S. Garner, P. Cimo, X.-S. Chai, G. Chen, L.-B. Hu, *Sci. Rep.***2014**, *4*, 1.

[195] Z. Fang, H. Zhu, W. Bao, C. Preston, Z. Liu, J. Dai, Y. Li, L. Hu, *Energy Environ. Sci.***2014**, *7*, 3313.

[196] C. Jia, T. Li, C. Chen, J. Dai, I. M. Kierzewski, J. Song, Y. Li, C. Yang, C. Wang, L. Hu, *Nano Energy***2017**, *36*, 366.

[197] D. Ha, Z. Fang, L. Hu, J. N. Munday, *Adv. Energy Mater.***2014**, *4*, 130184.

[198] J. He, C.-F. Ng, K. Young Wong, W. Liu, T. Chen, *Chempluschem***2016**, *81*, 1292.

[199] Z. Fang, H. Zhu, Y. Yuan, D. Ha, S. Zhu, C. Preston, Q. Chen, Y. Li, X. Han, S. Lee, G. Chen, T. Li, J. Munday, J. Huang, L. Hu, *Nano Lett.***2014**, *14*, 765.

[200] Z. Tang, A. Elfwing, A. Melianas, J. Bergqvist, Q. Bao, O. Inganäs, *J. Mater. Chem. A***2015**, *3*, 24289.

[201] H. Y. Chen, S. R. Wang, H. Lin, G. Wang, S. H. Wang, G. J. Yang, *Key Eng. Mater.***2012**, *512–515*, 1619.

[202] K. Yuwawech, J. Wootthikanokkhan, S. Wanwong, S. Tanpichai, *J. Appl. Polym. Sci.***2017**, *45010*, 1.

[203] S. Che Balian, A. Ahmad, N. Mohamed, *Polymers (Basel).***2016**, *8*, 163.

[204] D. Reishofer, T. Rath, H. M. Ehmann, C. Gspan, S. Dunst, H. Amenitsch, H. Plank, B. Alonso, E. Belamie, G. Trimmel, S. Spirk, *ACS Sustain. Chem. Eng.***2017**, *5*, 3115.

[205] H. Matsubara, M. Takada, S. Koyama, K. Hashimoto, A. Fujishima, *Chem. Lett.***1995**, *24*, 767.

[206] A. I. Maldonado-Valdivia, E. G. Galindo, M. J. Ariza, M. J. García-Salinas, *Sol. Energy***2013**, *91*, 263.

[207] D. Nunes, A. Pimentel, J. V Pinto, T. R. Calmeiro, S. Nandy, P. Barquinha, L. Pereira, P. A. Carvalho, E. Fortunato, R. Martins, *Catal. Today***2016**, DOI 10.1016/j.cattod.2015.10.038.

[208] A. Fujishima, K. Honda, *Nature***1972**, *238*, 37.

[209] D. Nunes, A. Pimentel, L. Santos, P. Barquinha, E. Fortunato, R. Martins, *Catalysts***2017**, *7*, 60.

[210] M. Ge, C. Cao, J. Huang, S. Li, Z. Chen, K.-Q. Zhang, S. S. Al-Deyab, Y. Lai, *J. Mater. Chem. A***2016**, *4*, 6772.

[211] T. G. Deepak, G. S. Anjusree, S. Thomas, T. a. Arun, S. V. Nair, a. Sreekumaran Nair, *RSC Adv.***2014**, *4*, 17615.

[212] R. Steim, F. R. Kogler, C. J. Brabec, *J. Mater. Chem.***2010**, *20*, 2499.

[213] Y. Bai, I. Mora-Seró, F. De Angelis, J. Bisquert, P. Wang, *Chem. Rev.***2014**, *114*, 10095.

[214] T. C. Liu, C. C. Wu, C. H. Huang, C. M. Chen, *J. Electron. Mater.***2016**, *45*, 6192.

[215] I. Chauhan, P. Mohanty, *Cellulose***2015**, *22*, 507.

[216] C. S. Lee, J. Y. Lim, W. S. Chi, J. H. Kim, *Electrochim. Acta***2015**, *173*, 139.

[217] E. Ghadiri, N. Taghavinia, S. M. Zakeeruddin, M. Grätzel, J.-E. Moser, *Nano Lett.***2010**, *10*, 1632.

[218] Y. Mee Jung, Y. Park, S. Sarker, J.-J. Lee, U. Dembereldorj, S.-W. Joo, *Sol. Energy Mater. Sol. Cells***2011**, *95*, 326.

[219] E. C. Muniz, M. S. Góes, J. J. Silva, J. A. Varela, E. Joanni, R. Parra, P. R. Bueno, *Ceram. Int.***2011**, *37*, 1017.

[220] S. Xu, L. Hu, J. Sheng, D. Kou, H. Tian, S. Dai, *Front. Optoelectron. China***2011**, *4*, 72.

[221] P. J. Holliman, D. K. Muslem, E. W. Jones, A. Connell, M. L. Davies, C. Charbonneau, M. J. Carnie, D. A. Worsley, *J. Mater. Chem. A***2014**, *2*, 11134.

[222] P. Pratheep, E. Vijayakumar, A. Subramania, *Appl. Phys. A***2015**, *119*, 497.

[223] V. Zardetto, G. De Angelis, L. Vesce, V. Caratto, C. Mazzuca, J. Gasiorowski, A. Reale, A. Di Carlo, T. M. Brown, *Nanotechnology***2013**, *24*, 255401.

[224] M. H. Khanmirzaei, S. Ramesh, K. Ramesh, *Sci. Rep.***2016**, *5*, 18056.

[225] M.-H. Kim, Y.-U. Kwon, *Mater. Trans.***2010**, *51*, 2322.

[226] M.-R. Ok, R. Ghosh, M. K. Brennaman, R. Lopez, T. J. Meyer, E. T. Samulski, *ACS Appl. Mater. Interfaces***2013**, *5*, 3469.

[227] X. Huang, Y. Liu, J. Deng, B. Yi, X. Yu, P. Shen, S. Tan, *Electrochim. Acta***2012**, *80*, 219.

[228] S. S. Mali, P. S. Patil, C. K. Hong, *ACS Appl. Mater. Interfaces***2014**, *6*, 1688.

[229] N. S. Samsi, N. A. S. Effendi, R. Zakaria, A. M. M. Ali, *Mater. Res. Express***2017**, *4*, 44005.

[230] H. Randriamahazaka, F. Vidal, P. Dassonville, C. Chevrot, D. Teyssié, *Synth. Met.***2002**, *128*, 197.

[231] F. Bella, J. R. Nair, C. Gerbaldi, *RSC Adv.***2013**, *3*, 15993.

[232] F. Bella, A. Chiappone, J. R. Nair, G. Meligrana, C. Gerbaldi, *Chem. Eng. Trans.***2014**, *41*, 211.

[233] F. Bella, S. Galliano, M. Falco, G. Viscardi, C. Barolo, M. Grätzel, C. Gerbaldi, *Green Chem.***2017**, *19*, 1043.

[234] W. Feng, L. Zhao, J. Du, Y. Li, X. Zhong, *J. Mater. Chem. A***2016**, *4*, 14849.

[235] M. Willgert, A. Boujemaoui, E. Malmström, E. C. Constable, C. E. Housecroft, *RSC Adv.***2016**, *6*, 56571.

[236] K. J. Jiang, T. Kitamura, Y. Wada, S. Yanagida, *Bull. Chem. Soc. Jpn.***2003**, *76*, 2415.

[237] S. K. Dhungel, J. G. Park, *Renew. Energy***2010**, *35*, 2776.

[238] R. Mori, T. Ueta, K. Sakai, Y. Niida, Y. Koshiba, L. Lei, K. Nakamae, Y. Ueda, *J. Mater. Sci.***2011**, *46*, 1341.

[239] H. Li, Z. Xie, Y. Zhang, J. Wang, *Thin Solid Films***2010**, *518*, e68.

[240] M. Boucharef, C. Di Bin, M. S. Boumaza, M. Colas, H. J. Snaith, B. Ratier, J. Bouclé, *Nanotechnology***2010**, *21*, 205203.

[241] A. Hu, Q. Wang, L. Chen, X. Hu, Y. Zhang, Y. Wu, Y. Chen, *ACS Appl. Mater. Interfaces***2015**, *7*, 16078.

[242] S. Ito, Y. Makari, T. Kitamura, Y. Wada, S. Yanagida, *J. Mater. Chem.***2004**, *14*, 385.

[243] H. Pettersson, T. Gruszecki, *Sol. Energy Mater. Sol. Cells***2001**, *70*, 203.

[244] A. P. Uthirakumar, in *Sol. Cells - Dye. Devices* (Ed.: L.A. Kosyachenko), InTech, **2011**, pp. 436–456.

[245] F. Bella, D. Pugliese, L. Zolin, C. Gerbaldi, *Electrochim. Acta***2017**, *237*, 87.

[246] J. Szlufcik, J. Majewski, A. Buczkowski, J. Radojewski, L. Jędral, E. B. Radojewska, *Sol. Energy Mater.***1989**, *18*, 241.

[247] Y.-S. Chiu, C.-L. Cheng, T.-J. Whang, C.-C. Chen, *Materials (Basel).***2013**, *6*, 4565.

[248] R. Li, H. Wang, Y. Tai, J. Bai, H. Wang, *RSC Adv.***2016**, *6*, 43732.

[249] J. Qin, S. Bai, W. Zhang, Z. Liu, H. Wang, *Circuit World***2016**, *42*, 77.

[250] M. Kaelin, D. Rudmann, F. Kurdesau, H. Zogg, T. Meyer, A. N. Tiwari, *Thin Solid Films***2005**, *480–481*, 486.

[251] S. Ahn, C. Kim, J. H. Yun, J. Gwak, S. Jeong, B.-H. Ryu, K. Yoon, *J. Phys. Chem. C***2010**, *114*, 8108.

[252] C.-L. Wang, A. Manthiram, *ACS Sustain. Chem. Eng.***2014**, *2*, 561.

[253] P. Liu, Z. Yu, N. Cheng, C. Wang, Y. Gong, S. Bai, X. Z. Zhao, *Electrochim. Acta***2016**, *213*, 83.

[254] I. Clemminck, R. Goossens, M. Burgelman, A. Vervaet, in *Conf. Rec. Twent. IEEE Photovolt. Spec. Conf.*, IEEE, **1988**, pp. 1579–1584 vol.2.

[255] J. Tian, R. Gao, Q. Zhang, S. Zhang, Y. Li, J. Lan, X. Qu, G. Cao, *J. Phys. Chem. C***2012**, *116*, 18655.

[256] G. Niu, W. Li, F. Meng, L. Wang, H. Dong, Y. Qiu, *J. Mater. Chem. A***2014**, *2*, 705.

[257] A. Chiappone, F. Bella, J. R. Nair, G. Meligrana, R. Bongiovanni, C. Gerbaldi, *ChemElectroChem***2014**, *1*, 1350.

[258] K. Miettunen, J. Vapaavuori, A. Tiihonen, A. Poskela, P. Lahtinen, J. Halme, P. Lund, *Nano Energy***2014**, *8*, 95.

[259] L. Teruel, Y. Bouizi, P. Atienzar, V. Fornes, H. Garcia, *Energy Environ. Sci.***2010**, *3*, 154.

[260] S. Ito, Y. Mikami, *Pure Appl. Chem.***2011**, *83*, 2089+.

[261] R. Cruz, L. Brandão, A. Mendes, *Int. J. Energy Res.***2013**, *37*, 1498.

[262] L. Valentini, S. Bittolo Bon, E. Fortunati, J. M. Kenny, *J. Mater. Sci.***2014**, *49*, 1009.

[263] K. Sakakibara, F. Nakatsubo, *Macromol. Chem. Phys.***2010**, *211*, 2425.

[264] Y. Saito, H. Kamitakahara, T. Takano, *Carbohydr. Res.***2016**, *421*, 40.

[265] Y. Saito, H. Kamitakahara, T. Takano, *Cellulose***2014**, *21*, 1885.

[266] Z. Shi, S. Zang, F. Jiang, L. Huang, D. Lu, Y. Ma, G. Yang, *RSC Adv.***2012**, *2*, 1040.

[267] Y. Song, Y. Jiang, L.-Y. Shi, S. Cao, X. Feng, M. Miao, J. Fang, *Nanoscale***2015**, *7*, 13694.

[268] Y. Rong, H. Han, *J. Nanophotonics***2013**, *7*, 73090.

[269] J. M. Feckl, A. Haynes, T. Bein, D. Fattakhova-Rohlfing, *New J. Chem.***2014**, *38*, 1996.

[270] Z. Du, H. Zhang, H. Bao, X. Zhong, *J. Mater. Chem. A***2014**, *2*, 13033.

[271] T. R. Chetia, M. S. Ansari, M. Qureshi, *ACS Appl. Mater. Interfaces***2015**, *7*, 13266.

[272] S. Smith, K. Moodley, U. Govender, H. Chen, L. Fourie, S. Ngwenya, S. Kumar, P. Mjwana, H. Cele, M. B. Mbanjwa, S. Potgieter, T.-H. Joubert, K. Land, *S. Afr. J. Sci.***2015**, *Volume 111*, 1.

[273] M. M. Hamedi, A. Ainla, F. Güder, D. C. Christodouleas, M. T. Fernández-Abedul, G. M. Whitesides, *Adv. Mater.***2016**, 5054.

[274] D. D. Liana, B. Raguse, J. J. Gooding, E. Chow, *Sensors***2012**, *12*, 11505.

[275] W. Zhao, A. van der Berg, *Lab Chip***2008**, *8*, 1988.

[276] A. W. Martinez, S. T. Phillips, M. J. Butte, G. M. Whitesides, *Angew. Chemie Int. Ed.***2007**, *46*, 1318.

[277] A. W. Martinez, S. T. Phillips, G. M. Whitesides, E. Carrilho, *Anal. Chem.***2010**, *82*, 3.

[278] M. S. Khan, D. Fon, X. Li, J. Tian, J. Forsythe, G. Garnier, W. Shen, *Colloids Surfaces B Biointerfaces***2010**, *75*, 441.

[279] M. N. Costa, B. Veigas, J. M. Jacob, D. S. Santos, J. Gomes, P. V Baptista, R. Martins, J. Inácio, E. Fortunato, *Nanotechnology***2014**, *25*, 94006.

[280] A. C. Marques, L. Santos, M. N. Costa, J. M. Dantas, P. Duarte, A. Gonçalves, R. Martins, C. A. Salgueiro, E. Fortunato, *Sci. Rep.***2015**, *5*, 9910.

[281] X. Li, J. Tian, T. Nguyen, W. Shen, *Anal. Chem.***2008**, *80*, 9131.

[282] A. C. Glavan, R. V. Martinez, A. B. Subramaniam, H. J. Yoon, R. M. D. Nunes, H. Lange, M. M. Thuo, G. M. Whitesides, *Adv. Funct. Mater.***2014**, *24*, 60.

[283] F. J. Pavinatto, C. W. A. Paschoal, A. C. Arias, *Biosens. Bioelectron.***2015**, *67*, 553.

[284] H. Schmidt, A. R. Hawkins, *Nat. Photonics***2011**, *5*, 598.

[285] D. Erickson, D. Sinton, D. Psaltis, *Nat. Photonics***2011**, *5*, 583.

[286] Y.-F. Chen, L. Jiang, M. Mancuso, A. Jain, V. Oncescu, D. Erickson, *Nanoscale***2012**, *4*, 4839.

[287] R. Zimmerman, G. Morrison, G. Rosengarten, in *ASME 2008 2nd Int. Conf. Energy Sustain. Vol. 2*, ASME, **2009**, p. 11005.

[288] Y.-S. Li, J. S. Church, *J. Food Drug Anal.***2014**, *22*, 29.

[289] R. Aroca, *Surface-Enhanced Vibrational Spectroscopy*, John Wiley And Sons, **2007**.

[290] S. Schlücker, *Angew. Chem. Int. Ed. Engl.***2014**, *53*, 4756.

[291] A. J. McQuillan, *Notes Rec. R. Soc.***2009**, *63*, 105.

[292] E. C. Le Ru, E. Blackie, M. Meyer, P. G. Etchegoin, *J. Phys. Chem. C***2007**, *111*, 13794.

[293] Z.-Y. Li, Y. Xia, *Nano Lett.***2010**, *10*, 243.

[294] F. J. García-Vidal, J. B. Pendry, *Phys. Rev. Lett.***1996**, *77*, 1163.

[295] Z. Yi, X. Xu, J. Luo, X. Li, Y. Yi, X. Jiang, *Phys. B Phys. Condens. Matter***2014**, *438*, 22.

[296] A. Araújo, C. Caro, M. J. Mendes, D. Nunes, E. Fortunato, R. Franco, H. Águas, R. Martins, *Nanotechnology***2014**, *25*, 415202.

[297] S. M. Stranahan, K. A. Willets, *Nano Lett.***2010**, *10*, 3777.

[298] J. Theiss, P. Pavaskar, P. M. Echternach, R. E. Muller, S. B. Cronin, *Nano Lett.***2010**, *10*, 2749.

[299] A. X. Wang, X. Kong, *Materials (Basel).***2015**, *8*, 3024.

[300] A. Otto, I. Mrozek, H. Grabhorn, W. Akemann, *J.Phys.:Condens.Matter***1992**, *4*, 1143.

[301] S. Lecomte, P. Matejka, M. H. Baron, **1998**, *7463*, 4373.

[302] W. Park, Z. H. Kim, *Nano Lett.***2010**, 4040.

[303] M. Käll, P. Apell, *Phys. Rev. E***2000**, 4318.

[304] A. M. Robinson, sensitive surface-enhanced R. spectroscopy (SERS) substrates for analytical applications. Zhao, Lilihe development of “fab-chips” as low-cost, M. Y. Shah Alam, P. Bhandari, S. G. Harroun, D. Dendukuri, J. Blackburn, C. L. Brosseau, *Analyst***2015**, *140*, 779.

[305] J. F. Betz, W. W. Yu, Y. Cheng, M. White, G. W. Rubloff, *Phys. Chem. Chem. Phys.***2014**, *16*, 2224.

[306] C. H. Lee, L. Tian, S. Singamaneni, *ACS Appl. Mater. Interfaces***2010**, *2*, 3429.

[307] R. F. Aroca, *Phys. Chem. Chem. Phys.***2013**, *15*, 5355.

[308] P. R. West, S. Ishii, G. V. Naik, N. K. Emani, V. M. Shalaev, a. Boltasseva, *Laser Photon. Rev.***2010**, *4*, 795.

[309] M. Rycenga, C. M. Cobley, J. Zeng, W. Li, C. H. Moran, Q. Zhang, D. Qin, Y. Xia, *Chem. Rev.***2011**, *111*, 3669.

[310] A. Araújo, A. Pimentel, M. J. Oliveira, M. J. Mendes, R. Franco, R. Fortunato, Elvira, Águas, Hugo, Martins, *Flex. Print. Electron.***2017**, *2*, 14001.

[311] D. Gaspar, S. N. Fernandes, A. G. De Oliveira, J. G. Fernandes, P. Grey, R. V Pontes, L. Pereira, R. Martins, M. H. Godinho, E. Fortunato, *Nanotechnology***2014**, *25*, 94008.

[312] K. L. Kelly, E. Coronado, L. L. Zhao, G. C. Schatz, *J. Phys. Chem. B***2003**, *107*, 668.

[313] M. J. Mendes, E. Hernández, E. López, P. García-Linares, I. Ramiro, I. Artacho, E. Antolín, I. Tobías, A. Martí, A. Luque, *Nanotechnology***2013**, *24*, 345402.

[314] V. A. Online, Y. Huang, D. Kim, *Nanoscale***2014**, *6*, 6478.

[315] D. Gaspar, A. C. Pimentel, M. J. Mendes, T. Mateus, B. P. Falcão, J. P. Leitão, J. Soares, A. Araújo, A. Vicente, S. A. Filonovich, H. Águas, R. Martins, I. Ferreira, *Plasmonics***2014**, 1.

[316] L.-L. Qu, D.-W. Li, J.-Q. Xue, W.-L. Zhai, J. S. Fossey, Yi-Tao Long, *Lab Chip***2012**, *12*, 876.

[317] L. Dongming, J. Shuhai, W. Jun, J. Yang, *Sensors Actuators A Phys.***2013**, *201*, 416.

[318] Q. Tao, S. Li, C. Ma, K. Liu, Q.-Y. Zhang, *Dalton Trans.***2015**, *44*, 3447.

[319] S. Cui, Z. Dai, Q. Tian, J. Liu, X. Xiao, C. Jiang, W. Wu, V. A. L. Roy, *J. Mater. Chem. C***2016**, *4*, 6371.

[320] G. Sinha, L. E. Depero, I. Alessandri, *ACS Appl. Mater. Interfaces***2011**, *3*, 2557.

[321] S. Faÿ, J. Steinhauser, N. Oliveira, E. Vallat-Sauvain, C. Ballif, *Thin Solid Films***2007**, *515*, 8558.

[322] J. Chen, Y. Huang, P. Kannan, L. Zhang, Z. Lin, J. Zhang, T. Chen, L. Guo, *Anal. Chim. Acta***2016**, *88*, 2149.

[323] Y. H. Ngo, W. L. Then, W. Shen, G. Garnier, *J. Colloid Interface Sci.***2013**, *409*, 59.

[324] W. W. Yu, I. M. White, *Anal. Chem.***2010**, *82*, 9626.

[325] L. Polavarapu, A. La Porta, S. M. Novikov, M. Coronado-Puchau, L. M. Liz-Marzán, *Small***2014**, *10*, 3065.

[326] L. Polavarapu, L. M. Liz-Marzán, *Phys. Chem. Chem. Phys.***2013**, *15*, 5288.

[327] R. Zhang, B. Xu, X. Liu, Y. Zhang, Y. Xu, Q. Chen, *Chem. Commun.***2012**, *48*, 5913.

[328] W. Wu, L. Liu, Z. Dai, J. Liu, S. Yang, L. Zhou, X. Xiao, *Sci. Rep.***2015**, 1.

[329] G. V. P. Kumar, *J. Nanophotonics***2012**, *6*, 64503.

[330] A. Martín, J. J. Wang, D. Iacopino, *RSC Adv.***2014**, *4*, 20038.

[331] B. Pietrobon, M. McEachran, K. Vladimir, *ASC NANO***2009**, *3*, 21.

[332] G. Zheng, L. Polavarapu, L. M. Liz-marza, I. Pastoriza-Santos, J. Pérez-Juste, *Chem. Commun.***2015**, *51*, 4572.

[333] S. Aksu, M. Huang, A. Artar, A. A. Yanik, S. Selvarasah, M. R. Dokmeci, H. Altug, *Adv. Mater.***2011**, *23*, 4422.

[334] K. D. Osberg, M. Rycenga, G. R. Bourret, K. A. Brown, C. A. Mirkin, *Adv. Funct. Mater.***2012**, *24*, 6065.

[335] M. Fan, G. F. S. Andrade, A. G. Brolo, *Anal. Chim. Acta***2011**, *693*, 7.

[336] J. Prakash, R. A. Harris, H. C. Swart, *Int. Rev. Phys. Chem.***2016**, *35*, 353.

[337] W.-S. Kim, J.-H. Shin, H.-K. Park, S. Choi, *Sensors Actuators B Chem.***2015**, *222*, 1112.

[338] Y. H. Ngo, D. Li, G. P. Simon, G. Garnier, *Langmuir***2012**, *28*, 8782.

[339] C. H. Lee, M. E. Hankus, L. Tian, P. M. Pellegrino, S. Singamaneni, *Anal. Chem.***2011**, *83*, 8953.

[340] A. J. Chung, Y. S. Huh, D. Erickson, *Nanoscale***2011**, *3*, 2903.

[341] P. M. Fierro-Mercado, S. P. Hernández-Rivera, *Int. J. Spectrosc.***2012**, *2012*, 1.

[342] R. Cha, D. Wang, Z. He, Y. Ni, *Carbohydr. Polym.***2012**, *88*, 1414.

[343] B. Veigas, J. M. Jacob, M. N. Costa, D. S. Santos, M. Viveiros, J. Inácio, R. Martins, P. Barquinha, E. Fortunato, P. V. Baptista, *Lab Chip***2012**, *12*, 4802.

[344] Y. Sun, J. a. Rogers, *Adv. Mater.***2007**, *19*, 1897.

[345] A. M. Robinson, S. G. Harroun, J. Bergman, C. L. Brosseau, *Anal. Chem.***2012**, *84*, 1760.

[346] E. P. Hoppmann, W. W. Yu, I. M. White, *Methods***2013**, *63*, 219.

[347] W. W. Yu, I. M. White, *Analyst***2013**, *138*, 1020.

[348] D. Wu, Y. Fang, *J. Colloid Interface Sci.***2003**, *265*, 234.

[349] M. J. Oliveira, P. Quaresma, M. P. Almeida, *Sci. Rep.***2017**, *7*, DOI 10.1038/s41598-017-02484-8.

[350] W. W. Yu, I. M. White, *Analyst***2012**, *137*, 1168.

[351] L. F. Sallum, F. L. F. Soares, J. A. Ardila, R. L. Carneiro, *Talanta***2014**, *118*, 353.

[352] A. Berthod, J. J. Laserna, J. D. Winefordner, *J. Pharm. Biomed. Anal.***1988**, *6*, 599.

[353] M. L. Cheng, B. C. Tsai, J. Yang, *Anal. Chim. Acta***2011**, *708*, 89.

[354] L. F. Sallum, F. L. F. Soares, J. A. Ardila, R. L. Carneiro, *Spectrochim. Acta. A. Mol. Biomol. Spectrosc.***2014**, *133*, 107.

[355] M. Wu, W. Su, H. Han, L. Chen, *Anal. Chem.***2012**, *84*, 5140.

[356] C. Novara, F. Petracca, A. Virga, P. Rivolo, S. Ferrero, A. Chiolerio, F. Geobaldo, S. Porro, F. Giorgis, *Nanoscale Res. Lett.***2014**, *9*, 527.

[357] A. Virga, P. Rivolo, E. Descrovi, A. Chiolerio, G. Digregorio, F. Frascella, M. Soster, F. Bussolino, S. Marchiò, F. Geobaldo, F. Giorgis, *J. Raman Spectrosc.***2012**, *43*, 730.

[358] K. Castro, E. Princi, N. Proietti, M. Manso, D. Capitani, S. Vicini, J. M. Madariaga, M. L. De Carvalho, *Nucl. Instruments Methods Phys. Res. Sect. B Beam Interact. with Mater. Atoms***2011**, *269*, 1401.

[359] Y. Li, K. Zhang, J. Zhao, J. Ji, C. Ji, B. Liu, *Talanta***2016**, *147*, 493.

[360] Y. Zhu, L. Zhang, L. Yang, *Mater. Res. Bull.***2015**, *63*, 199.

[361] W. Cao, H. E. Elsayed-Ali, *Mater. Lett.***2009**, *63*, 2263.

[362] M. A. Mohiddon, L. D. V. Sangani, M. G. Krishna, *Chem. Phys. Lett.***2013**, *588*, 160.

[363] D. Gaspar, A. C. Pimentel, T. Mateus, J. P. Leitão, J. Soares, B. P. Falcão, A. Araújo, A. Vicente, S. a Filonovich, H. Aguas, R. Martins, I. Ferreira, *Sci. Rep.***2013**, *3*, 1469.

[364] S. Sundarajoo, E. L. Izake, W. Olds, B. Cletus, E. Jaatinen, P. M. Fredericks, *J. Raman Spectrosc.***2013**, *44*, 949.

[365] J. B. Cooper, M. Abdelkader, K. L. Wise, *Appl. Spectrosc.***2013**, *67*, 973.

[366] D. Craig, M. Mazilu, K. Dholakia, *PLoS One***2015**, *10*, 1.

[367] M. Macias-Montero, R. J. Peláez, V. J. Rico, Z. Saghi, P. Midgley, C. N. Afonso, A. R. González-Elipe, A. Borras, *ACS Appl. Mater. Interfaces***2015**, *7*, 2331.

[368] H. Tang, G. Meng, Q. Huang, Z. Zhang, Z. Huang, *Adv. Funct. Mater.***2012**, *22*, 218.

[369] X. Zhao, B. Zhang, K. Ai, G. Zhang, L. Cao, X. Liu, H. Sun, H. Wang, L. Lu, *J. Mater. Chem.***2009**, *19*, 5547.

[370] A. Lamberti, A. Virga, A. Chiado, A. Chiodoni, *J. Mater. Chem. C***2015**, *3*, 6868.

[371] Z. Yi, Y. Yi, J. Luo, X. Li, X. Xu, X. Jiang, *Phys. B Phys. Condens. Matter***2014**, *451*, 58.

[372] T. Stelzner, G. Andra, M. Becker, V. Sivakov, U. Go, H. J. Reich, S. Hoffmann, J. Michler, S. H. Christiansen, *Small***2008**, *4*, 398.

[373] Z. Liu, W. He, Z. Guo, *Chem. Soc. Rev.***2013**, *42*, 1568.

[374] W. E. Buhro, V. L. Colvin, *Nat. Mater.***2003**, *2*, 138.

[375] L. Jing, S. V Kershaw, Y. Li, X. Huang, Y. Li, A. L. Rogach, M. Gao, *Chem. Rev.***2016**, *116*, 10623.

[376] A. M. Smith, S. Nie, *Acc. Chem. Res.***2010**, *43*, 190.

[377] A. Fu, W. Gu, C. Larabell, A. P. Alivisatos, *Curr. Opin. Neurobiol.***2005**, *15*, 568.

[378] C. Bertoni, D. Gallardo, S. Dunn, N. Gaponik, A. Eychmüller, *Appl. Phys. Lett.***2007**, *90*, 34107.

[379] V. A. Vlaskin, N. Janssen, J. van Rijssel, R. Beaulac, D. R. Gamelin, *Nano Lett.***2010**, *10*, 3670.

[380] K. D. Karlin, *Progress in Inorganic Chemistry*, **2012**.

[381] R. Beaulac, P. I. Archer, D. R. Gamelin, *J. Solid State Chem.***2008**, *181*, 1582.

[382] S. C. Qu, W. H. Zhou, F. Q. Liu, N. F. Chen, Z. G. Wang, H. Y. Pan, D. P. Yu, *Appl. Phys. Lett.***2002**, *80*, 3605.

[383] B. B. Srivastava, S. Jana, N. Pradhan, *J. Am. Chem. Soc.***2011**, *133*, 1007.

[384] D. Mocatta, G. Cohen, J. Schattner, O. Millo, E. Rabani, U. Banin, *Science (80-.).***2011**, *332*, 77.

[385] Y. Ito, K. Matsuda, Y. Kanemitsu, *Phys. Rev. B***2007**, *75*, 33309.

[386] M. Oshima, Y. Watanabe, S. Heun, M. Sugiyama, T. Kiyokura, *J. Electron Spectros. Relat. Phenomena***1996**, *80*, 129.

[387] W. Chen, A. G. Joly, J. Z. Zhang, *Phys. Rev. B***2001**, *64*, 41202.

[388] S. Dong, M. Roman, *J. Am. Chem. Soc.***2007**, *129*, 13810.

[389] B. Zhou, B. Shi, D. Jin, X. Liu, *Nat. Nanotechnol.***2015**, *10*, 924.

[390] G. G. Stokes, *Philos. Trans. R. Soc. London***1852**, *142*, 463.

[391] N. Bloembergen, *Phys. Rev. Lett.***1959**, *2*, 84.

[392] Q. Lu, Y. Hou, A. Tang, Y. Lu, L. Lv, F. Teng, *J. Appl. Phys.***2014**, *115*, 74309.

[393] Y. P. Rakovich, J. F. Donegan, in *Semicond. Nanocrystal Quantum Dots Synth. Assem. Spectrosc. Appl.* (Ed.: A.L. Rogach), Springer Vienna, Vienna, **2008**, pp. 257–275.

[394] N. Akizuki, S. Aota, S. Mouri, K. Matsuda, Y. Miyauchi, **2015**, *6*, 8920.

[395] E. M. Chan, *Chem. Soc. Rev.***2015**, *44*, 1653.

[396] F. M. Matysik, *Advances in Chemical Bioanalysis*, Springer International Publishing, **2014**.

[397] R. Dey, V. K. Rai, *Dalt. Trans.***2014**, *43*, 111.

[398] P. Ramasamy, P. Manivasakan, J. Kim, *RSC Adv.***2014**, *4*, 34873.

[399] J. Chen, J. X. Zhao, *Sensors***2012**, *12*, 2414.

[400] J. de Wild, A. Meijerink, J. K. Rath, W. G. J. H. M. van Sark, R. E. I. Schropp, *Energy Environ. Sci.***2011**, *4*, 4835.

[401] N. Hakmeh, C. Chlique, O. Merdrignac-Conanec, B. Fan, F. Cheviré, X. Zhang, X. Fan, X. Qiao, *J. Solid State Chem.***2015**, *226*, 255.

[402] H. Suo, C. Guo, L. Li, *Ceram. Int.***2015**, *41*, 7017.

[403] M. Reben, I. Wacławska, C. Paluszkiewicz, M. Środa, *J. Therm. Anal. Calorim.***2007**, *88*, 285.

[404] Q. A. Acton, *Advances in Nanotechnology Research and Application: 2011 Edition*, ScholarlyEditions, **2012**.

[405] D. H. Chávez, O. E. Contreras, G. A. Hirata, *Nanomater. Nanotechnol.***2016**, *6*, 1.

[406] X. Du, X. Wang, L. Meng, Y. Bu, X. Yan, *Nanoscale Res. Lett.***2017**, *12*, 163.

[407] I. Dugandžić, V. Lojpur, L. Mančić, M. D. Dramićanin, M. E. Rabanal, T. Hashishin, Z. Tan, S. Ohara, O. Milošević, *Adv. Powder Technol.***2013**, *24*, 852.

[408] E. Downing, L. Hesselink, J. Ralston, R. Macfarlane, *Science (80-.).***1996**, *273*, 1185.

[409] F. Zhang, *Photon Upconversion Nanomaterials*, Springer Berlin Heidelberg, **2014**.

[410] P. G. Kik, A. Polman, *J. Appl. Phys.***2003**, *93*, 5008.

[411] X. Huang, S. Han, W. Huang, X. Liu, *Chem. Soc. Rev.***2013**, *42*, 173.

[412] S. Fischer, J. C. Goldschmidt, P. Löper, G. H. Bauer, R. Brüggemann, K. Krämer, D. Biner, M. Hermle, S. W. Glunz, *J. Appl. Phys.***2010**, *108*, 44912.

[413] S. Hao, Y. Shang, D. Li, H. Agren, C. Yang, G. Chen, *Nanoscale***2017**, *9*, 6711.

[414] Y. Chen, H. Liang, *J. Photochem. Photobiol. B Biol.***2014**, *135*, 23.

[415] K. Börjesson, P. Rudquist, V. Gray, K. Moth-Poulsen, *Nat. Commun.***2016**, *7*, 1.

[416] M. Wang, G. Abbineni, A. Clevenger, C. Mao, S. Xu, *Nanomedicine Nanotechnology, Biol. Med.***2011**, *7*, 710.

[417] L. T. Canham, *Appl. Phys. Lett.***1990**, *57*, 1046.

[418] Y. Shang, S. Hao, C. Yang, G. Chen, *Nanomaterials***2015**, *5*, 1782.

[419] A. Gnach, A. Bednarkiewicz, *Nano Today***2012**, *7*, 532.

[420] W. Zou, C. Visser, J. A. Maduro, M. S. Pshenichnikov, J. C. Hummelen, *Nat Phot.***2012**, *6*, 560.

[421] L. T. Su, S. K. Karuturi, J. Luo, L. Liu, X. Liu, J. Guo, T. C. Sum, R. Deng, H. J. Fan, X. Liu, A. I. Y. Tok, *Adv. Mater.***2013**, *25*, 1603.

[422] F. Wang, D. Banerjee, Y. Liu, X. Chen, X. Liu, *Analyst***2010**, *135*, 1839.

[423] W. Liu, H. Zhang, H. Wang, M. Zhang, M. Guo, *Appl. Surf. Sci.***2017**, *422*, 304.

[424] S. Xu, B. Dong, D. Zhou, Z. Yin, S. Cui, W. Xu, B. Chen, H. Song, *Sci. Rep.***2016**, *6*, 23406.

[425] Q. Mei, H. Jing, Y. Li, W. Yisibashaer, J. Chen, B. Nan Li, Y. Zhang, *Biosens. Bioelectron.***2016**, *75*, 427.

[426] Q. Yanmin, G. Hai, *J. Rare Earths***2009**, *27*, 406.

[427] J. A. Capobianco, F. Vetrone, J. C. Boyer, A. Speghini, M. Bettinelli, *J. Phys. Chem. B***2002**, *106*, 1181.

[428] C. Lin, M. T. Berry, R. Anderson, S. Smith, P. S. May, *Chem. Mater.***2009**, *21*, 3406.

[429] K.-C. Liu, Z.-Y. Zhang, C.-X. Shan, Z.-Q. Feng, J.-S. Li, C.-L. Song, Y.-N. Bao, X.-H. Qi, B. Dong, *Light Sci Appl.***2016**, *5*, 1.

[430] M. Tzenka, Y. Vladimir, N. Gabriele, B. Stanislav, *New J. Phys.***2008**, *10*, 103002.

[431] B. J. Park, A. R. Hong, S. Park, K.-U. Kyung, K. Lee, H. Seong Jang, **2017**, *7*, 45659.

[432] S. Doughan, U. Uddayasankar, U. J. Krull, *Anal. Chim. Acta***2015**, *878*, 1.

[433] F. Zhou, M. Noor, U. Krull, *Nanomaterials***2015**, *5*, 1556.

[434] F. Zhou, M. O. Noor, U. J. Krull, *Anal. Chem.***2014**, *86*, 2719.

[435] K. Koren, M. Kühl, *Sensors Actuators B Chem.***2015**, *210*, 124.

[436] A. Pandey, V. K. Rai, *Dalt. Trans.***2013**, *42*, 11005.

[437] T. Otto, S. Geidel, A. Morschhauser, R. Streiter, T. Gessner, B. Heibutzki, J. Nestler, in *2015 Int. Conf. Signal Process. Commun.*, IEEE, **2015**, pp. 177–182.

[438] R. Radhakrishnan, I. I. Suni, C. S. Bever, B. D. Hammock, *ACS Sustain. Chem. Eng.***2014**, *2*, 1649.

[439] S. Thiemann, S. J. Sachnov, F. Pettersson, R. Bollström, R. Österbacka, P. Wasserscheid, J. Zaumseil, *Adv. Funct. Mater.***2014**, *24*, 625.

[440] M. Magliulo, K. Manoli, E. Macchia, G. Palazzo, L. Torsi, *Adv. Mater.***2015**, *27*, 7528.

[441] T. Sekitani, T. Yokota, U. Zschieschang, H. Klauk, S. Bauer, K. Takeuchi, M. Takamiya, T. Sakurai, T. Someya, *Science (80-.).***2009**, *326*, 1516.

[442] A. Guedes, M. J. Mendes, P. P. Freitas, J. L. Martins, *J. Appl. Phys.***2006**, DOI 10.1063/1.2162817.

[443] D.-H. Lien, Z.-K. Kao, T.-H. Huang, Y.-C. Liao, S.-C. Lee, J.-H. He, *ACS Nano***2014**, *8*, 7613.

[444] K. Nagashima, H. Koga, U. Celano, F. Zhuge, M. Kanai, S. Rahong, G. Meng, Y. He, J. De Boeck, M. Jurczak, W. Vandervorst, T. Kitaoka, M. Nogi, T. Yanagida, *Sci. Rep.***2015**, *4*, 5532.

[445] W. Zhang, X. Zhang, C. Lu, Y. Wang, Y. Deng, *J. Phys. Chem. C***2012**, *116*, 9227.

[446] J. Kawahara, P. Andersson Ersman, X. Wang, G. Gustafsson, H. Granberg, M. Berggren, *Org. Electron.***2013**, *14*, 3061.

[447] I. Cunha, R. Barras, P. Grey, D. Gaspar, E. Fortunato, R. Martins, L. Pereira, *Adv. Funct. Mater.***2017**, *27*, 1606755.

[448] Y. H. Jung, T.-H. Chang, H. Zhang, C. Yao, Q. Zheng, V. W. Yang, H. Mi, M. Kim, S. J. Cho, D.-W. Park, H. Jiang, J. Lee, Y. Qiu, W. Zhou, Z. Cai, S. Gong, Z. Ma, *Nat. Commun.***2015**, *6*, 7170.

[449] J.-H. Seo, T.-H. Chang, R. Sabo, Z. Cai, S. Gong, Z. Ma, in *2015 IEEE 15th Top. Meet. Silicon Monolith. Integr. Circuits RF Syst.*, IEEE, **2015**, pp. 83–85.